Streamflow Signature Analysis of Long-Term Effects of Urbanization on Hydrologic Alteration in the Southeastern United States

by

Reid McDaniel

A thesis submitted to the Graduate Faculty of
Auburn University
in partial fulfillment of the
requirements for the Degree of
Master of Science

Auburn, Alabama
May 4, 2019

Keywords: Streamflow, Hydrologic Alteration, Watershed Modeling, Urbanization, Land Cover Change

Approved by

Dr. Frances O'Donnell, Chair, Assistant Professor of Civil Engineering
Dr. Xing Fang, Arthur H. Feagin Chair Professor of Civil Engineering
Dr. Christopher Anderson, Associate Professor, School of Forestry and Wildlife Sciences

Abstract

Urbanization in the southeastern United States has risen exponentially over the past few decades. This increase causes runoff to have a greater surface flow, a smaller interflow, and sometimes a reduced baseflow by changing the natural infiltration characteristics of a watershed. As development continues, there is an increasing need for a better understanding of these effects on water resources and aquatic habitat. A study was performed to determine the overall effect urbanization has on hydrograph alteration over time. Streamflow and precipitation gauge data were analyzed over 36 years and compared with landcover changes to produce datasets for four watersheds. Datasets were split into pre-impact and post-impact periods to determine trends in hydrologic alteration. The 1-day, 3-day, 7-day, 30-day, and 90-day minimum and maximum were investigated for hydrologic alterations across each watershed. Maximums flows decreased over time in the urbanized watersheds whereas minimums flows varied in alteration.

Streamflow signature analysis was performed on each watershed to quantify long term trends in each watershed. The runoff ratio, slope of the flow duration curve, streamflow elasticity, and baseflow index were analyzed. The urbanized watersheds experienced increases to streamflow elasticity over time leading to a greater sensitivity to changes in precipitation. Runoff ratios increased with increases to urbanization in Alabama urban watershed but were reduced in all other cases. The change in the slope of the flow duration curve varied depending on the watershed and baseflow index decreased in most cases but increased in the urbanized Alabama watershed.

Watershed modeling with HEC-HMS was used to determine the effectiveness of large-scale hydrologic modeling methods in representing upstream tributary flows. Streamflow signature and hydrologic alteration analysis results derived from simulated flows proved less accurate to represent low flows and runoff ratio the farther away from the streamflow gage. However, increasing and decreasing trends between the gage location and upstream tributary locations were mostly maintained, even though the magnitude of alteration varied, showing that gage locations can at least provide a glimpse into the hydrologic alterations across the entire watershed. These trends can help identify the type of changes to the aquatic habitat that should be expected, but not necessarily an accurate depiction of the magnitude of the change.

Acknowledgements

I would like to thank my professor, Dr. Frances O'Donnell, for guidance throughout this entire process. Thank you for sharing your passion for hydrology and the environment with me as well as showing me the many ways we can protect our planet through engineering. Without your encouragement and willingness to invest in my education I would not be where I am today. I would also like to thank Dr. Xing Fang and Dr. Jose G. Vasconcelos Neto for their continued support and investment in my education and career preparation throughout both my graduate and undergraduate studies at Auburn University. I also want to thank Dr. Christopher Anderson for his perspective and guidance on the ecological work of this report. Finally, I want to thank my family for their unwavering support and prayer throughout my studies.

Table of Contents

Abstract ii

Acknowledgements iv

List of Tables viii

List of Figures x

1. Introduction 1

    1.1. Background Information 1

    1.2. Research Objectives 6

    1.3. Limitations 6

    1.4. Organization of Thesis 7

2. Literature Review 8

    2.1. Urbanization and Hydrology 8

    2.2. Streamflow Signatures 10

    2.3. Hydrologic Alterations 13

    2.4. Ecological Response to Urbanization 14

3. Methodology 17

    3.1. Streamflow Data 17

3.2. GIS Data 18
3.3 Precipitation 20
3.4 Watershed Selection 21
3.4.1 Site Descriptions 21
3.5 Indicators of Hydrologic Alteration 24
3.6 Streamflow Signature Analysis 27
3.6.1 Runoff Ratio 27
3.6.2 Slope of the Flow Duration Curve 28
3.6.3 Streamflow Elasticity 28
3.6.4 Baseflow Index 29
3.6.5 Baseflow Index Comparison 30
3.7 Comparison 31
3.8 HEC-HMS Model 31
3.8.1 Model Setup with ArcGIS 31
3.8.2 HEC-HMS Model Inputs 34
3.8.3 HEC-HMS Model Calibration 35
3.8.4 HEC-HMS Model Validation 37
3.8.5 HEC-HMS Model Comparison 38
4. Results & Analysis 39
4.1. Analysis Input Data 39

4.2. IHA Analysis Results 43
4.3. Streamflow Signature Analysis Results 56
4.4. HEC-HMS Model 60
5. Conclusions 76
References 78
Appendices 83
Appendix A: NLCD Information 84
NLCD Classification Changes 84
NLCD Urbanization Area Change Comparison 87
Appendix B: IHA Results 92
IHA Parameter Significance Test 92
Ecological Impacts 94
Appendix C: Streamflow Signature Analysis Results 95
Flow Duration Curves 95
Hydrographs 99
Appendix D: HEC-HMS Model Results 103
Model Calibration/Validation 103
Model Optimization Parameter Values 108

List of Tables

Table 3.1: NLCD Urban Classifications 20

Table 3.2: Watershed Identification Summary 22

Table 3.3: IHA Hydrologic Parameters 25

Table 3.3: NLCD Reclassification 32

Table 3.4: Curve Number Lookup Table 33

Table 3.5: Calibrated Model Performance Ratings 37

Table 4.1: NLCD Urbanization Change Comparison 43

Table 4.2: IHA Single Period Parameter P-Values 44

Table 4.3: IHA Two Period Parameter Means and CV for U1 46

Table 4.4: IHA Two Period Parameter Means and CV for C1 47

Table 4.5: IHA Two Period Parameter Means and CV for U2 48

Table 4.6: IHA Two Period Parameter Means and CV for C2 49

Table 4.7: Streamflow Signatures for U1 57

Table 4.8: Streamflow Signatures for C1 59

Table 4.9: Streamflow Signatures for U2 60

Table 4.10: Streamflow Signatures for C2 60

Table 4.11: Before Impact Year Model Performance 62

Table 4.12: After Impact Year Model Performance 62

Table 4.13: HEC-HMS Model Percent Urbanized by Subbasin 65

Table 4.14: Upstream Tributary Streamflow Signature Analysis Results 66

List of Figures

Figure 1.1: U.S. Land Cover Change (2001-2011) 1

Figure 1.2: United States Developed/Impervious Surface 1992 2

Figure 1.3: United States Developed/Impervious Surface 2011 2

Figure 1.4: Hydrologic/Water Cycle Diagram 3

Figure 2.1: Developmental Changes to Streamflow 10

Figure 2.2: Mean Annual Evapotranspiration for the United States, 1971-2000 11

Figure 3.1: Watershed Location Map 22

Figure 4.1: Watershed U1 Ariel View 40

Figure 4.2: Watershed C1 Ariel View 40

Figure 4.3: Watershed U2 Ariel View 41

Figure 4.4: Watershed C2 Ariel View 41

Figure 4.1: Hydrologic Alteration Values for U1 53

Figure 4.2: Hydrologic Alteration Values for C1 53

Figure 4.3: Hydrologic Alteration Values for U2 54

Figure 4.4: Hydrologic Alteration Values for C2 54

Figure 4.5: HEC-HMS Model for U1 61

Figure 4.6: HEC-HMS Ungaged Locations in Watershed U1 64

Figure 4.7: HEC-HMS Model Subbasins 64

Figure 4.8: Hydrologic Alteration Values for J358 70

Figure 4.9: Hydrologic Alteration Values for J310 71

Figure 4.10: Hydrologic Alteration Values for J384 72

Figure 4.11: Hydrologic Alteration Values for J399 73

Figure 4.12: Hydrologic Alteration Values for J313 73

Figure 4.13: Hydrologic Alteration Values for J417 74

Figure 4.14: Hydrologic Alteration Values for J304 75

1. Introduction

1.1. Background Information

Urbanization is defined as the change of land use from agricultural or forested areas to urban or peri-urban areas (National Research Council, 2009). In the southeastern United States (US) it has risen exponentially over the past few decades. It is expected that 84% of the U.S. population will reside in urban areas by the year 2030, with the urban land-cover area tripling the area measured in 2000 (Hopkins et al, 2015). This is already on top of the vast changes to the landscape in recent decades as more people move away from rural lands to cities and suburban areas (Homer et al., 2015). This change has predominantly taken place in the Southeastern United States (Figure 1.1) (Xian et al., 2011; Homer et al., 2015). To offset the high influx of population, cities have either become denser or expanded the urban footprint (Figure 1.2 and Figure 1.3) (Xian et al., 2011; Homer et al., 2015).

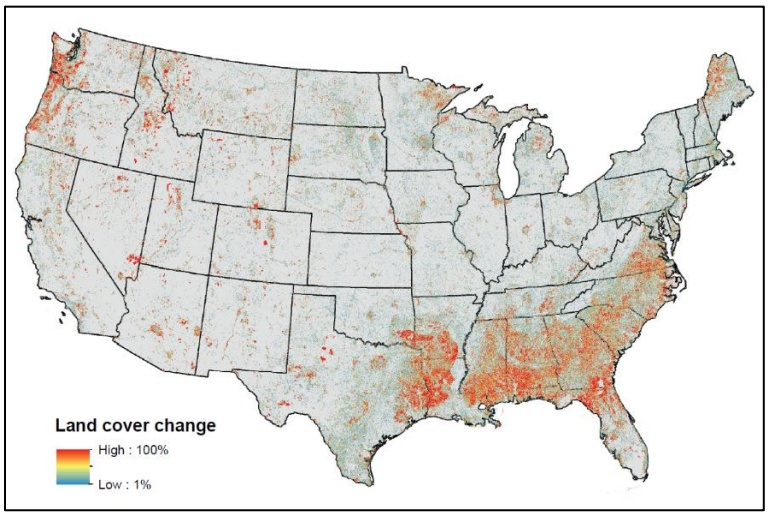

Figure 1.1: U.S. Land Cover Change (2001-2011) (Reference: Homer et al., 2015)

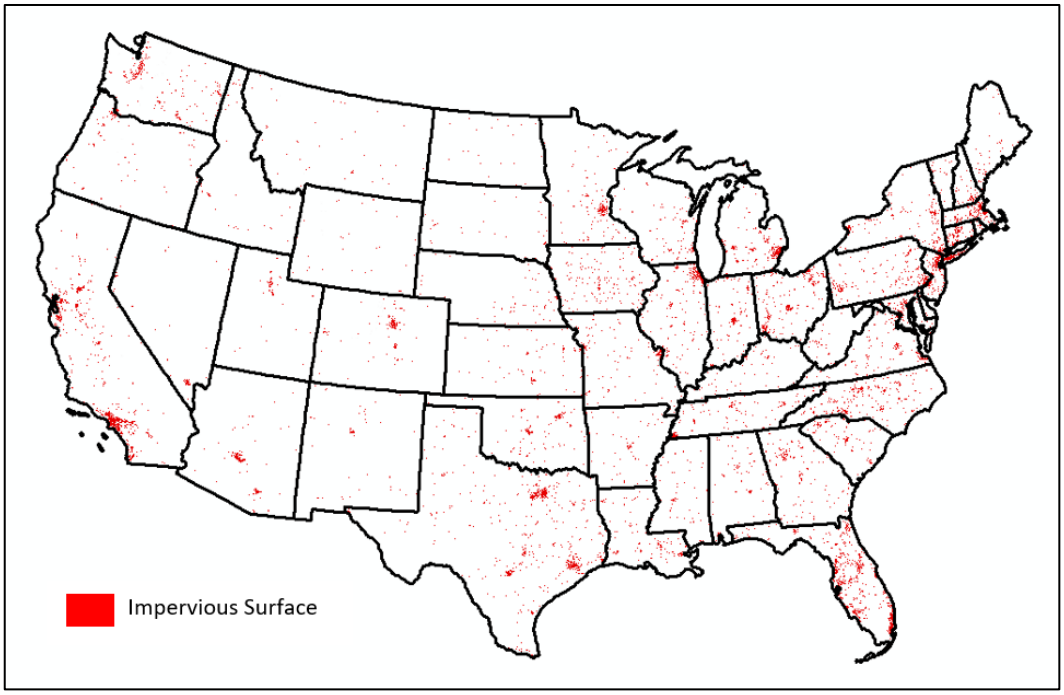

Figure 1.2: United States Developed/Impervious Surface 1992

(Reference: Fry et al., 2009)

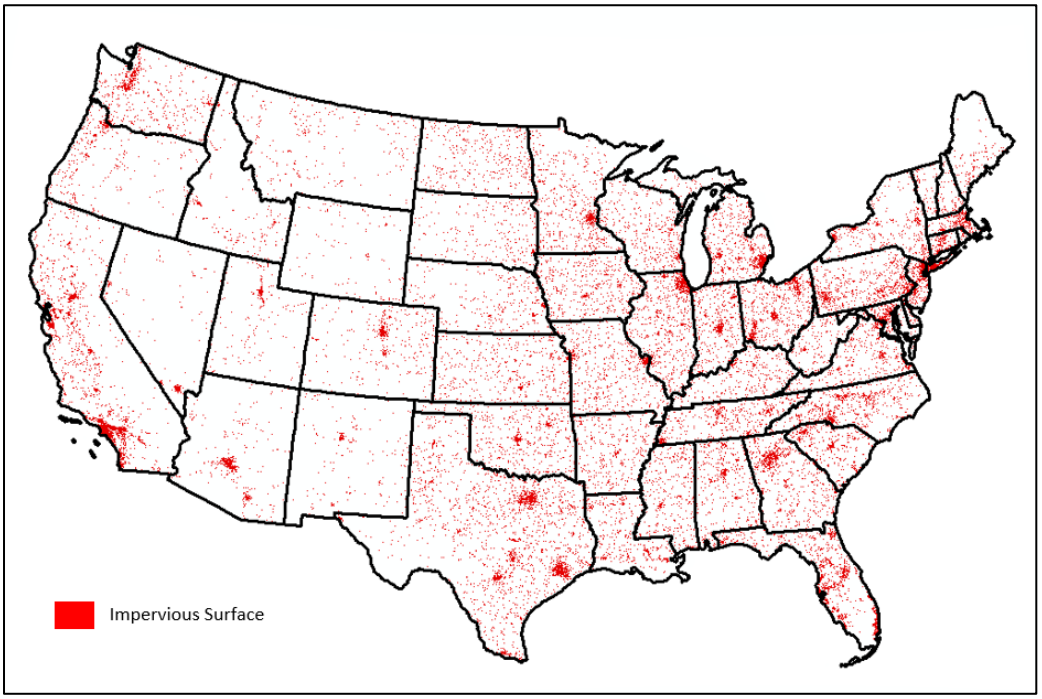

Figure 1.3: United States Developed/Impervious Surface 2011

(Reference: Homer et al., 2015)

These increases to urbanization have lasting effects on the hydrological processes of a watershed. In a natural watershed (Figure 1.4a), precipitation is distributed as either surface runoff, evapotranspiration, or infiltration into the soil. Infiltration refills underground aquifers and produces groundwater flow that seeps into streams, which makes up part of the baseflow during the dryer seasons and provides habitat for different aquatic life (USGS, 2016). However, in an urban watershed (Figure 1.4b), areas that were originally pervious and allowed precipitation to infiltrate into the soil are now covered by roadway pavements, roofs, and parking lots that prevent water from infiltrating and force most of the precipitation to become surface runoff, or stormwater (Cook and DeBell, 2002; National Research Council, 2009).

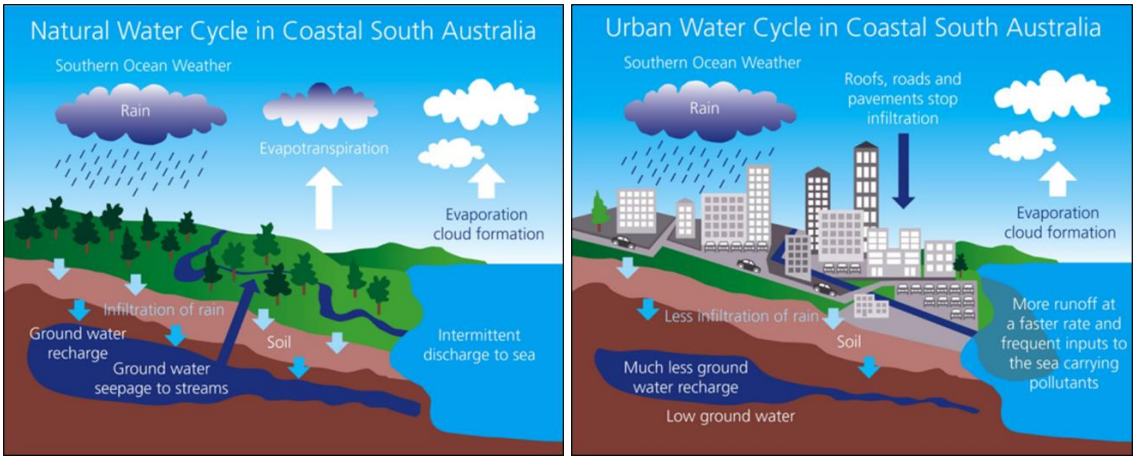

(a) **(b)**

Figure 1.4: Hydrologic/Water Cycle Diagram (Reference: EPA South Australia, 2017)

Stormwater can overwhelm a system by flooding streams and leaving negative effects on the ecology of aquatic habitat. In an urban setting it can lead to greater peak flows, smaller interflows, and sometimes a reduced baseflow by changing the natural infiltration characteristics of watersheds (US EPA, 1992). Urban stormwater can pollute waterways with oils, grease, chemicals, metals, bacteria, and nutrients; harm aquatic and wildlife habitats; cause erosion to

stream banks; contaminate food, drinking water, and recreational waterways; produce flashier hydrographs, alter channel geomorphology, increase dominance of tolerant species, and reduce biotic richness (Cook and DeBell, 2002; Walsh et al., 2005). For this reason, stormwater must be managed before it flows into bodies of water and becomes streamflow. Structural controls and drainage systems must be used to reroute the higher excess runoff and best management practices (BMPs) must be implemented to reduce excess runoff and the pollutants introduced by urban stormwater (National Research Council, 2009).

The United States Environmental Protection Agency (EPA) through the Federal Water Pollution Control Act, or the Clean Water Act (CWA), created regulations to manage the restoration and maintenance of the nation's water bodies. Through these regulations, the EPA established means to protect the quality and integrity of waterways by limiting the discharge of stormwater pollutants from point sources and nonpoint sources (Copeland, 2016). However, water quantity regulations are few and far between. Design standards may or may not require that pre-development peak flows be maintained for the post-development of a site depending on the state or locality (Galavotti, 2016; National Research Council, 2009). When these regulations are required, they are only managing one aspect of the hydrograph as baseflows and normal flow regime are not considered. This leads to major disparities in stream health across the United States as some sites may incorporate BMPs to try to maintain pre-development conditions and others may not (National Research Council, 2009). In addition, these management practices can possibly mask the effects of urbanization. By detaining streamflow or reducing peak flows through retention/detention basins or other control structures, it may seem as if the design has a neutral impact, but it affects larger basin characteristics. Seasonal floods, timing and frequency of peaks, and magnitude changes may be misrepresented at watershed stream gage observations

as stormwater is retained longer.

As development continues in the United States, there is an increasing need for a better understanding of how these urbanization impacts bring about hydrologic alterations to the water cycle and aquatic habitat within a watershed. Big data approaches using existing stream gage networks are one emerging method being used to assess anthropogenic impacts on watersheds. Long-term stream signature and hydrologic alteration analysis can quantify watershed characteristics and provide insight into the hydrologic response to change. By comparing signatures before and after urban growth, changes in the functional behavior can be understood.

Streamflow signature and hydrologic alteration analyses are typically performed using data from stream gages located at the outlet of a watershed. However, modeling methods using simulated flow values may provide more information. Stormwater managers may implement them to gather a greater understanding of conditions at different upstream tributary locations. This is especially important as these parts of the watershed stream network are the most valuable and/or threatened aspects of aquatic habitats. It is important to know whether these methods can be utilized for assessing ecological impacts as there is a potential disconnect between assessment at the gage location and assessment upstream in tributaries.

Land-cover changes have far reaching effects on a watershed. As baseflows and stream geomorphology change downstream from new developments, aquatic habitat can become degraded (National Research Council, 2009). Flow regimes must be preserved from the pre-development conditions to the post-development to prevent the loss of habitat in these ecosystems. Understanding how urban growth over long periods of time affect watershed characteristics, flow regimes, and aquatic ecosystems can provide stormwater managers valuable information for future growth and development.

1.2. Research Objectives

The following study aims to perform an investigation into streamflow to gain a better understanding of hydrologic alteration after urbanization. The specific research objectives are as follows:

- Identify urbanized and comparison watersheds in the Southeast and determine if IHA and streamflow signature analyses detect hydrologic change due to urbanization by using a before-after-control-impact approach.
- Assess the utility of IHA and streamflow signatures for identifying watersheds where urbanization has altered hydrologic dynamics and aquatic habitat.
- Use a large-scale hydrologic model to determine if analysis at a stream gage detects hydrologic alteration in upstream tributaries.

1.3. Limitations

There are a few limitations that had to be considered in the study. These limitations are as follows:

- Limited selection of continuous long term USGS streamflow and precipitation gage stations and data available for the Southeastern United States.
- The National Landcover Datasets was only produced at intervals of 5-year and 10-years for older data. Only datasets ranging from 1992 to 2011 were available for use. Updated landcover datasets on shorter intervals as well as newer data will not be available until December 28, 2019.

1.4. Organization of Thesis

The following thesis consists of five chapters. Each chapter is written and arranged with the intent to provide a clear and thorough summary of the work performed in meeting the previously outlined research objectives. Chapter 1: Introduction, gives necessary background information into urbanization and its relation to the hydrological cycle. Chapter 2: Literature Review, examines existing research and methods relating to urbanization, streamflow signatures, and hydrologic and ecologic alterations. Chapter 3: Methodology, outlines the process by which data was collected, the relevant information of each study area, and the methodologies used for the analyses. Chapter 4: Results, presents the data from the analyses and provides a detailed discussion of the findings. Chapter 5: Conclusions, examines the findings and provides recommendations for future work. After Chapter 5, the references used throughout the thesis and appendices for various data are given.

2. Literature Review

The effects of urbanization on the environment has become an emerging topic in the past decade. Multiple studies have performed in-depth analyses to explain how development affects hydrology as well as the ecology of water bodies. The following sections provide an explanation of these topics and a review of previous works.

2.1. Urbanization and Hydrology

Urbanization greatly affects the hydrological responses of a watershed by changing the natural landscape (Marsalek, 2008). In changing the land-cover of the watershed, many natural processes that help control stormwater runoff are bypassed. For example, studies have shown that when land-cover changes and vegetation is removed, evapotranspiration and infiltration will decrease whereas overland flows will increase (Maidment, 1992; Diem et al., 2017). Areas that are converted from forested to urban when compared to agricultural lands converted to urban areas see the greatest increases to stormwater runoff and streamflow as the decrease in evapotranspiration is magnified even more so (Diem et al., 2017). This is due to the increased impervious surface from parking lots, building roofs, and roadways in areas that were previously forested areas. In the case of newly grassed areas, stormwater that does not infiltrate moves rapidly as sheet flow without a barrier in place, i.e. trees and shrubs, to slow it down or soak part of it up (Rose and Peters, 2001). This leads to a more rapid response to storm events since a greater proportion of the precipitation becomes stormwater runoff, which ultimately increases peak streamflows (Rose and Peters, 2001; Schoonover et al., 2006).

In a study done by Rose and Peters, urbanized watersheds were found to have a significantly shortened recession period due to the stormwater management systems in place (Rose and Peters, 2001). Storm drains can transport runoff to streams in hours whereas undeveloped land may take days. This decrease in travel time is shown to produce flashier hydrographs when compared to more rural watersheds (Rose and Peters, 2001). The recession for urbanized watersheds can range from 1 to 2 days less than for nonurbanized watersheds (Rose and Peters, 2001). With a greater volume of stormwater discharging to streams in a shorter amount of time, peak flows and flood magnitudes for events with lower return periods easily increase (White and Greer, 2006; Hopkins et al., 2015).

In addition to increases in the peak flows, the low flow values of streams have been shown to decrease in some cases due to a lack of groundwater contribution (Rose and Peters, 2001; Wang et al., 2001). The removal of forested areas and paving over groundwater recharge areas with impervious surfaces produce consequences to groundwater recharge, storage, and discharge to streams (Rose and Peters, 2001; Schoonover et al., 2006; Barksdale and Anderson, 2015). Due to the efficiency in conveying urban stormwater to streams, surface and subsurface storage are reduced and lower long-term recharge to groundwater occurs leading to a reduction in groundwater discharge to nearby urban streams during the baseflow period (Rose and Peters, 2001). Studies show that a higher baseflow index is related to more constant flows as runoff takes longer flow paths to streams and a lower baseflow index is related to higher peak discharges and more flashiness due to increased volume and faster routing (Schoonover et al., 2006). However, it should be noted that baseflows can be increased when water is imported to urban watersheds for use in landscape irrigation (White and Greer, 2006). Therefore, urbanization commonly leads to differing peak flows, baseflows, recession periods, and total

runoff between pre- and post-development (Figure 2.1) (National Research Council, 2002).

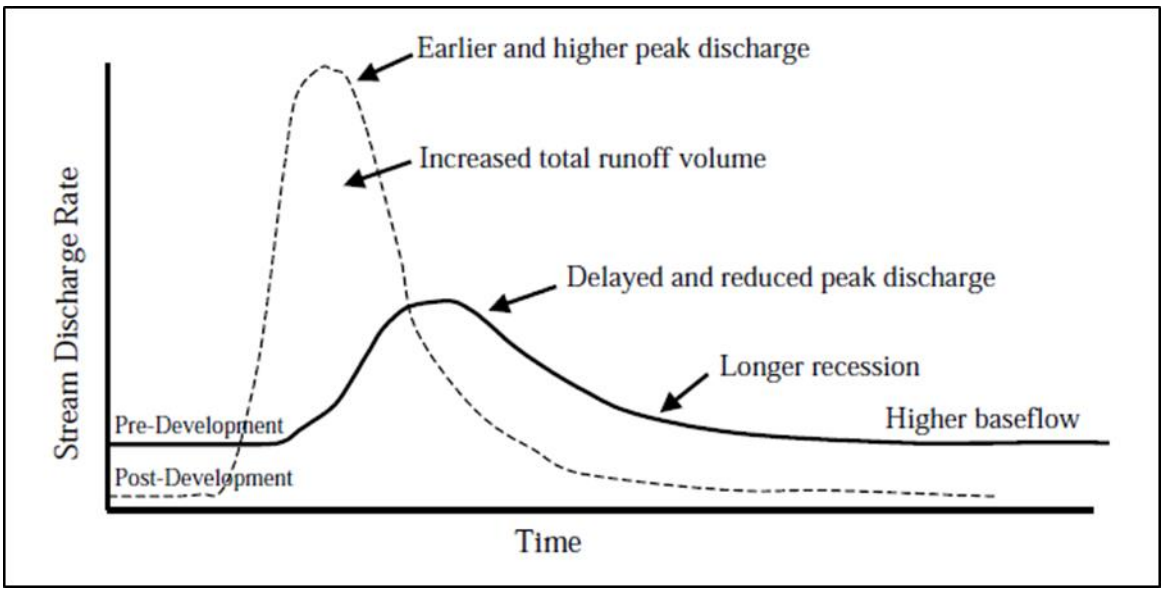

Figure 2.1: Developmental Changes to Streamflow

(Reference: National Research Council, 2002)

2.2. Streamflow Signatures

Developmental practices during urbanization may hinder the behavioral characteristics of a watershed and change the structure of the hydrograph. Big data approaches such as streamflow signature analysis can provide insight into the effect urbanization has on streamflow. By analyzing multiple watersheds, the hydrologic response to storm events can be quantified and used to look for similarity and trends across urbanized watersheds. (Yadav et al., 2007; Sawicz et al, 2011). Signatures are derived from time series data of streamflow and precipitation and have an interpretable link to watershed characteristics (Sawicz et al., 2011). These streamflow signatures do not scale with watershed size, can be applied to any watershed, and are not limited by calibration or model errors. This allows for an easier comparison between watersheds (Peel and Blöschl, 2011; Sawicz et al., 2011). The most common streamflow signatures used for

analysis are runoff ratio, flow duration curve, streamflow elasticity, and baseflow index.

The runoff ratio is the long-term ratio of runoff to precipitation for the watershed. Through its use, long-term water balance separation of streamflow and evapotranspiration exiting the watershed can be represented (Sawicz et al., 2011). A higher runoff ratio shows the system is streamflow dominated whereas a low runoff ratio represents an evapotranspiration dominated system (Sawicz et al., 2011). Studies from Sankarasubramanian and Vogel and Sawicz et al. show the runoff ratio for the southeastern United States is between 0.2 and 0.4 (Sankarasubramanian and Vogel, 2003; Sawicz et al., 2011). This makes sense as the southeastern United States has the highest regional mean annual evapotranspiration (Figure 2.2) (Sanford and Selnick, 2013).

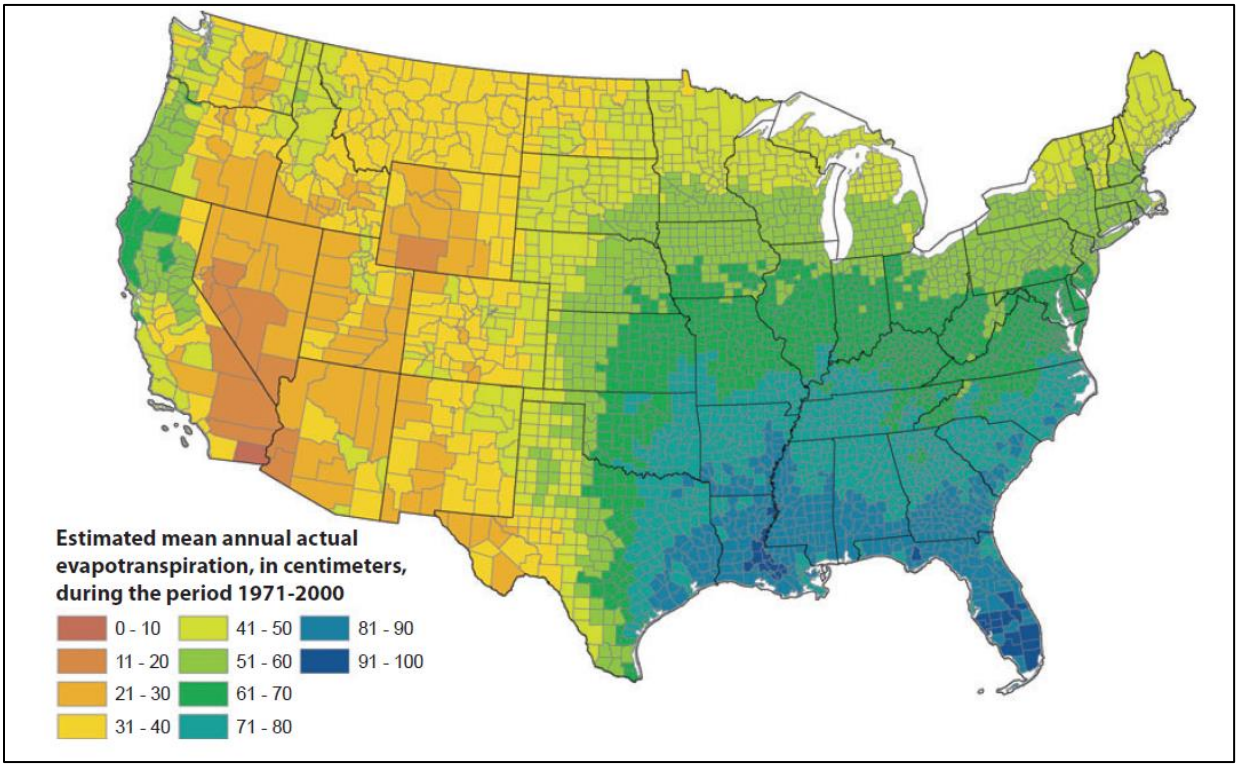

Figure 2.2: Mean Annual Evapotranspiration for the United States, 1971-2000

(Reference: Sanford and Selnick, 2013)

The flow duration curve (FDC) measures the percentage of time a flow will equal or exceed a specific value. The FDC can be used to characterize the "flashiness" of a watershed flow regime. Streams that are flashy experience rapid variations in streamflow over time (Rosburg et al., 2017). A decrease in high flows and increase in low flows dampens the flashiness of streams (Teutschbein et al., 2015). With an increase in flashiness, the slope of the flow duration curve will increase in magnitude. Urbanization has been shown to increase the flashiness of the watershed increasing magnitude of the slope of the flow duration curve (Nagy et al., 2012; Mejia et al., 2014).

Streamflow elasticity is a signature used to measure the sensitivity of streams to changes in precipitation. It represents the proportional change in streamflow to the proportional change in precipitation (Sankarasubramanian and Vogel, 2003). A study by Sankarasubramanian et al. (2007) demonstrated the usefulness of a nonparametric streamflow elasticity estimator. It produced low bias and was revealed to be just as good if not better than model-based approaches due to the lack of needing a calibration step or model assumption. The estimator is considered robust as it takes the median of the results and filters out outliers that could affect the analysis (Sawicz et al., 2011). Sankarasubramanian and Vogel (2003) showed that most streamflow elasticity values ranged from 1.0 to 2.5, which meant a 1% change in precipitation resulted in more than 1% change in streamflow.

The baseflow index is a streamflow signature used to determine the proportion of measured flow that is baseflow (Sawicz et al., 2014). To calculate the baseflow index, the baseflow must be separated from the streamflow (Dow, 2007). Previous works have developed estimators and methods to separate the baseflow from the streamflow data. The main baseflow separation methods used are the fixed-interval hydrograph separation program (HYSEP), sliding-

interval HYSEP, local minimum HYSEP, PART program, the United Kingdom Institute of Hydrology (UKIH) smoothed minima baseflow separation method, recursive digital filter technique from the program BFLOW, and recursive digital filter technique by Eckhardt (Eckhardt, 2007). Eckhardt compared these different baseflow methods and determined that the three HYSEP methods, PART, and UKIH were flawed because they utilize straight lines when connecting the data points, which would be uncharacteristic of the baseflow (Eckhardt, 2007). In addition, it was found that the recursive digital filter techniques provided smooth time series baseflow data, thus they are considered better estimators of the baseflow (Eckhardt, 2007; Rouhani and Malekian, 2013) and most closely follow experimental tracer results (Eckhardt, 2007).

2.3. Hydrologic Alterations

Increased urbanization produces changes in the hydrologic makeup of a watershed, specifically in the flow regime. These changes can be measured through another big data approach that quantifies hydrologic alteration. The best tool for measuring these alterations is the Indicators of Hydrologic Alteration (IHA) software (Richter et al., 1996; Richter et al., 1998; Schoonover et al., 2006). IHA uses a before and after approach to quantify hydrologic alterations, where time series data is divided into two periods based on an impact year (Richter et al., 1996; Richter et al., 1998). The time period before the impact year represents years where the watershed is less altered and more natural, or what is called the pre-development conditions (Richter et al., 1996). The time period after the impact year represents years where the watershed is more altered and urbanized, or the post-development conditions (Richter et al., 1996). The IHA software can provide detailed analysis of changes to flow frequency, flow magnitude, flow duration, and many other parameters useful for analyzing hydrologic alterations

(Richter et al., 1996).

Decadal-scale climate variation must be considered when using a before and after approach to assess changes in streamflow (Dale et al., 2015; Diem et al., 2017). These can result from climate phenomena such as the El Nino Southern Oscillation (ENSO) or the North Atlantic Oscillation (NAO), which drive climate fluctuations worldwide and in North America, respectively, and can results in anomalously wet or dry periods of 5-15 years. These patterns in precipitation can mask the trends in an analysis and skew results (Diem et al., 2017). To account for these effects, studies suggest using a long-term analysis approach with multiple decades of data (Rose and Peters, 2001; Diem et al., 2017). Therefore, an adequate amount of time series data must be available. Additionally, the use of a control helps deal with this issue. Change in the hydrology of an urbanized watershed due to decadal-scale climate fluctuations can be explained and verified if the specific change shows up in the control watershed as well.

2.4. Ecological Response to Urbanization

The goal of many streamflow signature and hydrologic alteration analyses is to assess the impact of urbanization on aquatic habitat. These impacts can affect the geomorphology and disturb aquatic plant and animal species habitat in streams and riparian areas (Richter et al., 1996; Walsh et al., 2005; National Research Council, 2002; White and Greer, 2006). Flow regimes act as a master variable in streams, meaning that changes can have far reaching effects on channel form, biological assemblages, and ecosystem process (Paul and Meyer, 2001). Increases in runoff frequency, volume, and peak flows put strain on the capacity of natural channels and river banks leading to increases to erosion and scouring of channel banks or channel incision (Paul and Meyer, 2001; Walsh et al., 2005). These increases can also produce flashiness, where more frequent, larger flow events have faster ascending and descending

hydrograph limbs leading to flooding downstream as storm drains transport runoff as fast as possible (National Research Council, 2002; Walsh et al., 2005). The increase in storm runoff can reduce the baseflow of the stream as well as restructure the physical and chemical makeup of the stream. This can lead to restructured biotic communities where riparian forest area and diversity and productivity of invertebrates and fish species declines (Richter et al., 1996; Wang et al., 2001; Paul and Meyer, 2001; National Research Council, 2002; Walsh et al., 2005; Barksdale and Anderson, 2015). These changes can all be correlated to increases in impervious cover, housing density, human population density, and total effluent discharge (Paul and Meyer, 2001).

Studies have shown that biological integrity and diversity is negatively correlated to the amount of urban land cover (Richter et al., 1996; Wang et al., 2001; National Research Council, 2002). Additionally, it has been shown that larger flow alterations are related to greater ecological change from the pre-development condition (Poff and Zimmerman, 2010). Certain thresholds have been found to represent trends in hydrological and ecological alteration. Wang et al. (2001) found that imperviousness levels below 8% of the total watershed area produced variable stream changes with either healthy fish communities and high baseflows or poor-quality fish communities and very low baseflows. Paul and Meyer (2001) found that imperviousness levels below 5% showed loss of sensitive fish species. Imperviousness between 5% and 15% led to a dramatic drop in maximum species numbers and biotic integrity as habitat degradation occurred and functional feeding groups are lost, and the baseflow decreased for imperviousness between 8% and 12% (Paul and Meyer, 2001; Wang et al., 2001). Anything over 15% imperviousness led to low baseflow values and severe degradation of fish communities as toxicity and organics increased. (Paul and Meyer, 2001; Wang et al., 2001; National Research

Council, 2002; Nagy et al., 2012).

Even though some management practices aim to address these issues, the majority only focus on maintaining the flow regime needed for a few targeted aquatic species instead of for the entire ecosystem of species (Richter et al., 1996). This creates a problem as biota that can thrive in these conditions or in altered conditions will replace all the other species that existed in the pre-development conditions and shift the community composition (White and Greer, 2006). The use of detention ponds and low impact development may ease the increase in flows caused by urbanization, but they will only increase the amount of urbanization a stream can take before it is degraded (Wang et al., 2001). It is also important to note that the biological community response usually lags behind changes to land use by a few years, (Wang et al., 2001). These management practices may seem to work at first until the biological community catches up to the land use changes.

Different types of biota respond to hydrologic alterations differently. A study by Poff and Zimmerman (2010) broke the different biota up into macroinvertebrates, fishes, and vegetation. The fish were the only group that was shown to respond negatively when the flows fluctuated (Poff and Zimmerman, 2010). A summary of the all the expected ecological responses from different hydrological alterations can be seen in Appendix B, Ecological Impacts.

3. Methodology

The study was performed to determine if streamflow signature and hydrologic alteration analysis of streamflow gage data is a good indicator of urbanization effects on aquatic resources in the entire watershed. It is primarily focused on the Southeastern United States and was analyzed on the watershed scale. All analyses used a water year defined as October 1st to September 30th. Multiple site locations were compiled and assessed to find locations with complete datasets of adequate length. An iterative approach was implemented for site selection, where processes were performed multiple times until ideal candidates for the study were found. Once appropriate site locations were determined, long-term streamflow signature and hydrologic alteration analyses were used to compare and quantify urbanization effects watershed characteristics. The following sections detail the methods used to perform the study and the site locations selected.

3.1. Streamflow Data

The United States Geological Survey (USGS) National Water Information System (NWIS) was used to compile streamflow data for all potential sites in the study. The USGS NWIS provides data for all streamflow gage stations on multiple time scales. Daily data was needed to accommodate the input requirements of the analyses implemented in the study. Daily average streamflow data for each gage station in Alabama and Georgia from the USGS website were assessed.

To refine the search for adequate watersheds to use for the analysis, each streamflow

gage station was investigated. The stations that had daily streamflow data going back at least to 1987 and up to 2017 were considered useful for further investigation. This allowed for the analysis of a least 30 water years, which was necessary for long term comparison. If a station met these requirements, the data was downloaded and checked for missing data points. If the number of missing data points was less than 5% of the total number of data points and missing data points did not occur in more than 10 consecutive days, the assessment continued. This was to make sure any analysis would be representative of the site and not be skewed by having too many missing data points.

For the third criterion, the days before and after the missing data points were checked to determine if the missing data was due to very large streamflow values. If the streamflow before and after the missing data points were very large, then it was an indication that the gage might not have been able to read the value because it was out of the measurement range of the instrumentation. These stations were not considered as they might be missing peak values of certain flow events and not produce an analysis that was truly representative of the site. If the values before and after the missing data points were not large, then these data points were marked as missing data and were gap filled by linear interpolation.

3.2. GIS Data

The streamflow gage stations that passed all the criteria were used for further assessment with the USGS StreamStats web application. The location of each station was used to delineate the boundary of the watershed it was associated with using the delineation tool on StreamStats producing a shapefile for the watershed. ArcMap 10.3.1 (ESRI, Redlands, CA) was used for all GIS analysis. Because most governmental agencies use the NAD83 for georeferencing purposes, all GIS data was projected to the NAD83 coordinate system (Craymer, 2006).

The National Land Cover Dataset (NLCD) from the Multi-Resolution Land Characteristics (MRLC) Consortium was used to determine land cover changes over time. The NLCD 1992/2001 Retrofit Land Cover Change dataset provides the land cover change from 1992 to 2001. Data for 1992 and 2001 were compiled by the MRLC using different methodologies, however, the retrofit dataset reclassified the datasets to the Anderson Level 1 classification scale to allow for a more accurate change comparison (Fry et al., 2009). The NLCD 2001 to 2006 Land Cover "from to" Change Index (2011 Edition) dataset is an updated dataset that indicates how each land cover classification changed from 2001 to 2006. A combined 2001/2006 land cover class index value was given to all possible class changes (Fry et al., 2011). The NLCD 2006 to 2011 Land Cover "from to" Change Index dataset shows how each land cover classification changed from 2006 to 2011. The same index for the 2001/2006 dataset was used for the 2006/2011 dataset (Homer et al., 2015). The identification numbers used to label each classification change for each dataset are provided in Appendix A, NLCD Classification Change.

These three datasets were used to assess land cover change to the urban classification for the time frames of 1992 to 2001, 2001 to 2006, and 2006 to 2011. The reclassify tool from ArcMap was used to remove all non-urban related classifications. The identification numbers for urban related classifications in each of the NLCD datasets used in the analysis are given in Table 3.1. For example, identification number 2 in the NLCD Retrofit 1992/2001 dataset represented the areas that remained urban from 1992 to 2001 and the identification number 12 in the NLCD Retrofit 1992/2001 dataset represented areas that were open water in 1992 and changed to urban by 2001. These new raster files were imported to ArcMap and overlain with the watershed shapefiles.

Table 3.1: NLCD Urban Classifications

NLCD Urban Classifications	
Dataset	**Identification Numbers**
NLCD Retrofit 1992/2001	2, 12, 23-28, 32, 42, 52, 62, 72, 82
NLCD 2001 to 2006	4-7, 21-24, 38-41, 52-119, 123-126, 140-143, 157-160, 174-177, 191-194, 208-211, 225-228, 242-245, 259-262, 276-279
NLCD 2006 to 2011	4-7, 21-24, 38-41, 52-119, 123-126, 140-143, 157-160, 174-177, 191-194, 208-211, 225-228, 242-245, 259-262, 276-279

To determine the overall change in urbanized development in each watershed, the NLCD datasets were clipped with each watershed. Once the datasets were clipped, the watershed and NLCD data were projected into the proper NAD83 Universal Transverse Mercator (UTM) Zone. This was done so the area of each pixel in the NLCD data could be calculated. The area urbanized was found by multiplying the number of cells reclassified as urbanized by the area of a cell. Next, the area of the NLCD data was divided by the total watershed area to get the percent urbanized.

3.3 Precipitation

Precipitation data was investigated for all the watersheds to determine which sites had adequate data for further analysis. Finding long-term data was a limiting factor as many gages either did not go far back enough in time or stopped recording precipitation sooner than was needed. A combination of searches with the National Oceanic and Atmospheric Administration (NOAA) National Climactic Data Center (NCDC) website, Iowa State Mesonet University Iowa Environmental Mesonet website, Weather Underground website, and USGS NWIS website provided gages with sporadic long-term data. Daily data from the Parameter-elevation

Regressions on Independent Slopes Model (PRISM) dataset (PRISM Climate Group, Orville, OR) from the Northwest Alliance for Computational Science & Engineering (NACSE) based at Oregon State University helped fill in the gaps where gages were missing data. PRISM products are the official spatial climate data sets for the United States Department of Agriculture (USDA) and can be used to create long-term climate maps for precipitation. It collects climate observations from monitoring networks, digital elevation models, and other spatial data sets to generate gridded estimates of precipitation. The gridded dataset went back to 1981, which allowed for up to 36 water years to be used in the analysis.

3.4 Watershed Selection

Watersheds were narrowed down based on the available data for streamflow, precipitation, and land cover change. Sites that had streamflow and precipitation data that met all the criteria were used for the land cover change assessment. Watersheds that had the most historical urbanization change were selected for the analysis and categorized as "Urbanized Watersheds". Watersheds that were close in proximity to the "Urbanized Watersheds" and had little to no urbanization were categorized as "Comparison Watersheds" and selected for the analysis. These watersheds were compared to the "Urbanized Watersheds" to act as a control to the study. The watersheds selected for the analysis are described in the following section.

3.4.1 Site Descriptions

Two watersheds located in Alabama in proximity to Birmingham and two watersheds located in Georgia in proximity to Atlanta were selected for further analysis in the study (Figure 3.1). The climate for each watershed was categorized as humid subtropical with mild winters and hot, humid summers. Table 3.2 summarizes the watershed identification information, where each watershed was given a unique code for use in the analysis.

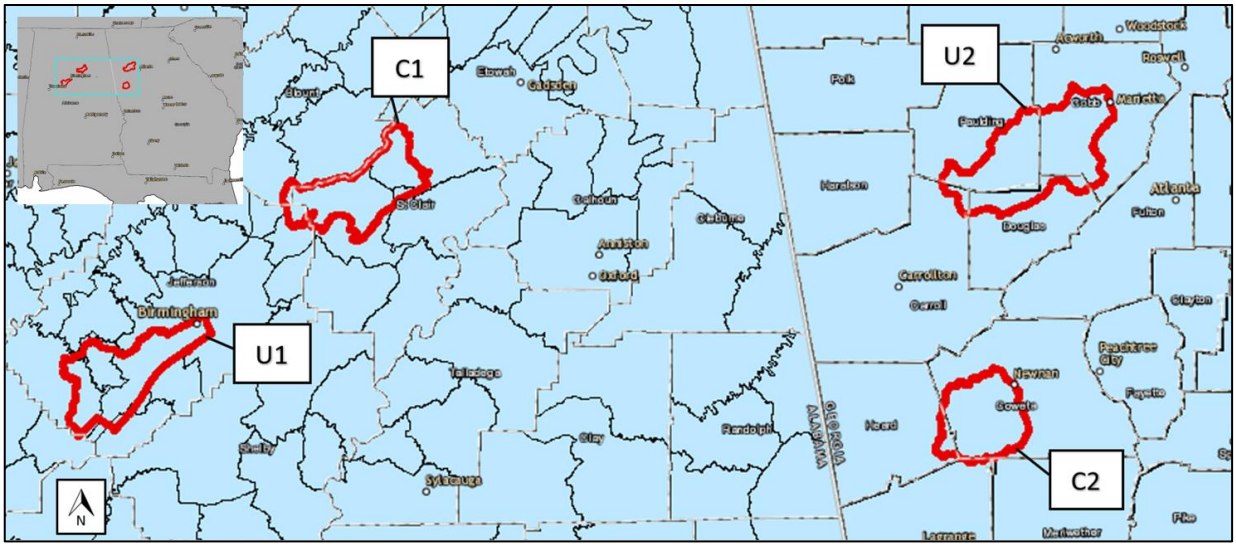

Figure 3.1: Watershed Location Map

Table 3.2: Watershed Identification Summary

Watershed Code	State	USGS Site Number	USGS Gage Location		Drainage Area (mi^2)	Comparison or Urbanized
			Latitude	Longitude		
U1	Alabama	02462000	33.44752	-87.12190	148.0	Urbanized
C1	Alabama	02401390	33.84005	-86.26276	141.0	Comparison
U2	Georgia	02337000	33.77296	-84.61415	238.0	Urbanized
C2	Georgia	02338660	33.23526	-84.98775	127.0	Comparison

Watershed U1 is located in the southwest corner of Jefferson County, Alabama, with a drainage area of 148.0 mi^2. For the water years 1982-2017, the mean annual precipitation was 56.57 inches and the mean annual temperature was 63.1°F. The land cover mostly consisted of a mixture of developed land types, deciduous forest, evergreen forest, and shrub land. The Hydrological Soil Group (HSG) breakdown in percent of watershed area was 12.49%, 34.58%, 19.80%, 31.67%, and 1.47% for A, B, C, D, and Other respectively. HSG A consisted mainly of deep, well drained to excessively drained sands and gravelly sands with high infiltration rates when wet and high rates of water transmission. HSG B consisted mostly of moderately deep, well drained soils (moderately fine to moderately coarse textures) with a moderate infiltration

rate when thoroughly wet and a moderate rate of water transmission. HSG C consisted mostly of soils having a layer that prevented downward movement of water or soils of moderately fine or fine textures with a slow infiltration rate when thoroughly wet and a slow rate of water transmission. HSG D consisted mainly of high shrink-swell potential clays and soils that have a high water table, have a claypan or clay later at or near the surface, are shallow over nearly impervious material, have a slow rate of water transmission, and have a very slow infiltration rate (high runoff potential). The Other group consisted of areas where the classification was unknown. The comparison watershed, C1, is located in the northwest corner of St. Claire County, Alabama, with a drainage area of 141.0 mi^2. For the water years 1982-2017, the mean annual precipitation was 55.23 inches and the mean annual temperature was 61.3°F. The land cover mostly consisted of open space, developed land, deciduous forest, evergreen forest, pasture/hay, and shrub land. The HSG breakdown in percent of watershed area was 2.37%, 47.44%, 17.42%, 25.22%, and 7.56% for A, B, C, D, and Other respectively. U1 and C1 were located in the Southwestern Appalachian and the Ridge and Valley physiographic regions.

Watershed U2 is located at the corners of Paulding, Cobb, and Douglas County, Georgia with the streamflow gage located in Douglas County. The drainage area of the watershed was 238.0 mi^2. For the water years 1982-2017, the mean annual precipitation was 50.48 inches and the mean annual temperature was 60.8°F. The land cover mostly consisted of a mixture of developed land types, deciduous forested, evergreen forested, pasture/hay, and a few wetlands. The HSG breakdown in percent of watershed area was 8.66%, 70.11%, 8.24%, 8.28%, and 4.71% for A, B, C, D, and Other respectively. The comparison watershed, C2, was located within the southwest corner of Coweta County, Georgia with the streamflow gage located in the southeast corner of Heard County, Georgia. The drainage area of the watershed was 127.0 mi^2.

For the water years 1982-2017, the mean annual precipitation was 50.35 inches and the mean annual temperature was 61.3°F. The land cover mostly consisted of open space developed land, deciduous forest, evergreen forest, pasture/hay, shrub land, and a few wetlands. The HSG breakdown in percent of watershed area was 0%, 95.92%, 1.13%, 0.86%, and 2.10% for A, B, C, D, and Other respectively. U2 and C2 were located in the Piedmont physiographic region.

3.5 Indicators of Hydrologic Alteration

Selected watersheds were analyzed for hydrologic alteration over time using the Indicators of Hydrologic Alteration (IHA) application from The Nature Conservancy (Richter et al., 1996). This application was used to perform a long-term hydrograph analysis of each watershed. The inputs to the application were the average daily streamflow gage data from the USGS.

The type of analysis was parametric to allow for the use of means and standard deviations. The analysis was run twice per watershed. The first analysis run used the single period option and the second run used the two-period comparison option. The single period run was used to find statistically significant trends over time for each IHA parameter. The two-period run allowed for the computation of the hydrologic alteration values and required an impact year, which was selected as the year when most of the development occurred. This year was found by looking at how satellite images from Google Earth changed during the years represented in the NLCD. The satellite images helped to narrow down when the development occurred since the NLCD was only given in 5- or 10-year intervals. Once the impact year was selected, the remainder of the analysis inputs were left as the default values and the analysis was run.

The IHA analysis produced 32 ecologically relevant hydrologic alteration parameters

(Table 3.3) (Richter et al., 1996). Inter-annual statistics were computed for each parameter using means and coefficient of variation to measure central tendency and dispersion, respectively. This produced a total of 64 inter-annual statistics to be compared between the before and after datasets.

Table 3.3: IHA Hydrologic Parameters

IHA Hydrologic Parameters		
IHA Statistics Group	**Regime Characteristics**	**Hydrologic Parameters**
Group 1: Magnitude of monthly water conditions	Magnitude Timing	Mean value for each calendar month
Group 2: Magnitude and duration of annual extreme water conditions	Magnitude Duration	Annual minima 1-day means
		Annual maxima 1-day means
		Annual minima 3-day means
		Annual maxima 3-day means
		Annual minima 7-day means
		Annual maxima 7-day means
		Annual minima 30-day means
		Annual maxima 30-day means
		Annual minima 90-day means
		Annual maxima 90-day means
Group 3: Timing of annual extreme water conditions	Timing	Julian date of each annual 1 day maximum
		Julian date of each annual 1 day minimum
Group 4: Frequency and duration of high and low pulses	Magnitude Frequency Duration	No. of high pulses each year
		No. of low pulses each year
		Mean duration of high pulses within each yea
		Mean duration of low pulses within each year
Group 5: Rate and frequency of water condition changes	Frequency Rate of Change	Means of all positive differences between consecutive daily means
		Means of all negative differences between consecutive daily values
		No. of rises
		No. of falls

The significance test in the single period run showed the parameters that exhibited statistically significant trends over the time period and were useful for investigation in the two-period run. The hydrologic alteration values found in the two-period runs were determined using the Range of Variability Approach (RVA). This approach is used to guide efforts in restoring or maintaining the natural streamflow regime of a river (Richter et al., 1998). A desirable outcome would attain the same flow frequencies in each targeted range (Low, Middle, and High RVA Categories) as the pre-development conditions in the period before the impact year. The Hydrologic Alteration (*HA*) value was determined using Equation 3.1, where the observed value (*O*) was the count of years that fell within the target range and expected (*E*) was the count of years expected to fall within the target range. Expected values were defined as the values in the pre-impact period and the observed values were defined as the values in the post-impact period.

$$HA = \frac{O-E}{E} \qquad \text{(Equation 3.1)}$$

A positive hydrologic alteration value indicates that the frequency in that category was increasing, whereas a negative value indicated that the frequency was decreasing. The three categories (or target ranges) for the RVA were the Low RVA, Middle RVA, and High RVA. The target range boundaries were set to the mean plus or minus the standard deviation for each parameter analyzed. Therefore, the Low RVA included values less than -1 standard deviation, the Middle RVA ranged from -1 to +1 standard deviation, and the High RVA included values greater than +1 standard deviation. For the low flows or minimum parameters, the Low RVA frequencies and hydrologic alterations were inspected; for the peak flows or maximum parameters, the High RVA frequencies and hydrologic alterations were inspected.

3.6 Streamflow Signature Analysis

Watersheds were then analyzed using a streamflow signature analysis. To perform this analysis, a MATLAB code was written to allow for the input of USGS streamflow gage station data and PRISM precipitation data.

The code was used to calculate the streamflow signatures chosen from those given in Yadav et al. (2007). These included the runoff ratio, slope of the flow duration curve, streamflow elasticity, and baseflow index. Streamflow signatures are used because they are uncorrelated, do not scale with catchment size, and have an interpretable link to watershed function (Sawicz et al., 2011). They are intended to better understand and quantify the hydrologic response to changes in watersheds and allow comparison of watersheds across a range of sizes. The following sections give further information for each streamflow signature.

3.6.1 Runoff Ratio

The runoff ratio (R_{QP}) is the proportion of precipitation that becomes streamflow in the watershed over the duration of the analysis:

$$R_{QP} = \frac{Q}{P} \qquad \text{(Equation 3.2)}$$

where Q is the long-term mean streamflow and P is the long-term mean precipitation (Sawicz et al., 2011). To determine average streamflow, the mean streamflow values were determined for each water year of the analysis. Then the mean of the water year values was taken to find Q. The long-term mean precipitation was found in the same manner. Runoff ratio shows how much water exits a watershed as streamflow and how much exits as either groundwater or evapotranspiration. Watersheds with a high runoff ratio will have a large amount of water exiting as streamflow, whereas a low runoff ratio shows a large amount exiting as groundwater or evapotranspiration (Sawicz et al., 2011). Runoff ratio would be expected to increase over

time with an increase in urbanization. The increase in impervious surface from development should produce more runoff as there is less area for the precipitation to infiltrate into the soil. However, stormwater management like detention or retention facilities may affect this signature by controlling the amount of runoff allowed to be discharged into streams.

3.6.2 Slope of the Flow Duration Curve

The flow duration curve is the cumulative distribution function of daily streamflow subtracted from 1, giving the probability that a streamflow value will be equaled or exceed at a randomly selected time. The slope of the flow duration curve (S_{FDC}) is used as an indicator of flow variability over time (Sawicz et al., 2014):

$$S_{FDC} = \frac{\ln(Q_{33\%}) - \ln(Q_{66\%})}{(0.66 - 0.33)} \quad \text{(Equation 3.3)}$$

where $Q_{33\%}$ is the 33rd percentile streamflow and $Q_{66\%}$ is the 66th percentile streamflow (Sawicz et al., 2011). A S_{FDC} value that is high in magnitude represents a flow regime that is very flashy, whereas a value with a low magnitude represents a flow regime that is more damped. Regimes that are more damped will show that precipitation is more year-round or have a large contribution of groundwater to streamflow (Sawicz et al., 2011). The flow duration curve is expected to increase in magnitude of flow at the higher percentages because of the increase in impervious surface and changes to hydrologic routing of stormwater (Rosburg et al., 2017). This increase would result in a decreased slope value as the bottom half of the plot shifts to the right.

3.6.3 Streamflow Elasticity

The streamflow elasticity shows a watershed's sensitivity to precipitation changes. It is defined as the proportional change in streamflow divided by the proportional change in precipitation (Sankarasubramanian et al., 2001). The equation for streamflow elasticity is given

by (Sawicz et al., 2011):

$$E_{QP} = \text{median}\left(\frac{dQ}{dP}\ \frac{P}{Q}\right) \quad \text{(Equation 3.4)}$$

where,

dQ = difference between previous year and current year streamflow

dP = difference between previous year and current year precipitation

Q = mean annual streamflow

P = mean annual precipitation

Median is a non-parametric estimator used in the calculation to describe the streamflow elasticity. Research done by Sankarasubramanian et al. (2001) and Sankarasubramanian and Vogel (2003) has demonstrated that using median to estimate streamflow elasticity has low bias, does not need model assumptions or a calibration method, and is as good as model-based approaches (Sankarasubramanian et al., 2001; Sankarasubramanian and Vogel, 2003). A streamflow elasticity value of 1 means that for every 1% change in precipitation there will be a 1% change in streamflow (Sawicz et al., 2011). Urbanized watersheds are thought to increase runoff volume and velocity as the infiltration and baseflow is decreased and make them less stable and flashier. However, stormwater management facilities may alter this.

3.6.4 Baseflow Index

The baseflow index represents the portion of the streamflow that is baseflow, which is the low flow in a stream during dryer weather (Sawicz et al., 2014). The higher the baseflow index, the higher the baseflow contribution to a system. It allows for the measurement of how much water is taking longer flow paths through the watershed (Sawicz et al., 2014). The equations used to solve for the baseflow index are

$$Q_{Dt} = cQ_{Dt-1} + \frac{1+c}{2}(Q_t - Q_{t-1}) \quad \text{(Equation 3.5)}$$

$$Q_{Bt} = Q_t - Q_{Dt} \quad \text{(Equation 3.6)}$$

$$BFI = \sum \frac{Q_B}{Q} \quad \text{(Equation 3.7)}$$

where,

BFI = Baseflow Index

c = 0.925

Q_t = Total flow at time step t

Q_{t-1} = Total flow at time step t-1

Q_{Dt} = Direct Flow at time step t

Q_{Dt-1} = Direct Flow at time step t-1

Q_{Bt} = Baseflow at time step t

Q_{Bt-1} = Baseflow at time step t-1

The one parameter single pass digital filter method from Lim et al. (2005) was used to solve for the direct flow values. Research done by Eckhardt (2008) proved a value of 0.925 for parameter *c* was sufficient. An estimate of 25% of the long-term average streamflow was used for Q_{Dt-1} and an estimate of 75% of the long-term average streamflow was used for Q_{t-1}. BFI is expected to decrease over time with an increase in urbanization. The increase in impervious surface is thought to decrease the amount of water taking the longer flow paths in the watershed.

3.6.5 Baseflow Index Comparison

After the baseflow index for each watershed was determined from the MATLAB code, the results were compared to other baseflow index methods. The Groundwater Toolbox software from USGS was used to calculate baseflow separation and baseflow index for the fixed-interval hydrograph separation program (HYSEP), sliding-interval HYSEP, local minimum HYSEP, PART program, the United Kingdom Institute of Hydrology (UKIH) smoothed minima baseflow separation method, recursive digital filter technique BFLOW, and recursive digital filter technique by Eckhardt. If the baseflow index calculated from the MATLAB code was close to the other methods, then it was acceptable.

3.7 Comparison

After the watersheds were analyzed using the IHA application and MATLAB code, the results for each watershed were compared. The differences in streamflow signatures and hydrologic alteration values were used to determine how the different tools characterized the effect of urbanization on watershed hydrology as well as how effective stormwater management was to maintain pre-development streamflow conditions.

3.8 HEC-HMS Model

A hydrologic model was created using the HEC-HMS 4.2.1 software from the United States Army Corps of Engineers and the data for watershed U1. The goal was to create a model that was representative of the watershed before the impact year and after the impact year to determine if streamflow signature and IHA analysis performed with stream gage data reflect impacts throughout the watershed. The following steps were followed to create the model and run the analysis.

3.8.1 Model Setup with ArcGIS

Before the HEC-HMS software could be used, an HMS project had to be created using ArcGIS. The ArcHydro and GeoHMS toolboxes were used to process input data. The software required Soil Conservation Service (SCS) curve number grid data, digital elevation model (DEM) grid data, and National Hydrography Dataset (NHD) data to create the HMS project. All data was clipped to the U1 watershed boundary before manipulation.

The SCS curve number grid was created from Soil Survey Geographic Database (SSURGO) soils data, NLCD grid data, and DEM grid data. The SSURGO soils data were download from the Web Soil Survey website run by the National Resource Conservation Service (NRCS). This data provided the most detailed digital soils information for the desired area of

interest. It was used to determine the hydrologic soil group (HSG) of each cell in the SCS curve number grid. The component table from the downloaded SSURGO database was joined to the soils polygon attribute table to pull the HSG information. All "null" values were replaced with HSG C because most of the watershed had type C soils. The DEM grid data and the NHD data were downloaded from the USGS National Map Viewer and Download Platform and in the format of "1/3 arc-second DEM" and "ArcGrid" and of HUC-8 subbasin and shapefile, respectively. NLCD for land use classification was reclassified using the reclassify tool in ArcMap to group similar land uses. The revised classifications can be seen in Table 3.3, where 4 classifications were created.

Table 3.3: NLCD Reclassification

Original NLCD classification		**Re-classification**	
Number	**Description**	**Number**	**Description**
11	Open water	1	Water
90	Woody wetlands		
95	Emergent herbaceous wetlands		
21	Developed, open space	2	Developed
22	Developed, low intensity		
23	Developed, medium intensity		
24	Developed, high intensity		
41	Deciduous forest	3	Forest
42	Evergreen forest		
43	Mixed forest		
31	Barren land	4	Agricultural
52	Shrub/Scrub		
71	Grassland/herbaceous		
81	Pasture/hay		
82	Cultivated crops		

The union tool in ArcMap was used to merge the revised SSURGO soils data and the reclassified NLCD data into one soil landuse polygon. A curve number lookup table (Table 3.4) was created using the SCS TR-55 manual to associate the curve number to the corresponding

landuse and HSG. The Create CN Grid tool from the HEC-GeoHMS toolbox in ArcMap along with the soil landuse polygon, curve number lookup table, and DEM data were used to create the curve number grid.

Table 3.4: Curve Number Lookup Table

Curve Number Lookup Table					
Number	**Description**	**A**	**B**	**C**	**D**
1	Water	100	100	100	100
2	Developed	57	72	81	86
3	Forest	30	58	71	78
4	Agricultural	67	77	83	87

The ArcHydro toolbox in ArcMap was used to perform terrain preprocessing of the watershed for the HEC-HMS. Various raster and vector data were created from the DEM and NHD data using the tools in the terrain preprocessing tab. The DEM data was reconditioned and sinks in the elevation were filled in. Outputs from this process were a flow direction grid, flow accumulation grid, stream definition grid, stream link grid , catchment delineation grid, watershed slope grid, catchment polygon, drainage line polygon, and adjoint catchment polygon. The stream definition grid determined how many cells were used to define the stream. A stream threshold of 20,000 cells was used, which allowed for delineation of the smaller upstream tributaries for the analysis.

The HEC-GeoHMS toolbox in ArcMap was used to create the HEC-HMS project file. The outlet point of the watershed was defined by the USGS gage station for watershed U1 and the curve number grid was used as a subbasin parameter. The SCS method was used for the loss method and transform method as they were the easiest to model in HEC-HMS given the data available. The baseflow method was defined as recession, which uses standard baseflow separation techniques to develop an exponentially declining baseflow (USACE, 2000). It is

derived from Equation 3.8 and represents drainage from natural storage in the watershed (USACE, 2000).

$$Q_t = Q_0 k^t \quad \text{(Equation 3.8)}$$

Where,

Q_t = Baseflow at any time t

Q_0 = Initial Baseflow at time zero

k = exponential decay constant (recession constant)

t = time

River routing followed the Muskingum method as it was the simplest to calibrate given the large number of subbasins. This method is derived from Equation 3.9, where the outflow is determined from the Muskingum *K* and *X* values.

$$O_t = \left(\frac{\Delta t - 2KX}{2k(1-X)+\Delta t}\right) I_t + \left(\frac{\Delta t + 2KX}{2k(1-X)+\Delta t}\right) I_{t-1} + \left(\frac{2K(1-X)-\Delta t}{2k(1-X)+\Delta t}\right) O_{t-1} \quad \text{(Equation 3.9)}$$

Where,

K = Travel time of the flood wave through routing reach, hours

X = Dimensionless weight, $0 \leq X \leq 0.5$

I_t = Inflow at time t

O_t = Outflow at time t

Δt = Change in time

The calculated basin characteristics were river length, river slope, basin slope, longest flowpath, basin centroid, centroid elevation, centroid longest flowpath, and curve number lag. The precipitation gage data for U1 was used to create the met model file, and the HMS tools tab was used to export the project from ArcMap to the HMS file type.

3.8.2 HEC-HMS Model Inputs

The model files were imported to the HEC-HMS software where the curve number, impervious percentage, area, and lag time were extracted from the ArcMap data. The initial

Muskingum *K* and *X* terms were 1.0 hours and 0.2, respectively. These were selected based on typical Muskingum values for use in the first trial run. The initial baseflow recession constant was 0.979, which was determined from the Groundwater Toolbox software from the USGS by using baseflow separation techniques. The precipitation data in the meteorological model was set to specified hyetograph and each subbasin was paired with the precipitation gage data. Time series were created for the precipitation gage and the discharge gage. The precipitation gage data was in inches and the discharge gage data was in cfs with a time interval of 1 day. The time series data in the first trial run was from a few years during the before impact year time period. The control specifications for the trial were setup to have a starting date and time equal to the time series data. The time interval for the control specifications had to be less than the lag time to prevent errors in the analysis.

3.8.3 HEC-HMS Model Calibration

The HEC-HMS model was calibrated before further analysis. This was done through the optimization run manager, where parameters were varied across each subbasin until they produced flows that fit the observed flow values. The program automatically adjusted the parameters so that the optimal values were reported. The Sum of Squared Residuals (SSR) method was used as the objective function (error) because it gave more weight to large errors than to small errors (Equation 3.10) (USACE, 2000). The univariate gradient method was used for the parameter search method because it evaluated and adjusted one parameter at a time.

$$SSR = \sum_{t=1}^{N} (Q_O(t) - Q_C(t))^2 \qquad \text{(Equation 3.10)}$$

Where,

Q_O = Observed Flow

Q_C = Calculated Flow (Model)

The Muskingum *K* and *X* values, Initial Baseflow, Baseflow Recession Constant, Baseflow Ratio to Peak, and Initial Abstraction were optimized in each reach and subbasin to calibrate the simulated flows, volumes, and time to peak terms. The observed flows and simulated flows were compared using the flow comparison plot. If the curves were close, then the scatter graph was inspected. The closer the data points were to a 1 to 1 line on the scatter graph, the better the calibration was. The flow residuals plot was used as well to determine goodness of fit. If the residuals were minimized (closer to zero) then it was representative of a good calibration. The objective function (error) plot showed the error across each iteration step. If the error leveled off after the last few iterations in the optimization run, then the model represented the observed flows well. These plots were used to help fit parameter values after each trial during calibration.

Once optimal values were found, the model performance was evaluated using goodness of fit statistics for watershed simulations (Moriasi et al., 2007; Ouédraogo et al., 2018). The Percent Error in Volume (PEV), Percent Error in Peak Flow (PEPF), Correlation Coefficient (R^2), Nash-Sutcliffe model Efficiency (NSE), and Root Mean Squared Error (RMSE) Standard Deviation Ration (RSR) were calculated and compared to the performance ratings outlined by Moriasi et al. (2007) (Table 3.5).

$$PEV = \left|\frac{Vol_O - Vol_S}{Vol_O}\right| \times 100 \qquad \text{(Equation 3.11)}$$

Where,

V_O = Observed Volume

V_S = Simulated Volume (Model)

$$PEPF = \left|\frac{Q_{O,Peak} - Vol_{S,Peak}}{Vol_{O,Peak}}\right| \times 100 \qquad \text{(Equation 3.12)}$$

Where,

$Q_{O,\ Peak}$ = Observed Peak Flow

$Q_{S,\ Peak}$ = Simulated Peak Flow (Model)

$$R^2 = \left[\frac{\sum_{t=1}^{n}(O_i - \bar{O}) \times (S_i - \bar{S})}{\sqrt{\sum_{t=1}^{n}(O_i - \bar{O})^2 \times \sum_{t=1}^{n}(S_i - \bar{S})^2}}\right]^2 \quad \text{(Equation 3.13)}$$

Where,

O_i = Observed Flow at time t

S_i = Simulated Flow at time t

$\bar{O}$ = Average Observed Flow

$\bar{S}$ = Average Simulated Flow

$$NSE = \frac{\sum_{t=1}^{n}(O_i - \bar{O})^2 \times \sum_{t=1}^{n}(S_i - \bar{S})^2}{\sum_{t=1}^{n}(O_i - \bar{O})^2} \quad \text{(Equation 3.14)}$$

$$RSR = \frac{RMSE}{ST.Dev._{obs}} = \frac{\sqrt{\sum_{t=1}^{n}(O_i - S_i)^2}}{\sqrt{\sum_{t=1}^{n}(O_i - \bar{O})^2}} \quad \text{(Equation 3.15)}$$

Table 3.5: Calibrated Model Performance Ratings

Calibrated Model Performance Ratings					
Performance Rating	**PEV (%)**	**PEPF (%)**	**R^2**	**NSE**	**RSR**
Very good	< ± 10	< 15	0.75 to 1	0.75 to 1	0 to 0.50
Good	± 10 to ± 15	15 to 30	0.65 to 0.75	0.65 to 0.75	0.50 to 0.60
Satisfactory	± 15 to ± 25	30 to 40	0.50 to 0.65	0.50 to 0.65	0.60 to 0.70
Unsatisfactory	> ± 25	> 40	< 0.50	< 0.50	> 0.70

3.8.4 HEC-HMS Model Validation

The HEC-HMS model was validated by using data from a different set of years during the before time period. The goal was to achieve relatively the same degree of accuracy in the simulation as the calibration step. The model was run with all the same parameters from the calibration step and again the variation in observed and simulated hydrographs were checked.

The validation included the same goodness of fit statistics and performance criteria comparison. If the simulated data fit the observed data, then the model was validated.

3.8.5 HEC-HMS Model Comparison

The HEC-HMS model was used to simulate flows based off data from the before impact year time period and after impact year time period. These results were used to reproduce the IHA and streamflow signature analysis. The resultant values were compared to the before and after results from the original analyses to determine the effectiveness of HEC-HMS to model the upstream tributaries.

4. Results & Analysis

The results of the study are presented in this chapter. The streamflow signature and IHA analysis were run using data from the four selected watersheds. The results were compared to determine if the effects urbanization were detected by these analysis methods. The HEC-HMS model analysis was conducted for watershed U1 to determine if streamflow signatures and IHA analysis capture the impact of urbanization on small headwater streams.

4.1. Analysis Input Data

The USGS NWIS streamflow gage data for each watershed was compiled and all missing data was gap filled through linear interpolation. The precipitation gage data was a limiting factor in the data collection phase as the few gauges available with long term data were sparse and incomplete. To overcome this limitation the PRISM precipitation product was used to help fill the gaps in these datasets. In addition, for watershed C2, a precipitation gage just outside the watershed was used to fill in missing data as it had a more complete record. A time frame of water year 1982 to 2017 was selected for the streamflow signature analysis. However, since the IHA analysis did not require precipitation data, a longer time frame of water year 1979 to 2017 could be used. This allowed for 36 years in the streamflow signature analysis and 40 years in the IHA analysis, which is long enough to cover any decadal-scale climate variations (Rose and Peters, 2001; Dow, 2007; Diem et al., 2017). Watershed boundaries with stream and precipitation gage locations can be seen in Figure 4.1, Figure 4.2, Figure 4.3, and Figure 4.4.

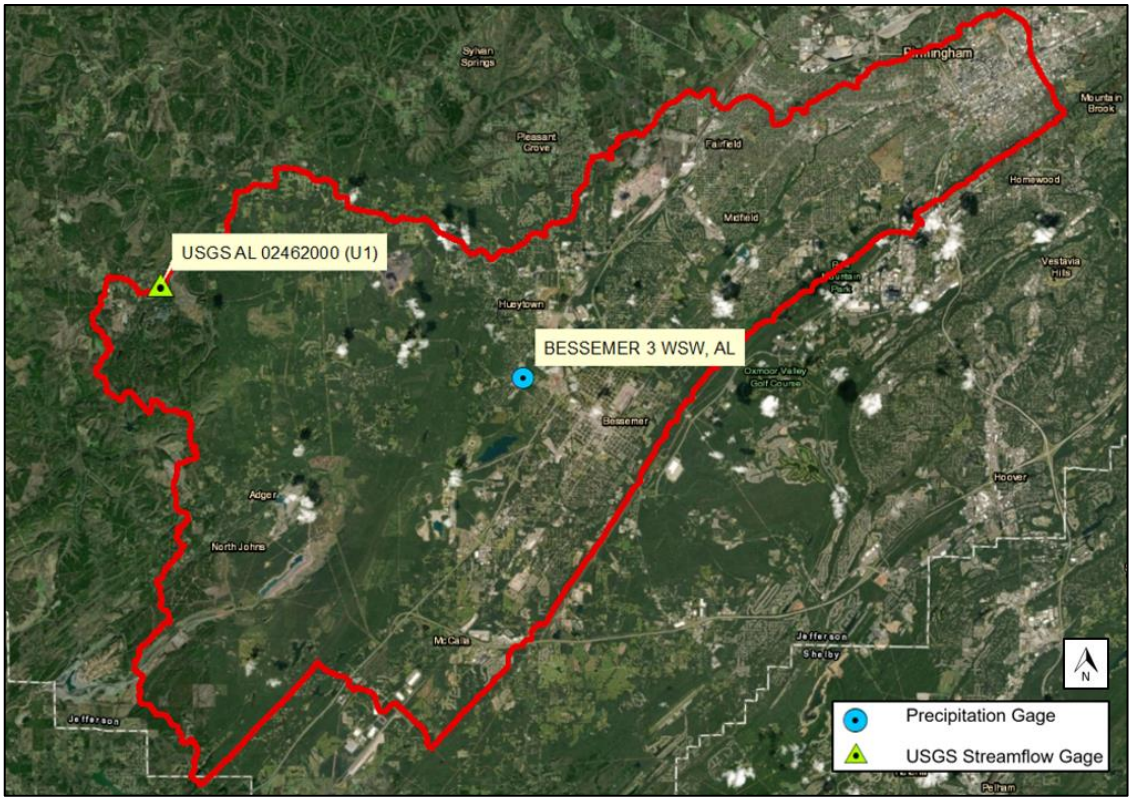

Figure 4.1: Watershed U1 Ariel View

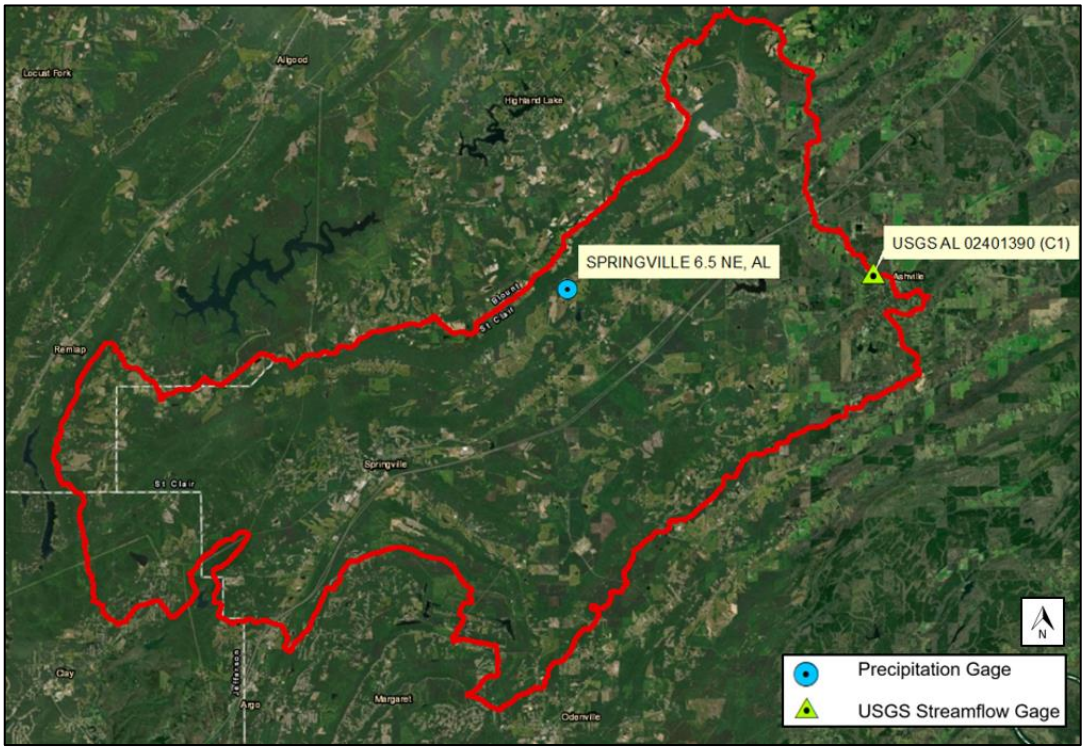

Figure 4.2: Watershed C1 Ariel View

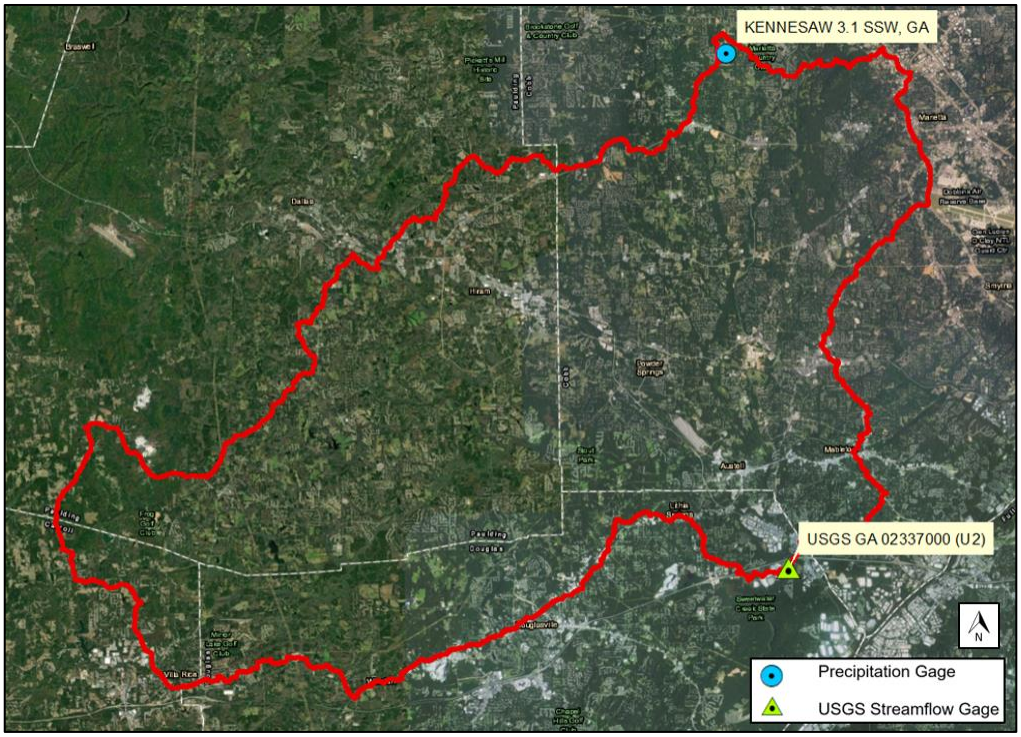

Figure 4.3: Watershed U2 Ariel View

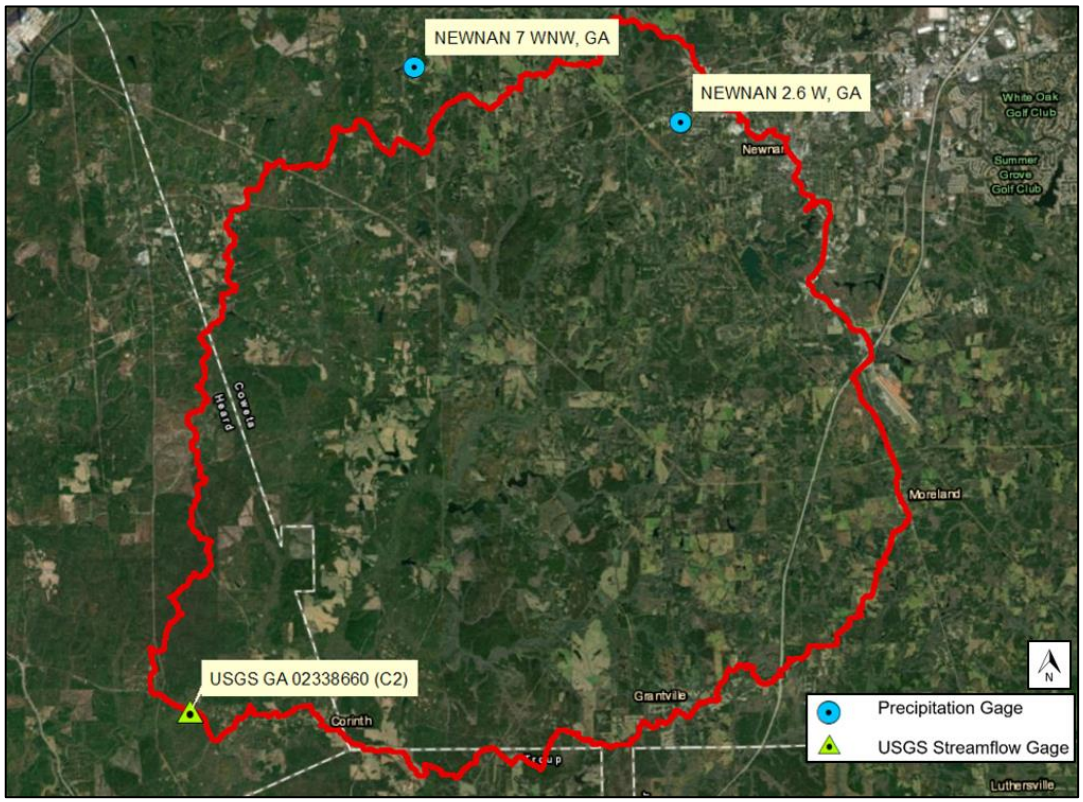

Figure 4.4: Watershed C2 Ariel View

The NLCD was used to determine when the greatest increase in urbanization occurred. The datasets were limited because they only presented information in 5- or 10-year intervals. Google Earth satellite images helped to narrow down the search to a yearly scale, but this was only through a qualitative analysis. ArcGIS was used to calculate the area of urbanization change and percent increase compared to the watershed size. The results can be seen in Appendix A, NLCD Urbanization Area Change Comparison. The majority of the change for NLCD 1992 to 2001 came from forest areas being converted to urban areas. The majority of the change in the NLCD 2001 to 2006 and NLCD 2006 to 2011 came from areas being converted from forest to urban or pasture and hay to urban. These changes are associated with a decrease in interception and travel time for runoff with less pervious surfaces and plant biota present in the watershed.

The NLCD 1992 to 2001 had the greatest change in urban area and percent increase in urbanization. For watershed U1, the urban area change was 2.12 mi^2 and the percent increase based off the 148 mi^2 watershed was 1.42%. For watershed U2, the urban area change was 12.15 mi^2 and the percent increase was 5.10% of the 238 mi^2 watershed (Table 4.1). Therefore, qualitative inspection of Google Earth satellite images was performed from 1992 to 2001. The most visible change in landscape occurred during 1995 and 1996 for both watersheds, where the majority of urban change was observed to be forested areas converted to suburban/residential or medium intensity commercial.

Table 4.1: NLCD Urbanization Change Comparison

Urbanization Change			
	NLCD 1992-2001	**NLCD 2001-2006**	**NLCD 2006-2011**
U1 Urban Change Area (mi^2)	2.12	2.04	0.96
U2 Urban Change Area (mi^2)	12.15	11.73	4.00
U1 Urbanization Increase	1.42%	1.37%	0.65%
U2 Urbanization Increase	5.10%	4.92%	1.68%
C1 Urban Change Area (mi^2)	0.37	0.52	0.08
C2 Urban Change Area (mi^2)	0.45	0.58	0.05
C1 Urbanization Increase	0.25%	0.35%	0.05%
C2 Urbanization Increase	0.31%	0.39%	0.04%

4.2. IHA Analysis Results

The IHA analysis was run using the single period parametric option first to test parameters for a significant trend in time. The analysis was ran using the water years 1982 to 2017. A significance level of 0.05 was used to test for the significance of the parameter mean values. The p-values obtained from IHA that were less than or equal to the significance level (p-value ≤ 0.05) were considered to be statistically significant. The significant results of the single period analysis can be seen below for each watershed, where statistically significant values were highlighted.

Table 4.2: IHA Single Period Parameter P-Values

IHA Parameter Significance Test				
	U1	**C1**	**U2**	**C2**
IHA Parameter	**P-Value**	**P-Value**	**P-Value**	**P-Value**
1-day minimum	0.025	0.5	0.25	0.05
3-day minimum	0.025	0.5	0.25	0.05
7-day minimum	0.025	0.5	0.25	0.025
30-day minimum	0.25	0.5	0.25	0.005
90-day minimum	0.25	0.5	0.25	0.1
1-day maximum	0.05	0.5	0.5	0.25
3-day maximum	0.05	0.5	0.5	0.25
7-day maximum	0.05	0.5	0.5	0.5
30-day maximum	0.05	0.25	0.5	0.25
90-day maximum	0.05	0.25	0.5	0.5
Extreme low peak	0.1	0.25	0.25	0.05
Extreme low freq.	0.01	0.5	0.005	0.01
High flow peak	0.25	0.5	0.5	0.005
High flow frequency	0.5	0.5	0.5	0.5

The majority of the parameters for U1 were statistically significant showing there was a difference in the means across this time frame. The single period run for C1 did not produce any meaningful parameters with statistical significance, which showed there was not a significant change in the hydrology for this comparison watershed. These results were of value because they showed that the urbanized watershed showed some significant change over time and the comparison watershed remained relatively constant.

The opposite situation occurred in the U2 and C2 watersheds. The p-values for the IHA parameters in the single period run were not statistically significant except for the extreme low flow frequency, where the p-value was significant to the 0.05 significant level. However, p-values for C2 were significant for the 1-, 3-, 7-, 30-day minimum flows, the extreme low flow peak and frequency values, and the high flow peak value. A significant change occurred in the low flows of C2 that was not represented in U2. This was of value because as the comparison

watershed exhibited a change, the urbanization in U2 apparently kept this change from taking place. Therefore, U2 was prevented from following the natural trend that should have taken place if it were not for the disturbance of urbanization.

The results from the single period analysis were used as guidance for the hydrologic alterations measured in the two-period analysis. He two-period analysis was ran using water years 1982 to 1995 for the pre-impact period and water years 1996 to 2017 for the post-impact period. The 32 indicators of hydrologic alteration, or parameters, were calculated for each watershed and can be seen in Appendix B, IHA Parameter Significance Test. Only the statistically significant parameters were analyzed further. The means and coefficient of variation (CV) were used to determine central tendency and dispersion of the parameters. The results for before and after the impact year were determined and presented in Table 4.3, Table 4.4, Table 4.5, and Table 4.6 for U1, C1, U2, and C2, respectively.

Table 4.3: IHA Two Period Parameter Means and CV for U1

U1	IHA Two Period Analysis			
	Mean (cfs)		Coefficient of Variation	
IHA Parameter	Pre-Impact	Post-Impact	Pre-Impact	Post-Impact
1-day minimum [2]	61.9	68.8	27.3%	20.0%
3-day minimum [2]	65.7	74.0	25.8%	16.1%
7-day minimum [2]	70.1	78.3	23.1%	16.0%
30-day minimum	88.3	96.5	22.5%	18.8%
90-day minimum	125	149	32.7%	31.9%
1-day maximum [1]	5981	4513	87.2%	43.9%
3-day maximum [1]	3545	2647	90.1%	41.7%
7-day maximum [1]	2121	1630	82.6%	34.0%
30-day maximum [1]	971	817	53.1%	29.4%
90-day maximum [1]	649	564	43.6%	22.0%
Extreme low peak	69.9	72.7	9.6%	6.6%
Extreme low freq. (Unitless) [3]	7.35	4.68	77.2%	86.8%
High flow peak	964	861	23.2%	24.2%
High flow freq. (Unitless)	19.4	19.9	30.6%	26.4%

Note: [1] Indicates $p < 0.05$ [2] Indicates $p < 0.025$ [3] Indicates $p < 0.01$
[4] Indicates $p < 0.005$

Table 4.4: IHA Two Period Parameter Means and CV for C1

C1	IHA Two Period Analysis			
	Mean (cfs)		Coefficient of Variation	
IHA Parameter	Pre-Impact	Post-Impact	Pre-Impact	Post-Impact
1-day minimum	15.4	15.7	26.7%	42.2%
3-day minimum	15.7	16.2	26.9%	42.0%
7-day minimum	16.6	16.8	30.2%	41.4%
30-day minimum	21.0	21.1	29.1%	48.4%
90-day minimum	48.8	52.7	63.7%	80.1%
1-day maximum	4987	5450	41.5%	43.1%
3-day maximum	3330	3665	41.1%	46.4%
7-day maximum	2017	2090	39.2%	42.9%
30-day maximum	923	873	43.1%	34.8%
90-day maximum	620	560	39.7%	30.6%
Extreme low peak	17.2	15.8	10.9%	25.6%
Extreme low freq. (Unitless)	4.35	3.14	86.7%	103.8%
High flow peak	1033	957	28.6%	23.0%
High flow freq. (Unitless)	12.7	13.7	25.6%	26.1%

Note: [1] Indicates $p < 0.05$ [2] Indicates $p < 0.025$ [3] Indicates $p < 0.01$
[4] Indicates $p < 0.005$

Table 4.5: IHA Two Period Parameter Means and CV for U2

U2	IHA Two Period Analysis			
	Mean (cfs)		Coefficient of Variation	
IHA Parameter	Pre-Impact	Post-Impact	Pre-Impact	Post-Impact
1-day minimum	28.2	22.6	62.9%	108.2%
3-day minimum	31.1	23.9	59.4%	108.3%
7-day minimum	34.4	27.1	58.2%	112.1%
30-day minimum	59.5	45.1	55.3%	89.5%
90-day minimum	122	109	70.3%	80.9%
1-day maximum	4113	4888	60.1%	109.3%
3-day maximum	3417	3731	55.7%	86.7%
7-day maximum	2114	2264	47.9%	78.7%
30-day maximum	1038	959	39.5%	48.3%
90-day maximum	682	634	37.7%	39.3%
Extreme low peak	40.4	33.2	21.6%	28.0%
Extreme low freq. (Unitless) [4]	3.94	6.50	81.5%	71.8%
High flow peak	948	1024	19.1%	19.5%
High flow freq. (Unitless)	15.5	14.7	39.4%	32.1%

Note: [1] Indicates $p < 0.05$ [2] Indicates $p < 0.025$ [3] Indicates $p < 0.01$
[4] Indicates $p < 0.005$

Table 4.6: IHA Two Period Parameter Means and CV for C2

C2	IHA Two Period Analysis			
	Mean (cfs)		Coefficient of Variation	
IHA Parameter	Pre-Impact	Post-Impact	Pre-Impact	Post-Impact
1-day minimum [1]	8.81	5.12	80.6%	144.1%
3-day minimum [1]	9.15	5.36	79.5%	140.5%
7-day minimum [2]	9.93	5.95	74.2%	133.7%
30-day minimum [2]	19.2	10.7	54.1%	110.5%
90-day minimum	47.9	33.6	65.2%	109.4%
1-day maximum	2745	2173	64.2%	72.4%
3-day maximum	1580	1363	55.2%	66.4%
7-day maximum	946	848	46.5%	67.7%
30-day maximum	482	403	39.5%	53.1%
90-day maximum	313	274	39.3%	51.8%
Extreme low peak [1]	11.2	10.5	28.9%	25.9%
Extreme low freq. (Unitless) [3]	2.71	4.77	77.0%	52.5%
High flow peak [4]	448	504	22.2%	28.9%
High flow freq. (Unitless)	15.1	13.2	34.1%	30.3%

Note: [1] Indicates $p < 0.05$ [2] Indicates $p < 0.025$ [3] Indicates $p < 0.01$
[4] Indicates $p < 0.005$

According to Richter et al. (1996), statistical comparison of the IHA parameters between the pre- and the post-impact year periods can be performed. Instead of using the mean and coefficient of variation to determine whether or not the central tendency and dispersion has changed, the deviation in the central tendency and dispersion is used to determine the magnitude of change. This allows for a total of 64 indicators of hydrologic alteration to quantify the alteration between pre- and post-impact year periods.

The results for U1 showed the 1-, 3-, and 7- day minimums significantly increased from pre-impact to post-impact year with an increase in CV. The average deviation of impact period

values from the pre-impact period mean for these three IHA parameters was 7.88 cfs (11.96%) and the percent deviation from the CV ranged from -27.01% to -37.51%. This showed the mean minimum flows not only increased but also became less variable after the impact year. The 1-, 3-, 7-, 30-, 90-day maximum showed a significant decrease in the post-impact period. The average deviation from the mean was -619.27 cfs (-20.414%) and the percent deviation from the CV ranged from -58.84% to -44.73%. This showed the mean maximum flows decreased became less variable after the impact year. The extreme low flow frequency showed a significant increase with a mean deviation of -2.67 cfs (-36.33%) and a percent deviation from the CV of 12.39%, meaning it become more dispersed after the impact year.

The results for C1 showed the 1-, 3-, and 7- day minimums did not significantly change from pre-impact to post-impact year. The average deviation from the mean was 0.37 cfs (2.35%) and the percent deviation from the CV ranged from 37.18% to 58.38%. This showed the mean minimum flows became just slightly more dispersed after the impact year. The 1-, 3-, 7-, 30-, 90-day maximum did not significantly change in the post-impact period. The average deviation from the mean was 152.51 cfs (1.59%) and the percent deviation from the CV ranged from -22.88% to 12.86%. This showed the mean maximum flows became slightly more dispersed in some flows and less dispersed in others after the impact year. The extreme low flow frequency did not significantly change and had a mean deviation of -1.22 cfs (-27.95%) with a percent deviation from the CV of 19.73%, meaning it become slightly more dispersed after the impact year. These deviations were relatively small when compared to U1.

The results for U2 showed the 1-, 3-, 7-, 30-day minimums did not significantly change after the impact year. The average deviation from the mean for these parameters was -8.66 cfs (-22.21%) and the percent deviation from CV ranged from 61.73% to 92.6%. This showed that

these flows grew very dispersed after the impact year. The extreme low flow peak did not significantly change and had a mean deviation of -7.16 cfs (-17.72%) with a percent deviation from the CV of 29.30%, where it became slightly more dispersed after the impact year. The extreme low flow frequency showed a significant increase with a mean deviation of 2.56 cfs (64.93%) with a percent deviation from the CV of -11.86%, where it became slightly less dispersed after the impact year. The extreme high flow peak did not significantly change and had a mean deviation of 76.20 cfs (8.04%) with a percent deviation from the CV of 1.86%, where it became slightly more dispersed after the impact year. The extreme high flow frequency mean deviation was -0.80 cfs (-5.17%) with a percent deviation from the CV of -18.70%, where it became slightly less dispersed after the impact year.

The results for C2 showed the 1-, 3-, 7-, 30-day minimums showed a significant decrease after the impact year. The average deviation from the mean for these parameters was -4.98 cfs (-41.87%) and the percent deviation from CV ranged from 76.61% to 104.20%. This showed that these flows grew more dispersed after the impact year. The extreme low flow peak showed a significant decrease and had a mean deviation of -0.75 cfs (-6.67%) with a percent deviation from the CV of -10.44%, where it became less dispersed after the impact year. The extreme low flow frequency mean showed a significant increase and had a deviation of 2.07 cfs (76.38%) with a percent deviation from the CV of -31.85%, where it became slightly less dispersed after the impact year. The extreme high flow peak showed a significant increase and had a mean deviation of 55.41 cfs (12.36%) with a percent deviation from the CV of 30.41%, where it became more dispersed after the impact year. The extreme high flow frequency mean deviation was -1.83 cfs (-12.16%) with a percent deviation from the CV of -11.18%, where it became less dispersed after the impact year. When compared to U2, the deviations for C2 were much greater.

This showed that the control watershed experienced a difference between the pre-impact and post-impact period most likely due to climate variability that should have shown up in the urbanized watershed but did not. The reason could be that the stormwater management associated with increased urbanization after the impact year in U2 kept the watershed from going through changes such as increased peak flow.

These deviations from the parameter means after the impact year were further analyzed through the RVA and HA analysis. The three categories (or target ranges) for the RVA were the Low RVA, Middle RVA, and High RVA, where the upper and lower boundaries of the Middle RVA were set as 1 standard deviation from the mean for the analysis. A positive hydrologic alteration value indicated the frequency in that category was increasing, whereas a negative value indicated the frequency was decreasing. For example, a positive HA for the Low and High RVA and a negative HA for the Middle RVA would indicate more variability in the flow regime and vice versa. The hydrologic alteration value in each RVA category was plotted for the 1-, 3-, 7-, 30-, 90-day minimum flow and the 1-, 3-, 7-, 30-, 90-day maximum flow. These can be seen in Figure 4.1, Figure 4.2, Figure 4.3, and Figure 4.4 for U1, C1, U2, and C2, respectively.

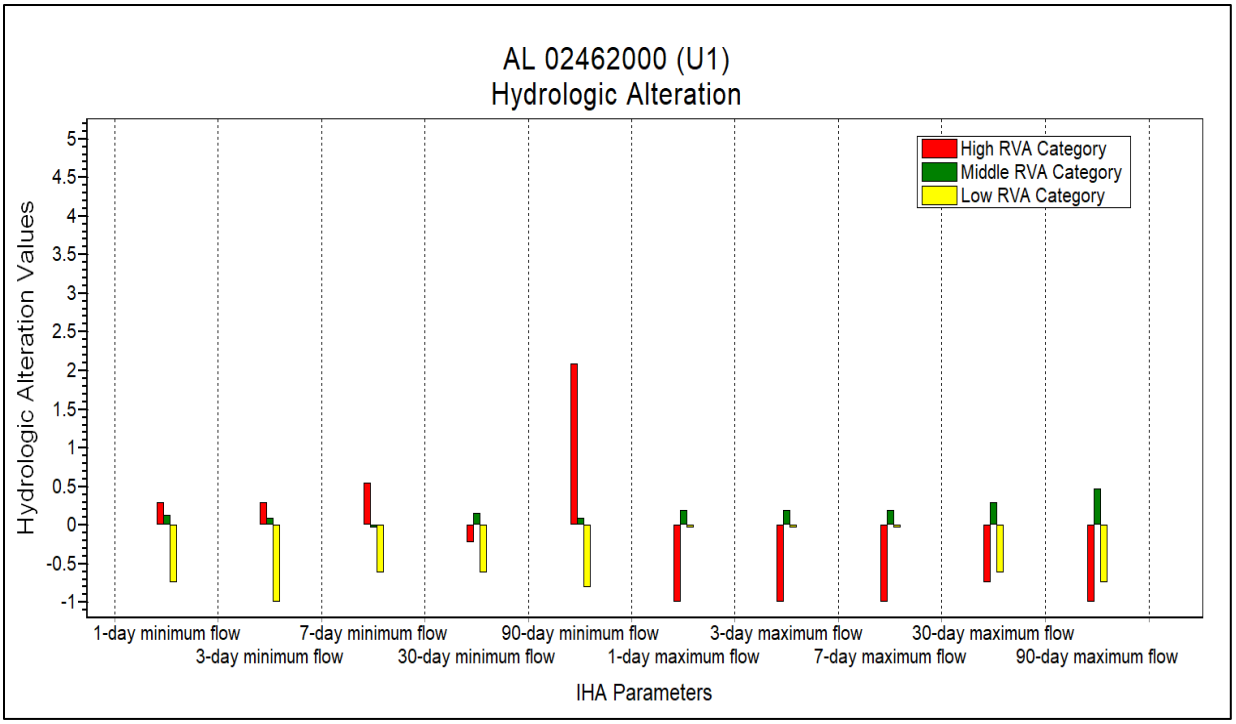

Figure 4.1: Hydrologic Alteration Values for U1

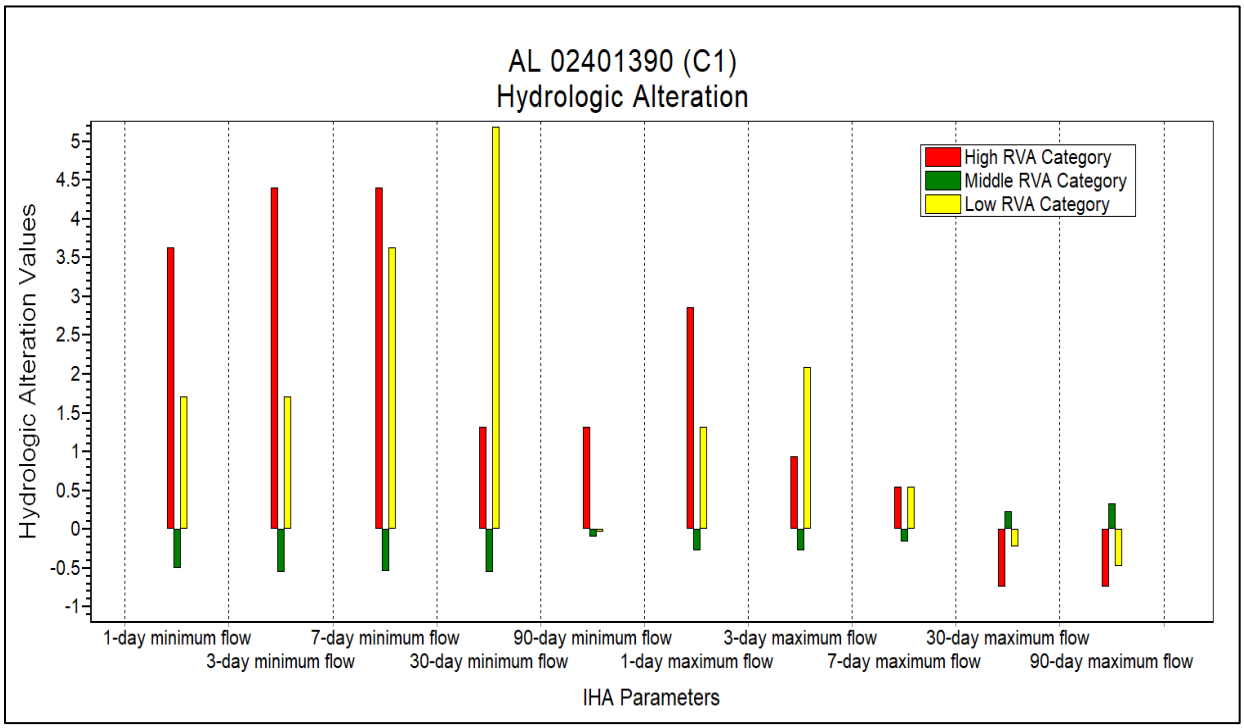

Figure 4.2: Hydrologic Alteration Values for C1

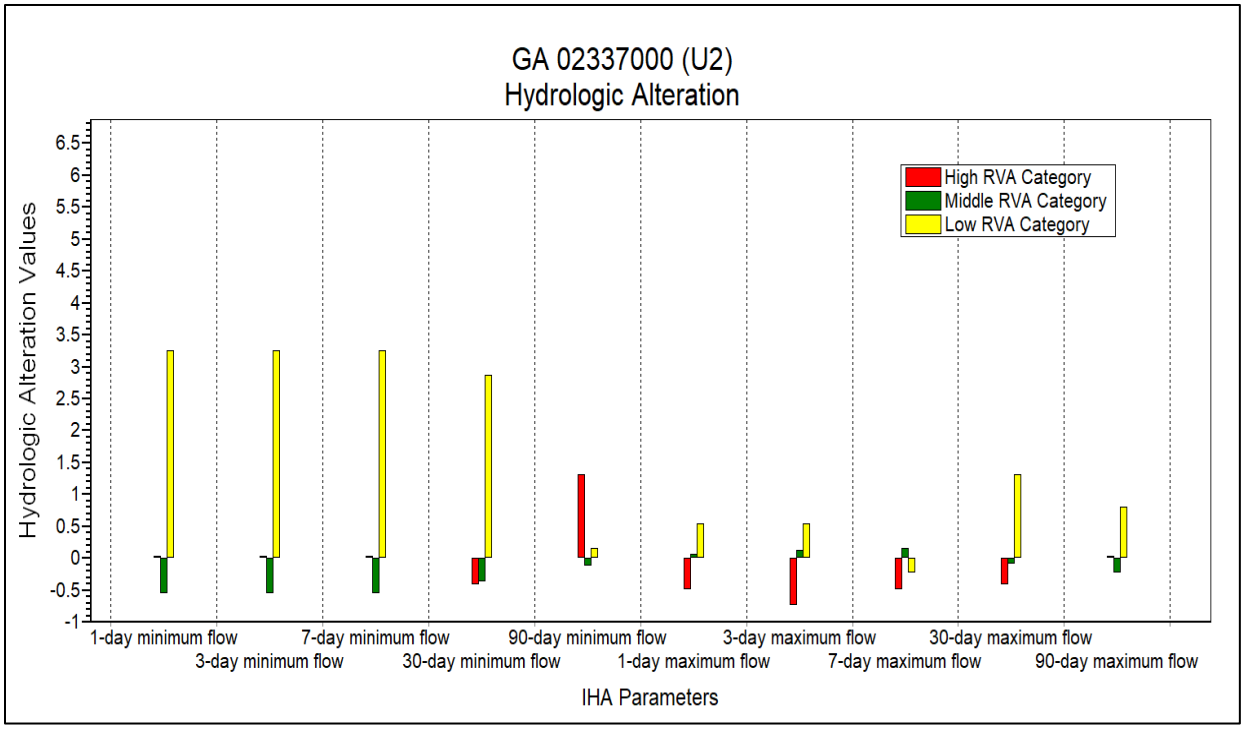

Figure 4.3: Hydrologic Alteration Values for U2

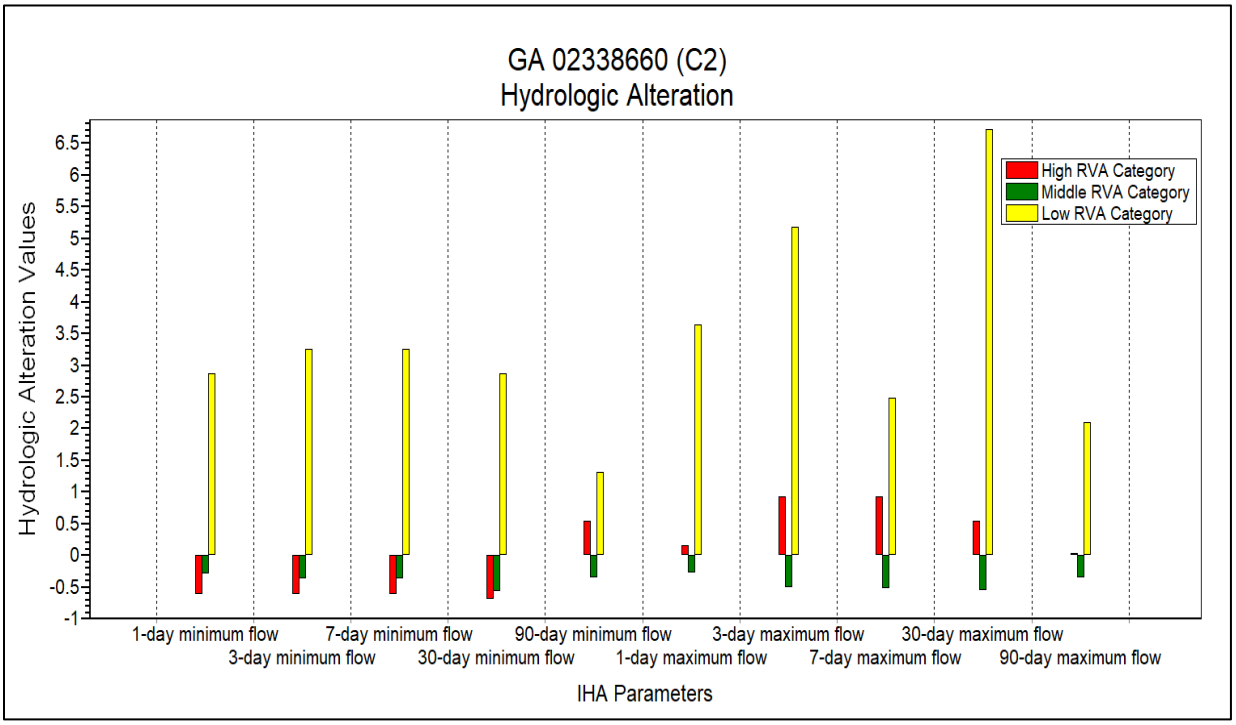

Figure 4.4: Hydrologic Alteration Values for C2

The change in frequency in each RVA category was mostly consistent across each watershed. However, differences arose between the Alabama and Georgia sites with respect to minimum flows for the urbanized watersheds. In watershed U1 in Alabama, the 1-, 3-, and 7-day minimum flows experienced an increase in the high RVA, decrease in the low RVA, and relatively no change in the middle RVA. This represented an increase in the overall minimum flow values. This change in minimum flows was most likely caused by the increase in stormwater management control structures used to offset urbanization and impervious surfaces and the reduced groundwater recharge due to reduced infiltration after the impact year. The 1-, 3-, 7-, 30-, and 90-day maximum flows experienced a decrease in high and low RVA with an increase in the middle RVA. This change shows the stormwater management facilities in this watershed may have been over designed. Standard practice requires that peak flows from a developed site must match the pre-development conditions. However, changes to the high- and low-flow regimes may affect the ecology and sediment transport dynamics of streams in the watershed.

Watershed C1 experienced increases to the low and high RVA for the 1-, 3-, and 7-day minimum flows, the 1-, 3-, and 7-day maximum flows, and the middle RVA for 30- and 90-day maximum flows. This showed an increase in the overall number of minimum flow values, which meant the watershed may have experienced low flows more often. U1 results contrasted this, which showed the increase to the baseflow in U1 was not caused from natural events. A decrease was shown in the middle RVA for the 1-, 3-, and 7-day minimum and maximum flows and the low and high RVA for the 30- and 90-day maximum flows. These results followed U1 as expected but the degree of alteration to peak flow values was much smaller. This once again showed that the decrease in U1 peak flows was not caused by differences in climate between the

pre- and post-impact periods.

Watershed U2 in Georgia was interesting in that it experienced an increase in the low RVA for all parameters except the 7-day maximum flow where it decreased. The middle RVA for all minimum flows decreased and the high RVA decreased for the 30-day minimum, increased for the 90-day minimum, and was negligible for the 1-, 3-, and 7-day minimum flows. The high RVA decreased for all maximum parameters. The 1-, 3-, and 7-day maximums experienced an increase and the 30- and 90-day maximums experienced a slight decrease in the middle RVA. Overall, this led to lower baseflow values as the minimum flow parameters were increased in frequency. The maximum flows decreased as was observed in the other urbanized watershed.

The low RVA in C2 experienced a significant increase in all parameters and the middle RVA decreased slightly in all parameters. The high RVA values decreased slightly for all the minimum parameters except the 90-day minimum and decreased for all the maximum parameters. Therefore, the overall streamflow may have decreased in the watershed and baseflow may have been reduced. The U2 minimum flow results matched this trend and showed a similar degree of alteration. These parameters for U2 experienced a decent decreasing alteration in the middle RVA about twice that of C2. This, in addition to the high RVA change in these parameters for U2 being negligible, produced a low flow reduction less than that found in C2. Therefore, the low flows might have been reduced more in U2 if urbanization had not increased the impervious surfaces and led to more stormwater runoff.

4.3. Streamflow Signature Analysis Results

Streamflow signatures for each watershed were calculated using the streamflow and precipitation data with the MATLAB code. Data was broken up for a before-after approach with

the before period ranging from water year 1982 to 1995 and the after period from water year 1996 to 2017, which totaled to 36 water years in the analysis. The streamflow elasticity coefficient, runoff ratio, slope of the flow duration curve and baseflow index were calculated and hydrographs and FDR curves were plotted for each for the before and after periods for each watershed. Unpaired, two-sided, heteroscedastic *t*-tests were used to compare the means of pre- and post-impact period streamflow signatures. The before and after flow duration curves and hydrographs can be seen in Appendix C.

The results for U1 can be seen in Table 4.7. None of the streamflow signatures were found to be statistically significant, however, the following observations were made. The streamflow elasticity coefficients and runoff ratios did not change between the before and after periods, whereas slope of the flow duration curve decreased and the baseflow index increased. The percent difference for the slope of the flow duration curve was 10.04% moving in the negative direction, which showed the flow regime become more dampened and less variable. The baseflow index had a percent difference of 5.62% in the positive direction. The increase in baseflow is consistent with the IHA analysis results and affirmed changes to the landcover from urbanization caused these effects.

Table 4.7: Streamflow Signatures for U1

U1			
Streamflow Signatures	**Before**	**After**	**Percent Difference**
Streamflow Elasticity Coefficient	0.7894	0.7912	0.23%
Runoff Ratio	0.4927	0.5011	1.69%
Slope of the Flow Duration Curve	-2.2006	-1.9902	10.04%
Baseflow Index	0.6343	0.671	5.62%
Note: [1] Indicates $p < 0.05$ [2] Indicates $p < 0.025$ [3] Indicates $p < 0.01$ [4] Indicates $p < 0.005$			

The results for C1 showed an opposite trend when compared to U1 and can be seen in Table 4.8. None of the streamflow signatures were found to be statistically significant, however, the following observations were made. The streamflow elasticity coefficient and slope of the flow duration curve increased whereas the runoff ratio and baseflow index decreased. The percent difference for the streamflow elasticity coefficient was 6.61% compared to 0.23% in U1. A greater difference in C1 showed that stormwater management in U1 performed well in controlling stream sensitivity to precipitation. Both coefficients were below 1.0, meaning a 1% change in precipitation produced a less than 1% change in streamflow. The runoff ratio for C1 decreased with a percent difference of 8.68% whereas it increased in U1 with a percent difference of 1.69%. This showed that the runoff ratio would have decreased for U1 if not for increases to urban landcover. With less impervious surface, C1 was able to infiltrate more precipitation into the soil where U1 routed more precipitation to streams. The slope of the flow duration curve for C1 increased with a percent difference of 5.43%, so the flow regime became more variable. The baseflow index was also opposite than U1 with a decrease and a percent difference of 1.45%. Even though more baseflow seemed to show up in U1, from the IHA analysis these baseflow values were shown to be increasing in magnitude.

Therefore, with an increase in urbanization, baseflow frequency was increasing but the magnitude of the baseflow norm increased. This is concerning as it can change the ecology of the watershed over this long span of increases in flow. As reported in Poff and Zimmerman (2010), this increase in magnitude of low flow values and loss of flow variability has potential to disrupt species life cycles, reduce species richness and diversity, alter assemblages and dominant taxa, and increase invasive species.

Table 4.8: Streamflow Signatures for C1

C1			
Streamflow Signatures	**Before**	**After**	**Percent Difference**
Streamflow Elasticity Coefficient	0.7607	0.8127	6.61%
Runoff Ratio	0.4606	0.4223	8.68%
Slope of the Flow Duration Curve	-4.0469	-4.2728	5.43%
Baseflow Index	0.541	0.5332	1.45%
Note: [1] Indicates $p < 0.05$ [2] Indicates $p < 0.025$ [3] Indicates $p < 0.01$ [4] Indicates $p < 0.005$			

The results for U2 and C2 can be seen in Table 4.9 and Table 4.10, respectively. Results for U2 baseflow index and C2 runoff ratio, slope of the flow duration curve, and baseflow index showed statistical significance. The remaining signatures showed no statistical significance; however, the following observations were found. U2 showed an increase in streamflow elasticity coefficient and slope of the flow duration curve and a decrease in runoff ratio and baseflow index. The percent difference for the streamflow elasticity coefficient was very low and similar for both watersheds. However, the runoff ratio and slope for the flow duration curve for C2 was almost three times that of U2. The percent difference in the baseflow index was slightly higher for C2 (8.10%) than for U2 (7.31%). The flow duration curves for U2 show an overall decrease in flow values, which is supported from the IHA results as well. These trends led to a more variable flow regime, which are known to affect plant growth, the germination period of plants is disrupted, and survival is reduced (Poff and Zimmerman, 2010). The reduction in overall flows can lead to many ecological problems such as terrestrialization and vegetative encroachment to channels, increased invasive species, increased riparian cover, and alteration to plant assemblages.

Table 4.9: Streamflow Signatures for U2

U2			
Streamflow Signatures	**Before**	**After**	**Percent Difference**
Streamflow Elasticity Coefficient	0.7674	0.7769	1.23%
Runoff Ratio	0.3906	0.3654	6.67%
Slope of the Flow Duration Curve	-2.3397	-2.5516	8.66%
Baseflow Index[3]	0.6198	0.5761	7.31%
Note: [1] Indicates $p < 0.05$ [2] Indicates $p < 0.025$ [3] Indicates $p < 0.01$ [4] Indicates $p < 0.005$			

Table 4.10: Streamflow Signatures for C2

C2			
Streamflow Signatures	**Before**	**After**	**Percent Difference**
Streamflow Elasticity Coefficient	0.7823	0.7939	1.47%
Runoff Ratio[1]	0.3169	0.2673	16.98%
Slope of the Flow Duration Curve[3]	-2.6439	-3.3824	24.51%
Baseflow Index[2]	0.6472	0.5968	8.10%
Note: [1] Indicates $p < 0.05$ [2] Indicates $p < 0.025$ [3] Indicates $p < 0.01$ [4] Indicates $p < 0.005$			

4.4. HEC-HMS Model

A HEC-HMS model (Figure 4.5) using data from watershed U1 for water years 1981 to 2017 was created to simulate streamflow at upstream tributaries. The goal was to analyze simulated streamflow at upstream tributaries using IHA and the streamflow signatures and compare it with the IHA and streamflow signature analysis results for the observed streamflow at the outlet. However, before the model could be used, it was calibrated and validated for the before and after impact year periods.

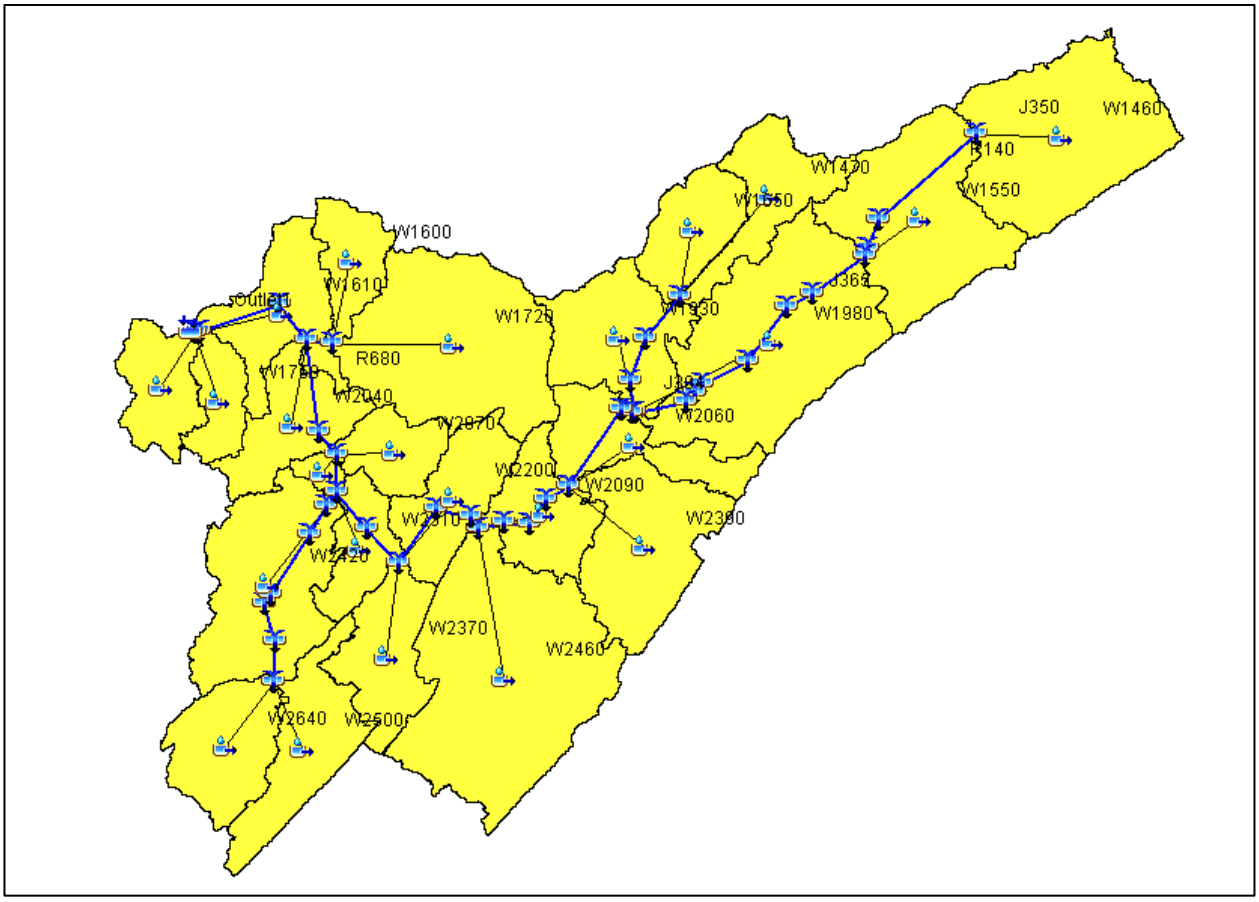

Figure 4.5: HEC-HMS Model for U1

The model was auto calibrated using optimization runs with parameters for the Muskingum *K* and *X* terms, Initial Baseflow, Baseflow Recession Constant, Baseflow Ratio to Peak, and Initial Abstraction. The optimized parameters can be seen in Appendix D, Model Optimized Parameter Values. The calibration period was water years 1981 to 1985 and the validation period was water years 1989 to 1993 for the before impact year data. Each period was analyzed for goodness of fit using hydrographs, flow comparison plots, and model performance ratings. The calibrated model performance for before the impact year can be seen in Table 4.11 and for the after the impact year in Table 4.12. Comparison hydrographs and flow plots can be seen in Appendix D, Model Calibration/Validation.

Table 4.11: Before Impact Year Model Performance

Before Impact Year Model Performance					
	PEV (%)	**PEPF (%)**	**R^2**	**NSE**	**RSR**
Calibration (WY 1982-1985)	14.7% [2]	11.7% [1]	0.74 [2]	0.70 [2]	0.55 [2]
Validation (WY 1990-1993)	22.8% [3]	21.3% [2]	0.65 [2]	0.56 [3]	0.66 [2]
Note: [1] Very Good [2] Good [3] Satisfactory [4] Unsatisfactory					

Table 4.12: After Impact Year Model Performance

After Impact Year Model Performance					
	PEV (%)	**PEPF (%)**	**R^2**	**NSE**	**RSR**
Calibration (WY 1997-2000)	4.3% [1]	31.3% [3]	0.74 [2]	0.71 [2]	0.54 [2]
Validation (WY 2011-2014)	1.9% [1]	7.9% [1]	0.67 [2]	0.51 [3]	0.69 [3]
Note: [1] Very Good [2] Good [3] Satisfactory [4] Unsatisfactory					

The model was shown to perform well overall for the before impact year period. The PEV was 14.7% for the calibration and 22.8% for the validation, which corresponded to a performance rating of Good and Satisfactory, respectively. The PEPF was 11.7% for the calibration and 21.3% for the validation, which corresponded to a performance rating of Very Good and Good, respectively. The R^2 was 0.74 and 0.65 for the calibration and validation, respectively. This showed a performance rating of Good for both periods. The NSE was 0.70 for the calibration and 0.56 for the validation, which corresponded to a performance rating of Good and Satisfactory, respectively. The RSR was found to be 0.55 for the calibration and 0.66 for the validation, which showed Good model performance for both periods. The model slightly underestimated streamflow values which led to the differences in the performance statistics.

The model performed well in the after impact year period, but it slightly underestimated the streamflow values when compared to the observed values. The PEV was 4.3% for the

calibration and 1.9% for the validation, which corresponded to a performance rating of Very Good in both. The PEPF was 31.3% for the calibration and 7.9% for the validation, which corresponded to a performance rating of Satisfactory and Very Good, respectively. The R^2 was 0.74 and 0.67 for the calibration and validation, respectively. This showed a performance rating of Good for both periods. The NSE was 0.71 for the calibration and 0.51 for the validation, which corresponded to a performance rating of Good and Satisfactory, respectively. The RSR was found to be 0.54 for the calibration and 0.69 for the validation, which showed Good and Satisfactory model performance, respectively.

The model was used to simulate streamflow at ungaged locations in upstream tributaries of watershed U1. The goal was to determine how effective streamflow signatures and hydrologic alterations calculated at a downstream gage were at detecting hydrologic alteration in the upstream subcatchments. Seven points throughout the watershed were selected to give a good representation of the watershed. The points were at J358, J310, J384, J399, J417, J314, J304 in the model (Figure 4.6). The percent urbanized for each subbasin in the model (Figure 4.7) was determined for the before- and after-impact year time periods (Table 4.13).

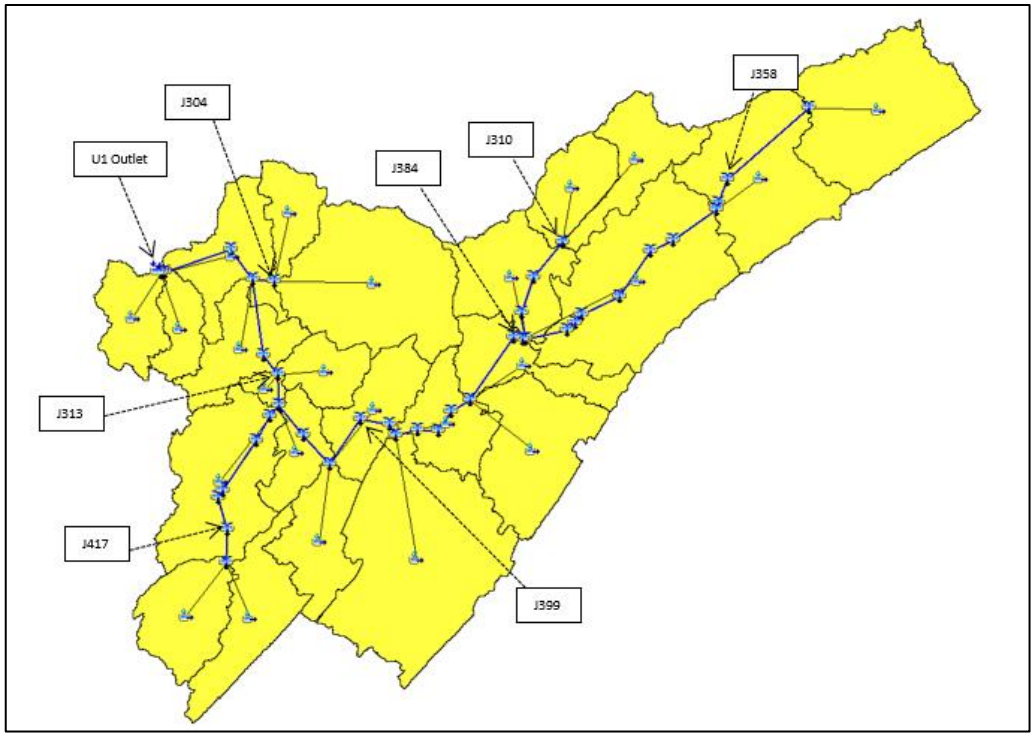

Figure 4.6: HEC-HMS Ungaged Locations in Watershed U1

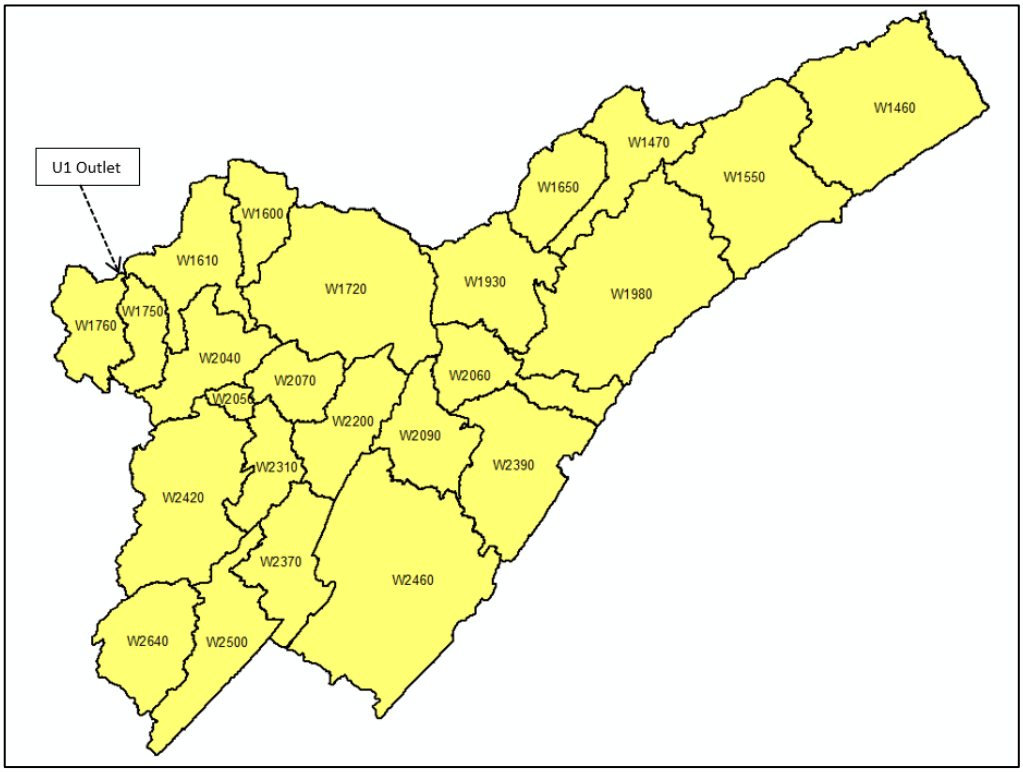

Figure 4.7: HEC-HMS Model Subbasins

Table 4.13: HEC-HMS Model Percent Urbanized by Subbasin

Percent Urbanized Area				
Subbasin	**Percentage of Area Urbanized (Before)**	**Percentage of Area Urbanized (After)**	**Change in Percent**	**HMS Junction**
W1460	79.70%	98.14%	18.44%	
W1470	63.57%	95.92%	32.36%	
W1550	65.75%	91.37%	25.62%	J358
W1600	3.54%	21.64%	18.10%	
W1610	0.66%	9.48%	8.82%	
W1650	38.66%	72.47%	33.81%	
W1720	5.97%	23.73%	17.76%	J304
W1750	0.13%	0.48%	0.35%	
W1760	0.19%	7.91%	7.73%	
W1930	32.61%	82.51%	49.90%	J310
W1980	47.49%	85.07%	37.58%	
W2040	0.04%	5.27%	5.23%	
W2050	0.01%	0.75%	0.74%	
W2060	47.94%	79.13%	31.19%	J384
W2070	9.06%	33.71%	24.66%	J313
W2090	7.31%	44.09%	36.78%	
W2200	0.46%	5.27%	4.82%	J399
W2310	0.33%	3.11%	2.78%	
W2370	0.07%	0.69%	0.62%	
W2390	46.02%	84.48%	38.46%	
W2420	1.46%	8.15%	6.69%	J417
W2460	4.92%	44.45%	39.52%	
W2500	2.08%	3.28%	1.20%	
W2640	0.04%	2.46%	2.42%	

The simulated flows were used in the MATLAB code to determine the streamflow signatures at each upstream tributary location. The results can be seen in Table 4.14, where the U1 results are highlighted in yellow for comparison.

Table 4.14: Upstream Tributary Streamflow Signature Analysis Results

Upstream Tributary Streamflow Signature Comparison			
Streamflow Signatures	**Before**	**After**	**Percent Difference**
U1			
Streamflow Elasticity Coefficient	0.7894	0.7912	0.23%
Runoff Ratio	0.4927	0.5011	1.69%
Slope of the Flow Duration Curve	-2.2006	-1.9902	10.04%
Baseflow Index	0.6343	0.671	5.62%
J358			
Streamflow Elasticity Coefficient	0.7856	0.7851	0.06%
Runoff Ratio	0.0277	0.031	11.24%
Slope of the Flow Duration Curve	-7.9979	-6.991	13.44%
Baseflow Index	0.2062	0.2011	2.50%
J310			
Streamflow Elasticity Coefficient	0.7858	0.7882	0.30%
Runoff Ratio	0.0253	0.0283	11.19%
Slope of the Flow Duration Curve	-4.4108	-5.3955	20.08%
Baseflow Index	0.4302	0.4254	1.12%
J384			
Streamflow Elasticity Coefficient	0.7881	0.7862	0.24%
Runoff Ratio	0.1363	0.1525	11.22%
Slope of the Flow Duration Curve	-4.041	-5.3393	27.68%
Baseflow Index	0.3441	0.3492	1.47%
J399			
Streamflow Elasticity Coefficient	0.7903	0.7860	0.55%
Runoff Ratio [4]	0.2185	0.3341	41.84%
Slope of the Flow Duration Curve [4]	-3.6865	-2.1321	53.43%
Baseflow Index [4]	0.3223	0.5163	46.27%
J417			
Streamflow Elasticity Coefficient	0.7931	0.7833	1.24%
Runoff Ratio	0.0281	0.0298	5.87%
Slope of the Flow Duration Curve [1]	-4.7893	-5.2098	8.41%
Baseflow Index	0.2919	0.2752	5.89%
J313			
Streamflow Elasticity Coefficient	0.7935	0.7854	1.03%
Runoff Ratio [4]	0.3193	0.4375	31.24%
Slope of the Flow Duration Curve [4]	-3.9054	-2.4393	46.21%
Baseflow Index [4]	0.3526	0.4721	28.98%

J304			
Streamflow Elasticity Coefficient	0.7937	0.7918	0.24%
Runoff Ratio [4]	0.0381	0.1226	105.16%
Slope of the Flow Duration Curve [4]	-4.4434	-0.3352	171.94%
Baseflow Index [4]	0.2873	0.7473	88.92%
Note: [1] Indicates $p < 0.05$ [2] Indicates $p < 0.025$ [3] Indicates $p < 0.01$ [4] Indicates $p < 0.005$			

The simulated flows at each location were able to match the magnitude of the streamflow elasticity coefficient of the U1 outlet location and fell within the range of 0 to 2 given by Sawicz et al. (2011) for watersheds in Alabama, but it was not statistically significant at any of the locations. However, the values for the other three signatures varied across each tributary location. The runoff ratio showed a significant increase at J399, J313, and J304, but was not statically significant at the other locations. The slope of the flow duration curve showed a significant increase at J417, a significant decrease at J399, J313, and J304, and no statistical significance at the other locations. The baseflow index showed a significant increase at J399, J13, and J04, but was not statistically significant at the other locations.

The runoff ratios for J399 and J313 ranged from 0.21 to 0.44, which fell within the expected range of 0.2 to 0.6 given by Sawicz et al. (2011) for watersheds within Alabama. However, the other five locations fell drastically short of this by ranging from 0.02 to 0.15. These locations were further away from the main stream than J399 and J313, which shows the simulated flows may not represent the runoff ratio that well the further upstream the location is.

The slope of the flow duration curve varied at each upstream location, but it followed the same decreasing trend from the before- to the after- impact year time period just as the U1 outlet did. The magnitude for each location was within the range of 2 to 6 given by Sawicz et al. (2011) for watersheds in Alabama, except for J358 which decreased from 7.99 to 6.99. The

baseflow index at each upstream location was about half of the values of U1 in most cases. The increasing trend from the before- to the after- impact year time period was maintained in upstream tributary locations J384, J399, J313, and J304, but exhibited a decreasing trend in J358, J310, and J417. The values fell within the range of 0.4 to 0.8 given by Sawicz et al. (2011) for watersheds in Alabama but ranged from 1/3 to 2/3 the magnitude of baseflow index at U1 outlet. The results showed that the further the location was from the U1 outlet, the less accurate the simulated results were in measuring the streamflow signatures. However, for J313 and J304, which were the closest sample locations to the U1 outlet, the results matched well. The runoff ratios and baseflow indices for both significantly increased and the slope of the flow duration curves significantly decreased. The subbasins where J313 and J304 were located had a percentage of urban area that changed from 9.06% to 33.71% and 5.97% to 23.73%, respectively. Basins over 15% imperviousness often support poor stream habitats (National Research Council, 2002; Nagy et al., 2012). Therefore, both subbasins where these two upstream tributary locations likely became poor stream habitats as a result of the increased urban area after the impact year. The other locations were either already well over the 15% mark before the impact year or did not reach 15% after the impact year. A streamflow signature analysis considering just the gage data would not have detected the impact of urbanization on this watershed (Table 4.7).

The streamflow signature changes followed what was expected for an urbanized watershed for the streamflow elasticity coefficient and runoff ratio but not for the slope of the flow duration curve and baseflow index. The increasing runoff ratio was expected with an increase in urbanization over time due to the increases to impervious surface and reduced infiltration. However, the change in the slope of the flow duration curve suggested streamflow

was becoming less flashy, which is not what would be expected in an urbanized watershed. Stormwater management may be the cause of this unexpected outcome as the peak flows were reduced through certain practices. The baseflow index increased over time, which is the opposite of what would be expected for an urbanized watershed. The baseflow index would be expected to decrease as increases to impervious surface decrease the amount of runoff taking longer flow paths in the watershed. This unexpected change may have represented the gradual release of water from detention storage rather than actual groundwater sourced baseflow. Overall, stormwater management may cause unexpected effects of urbanization and future study should investigate how stormwater management was done in these two watersheds.

The streamflow at each point was analyzed using the IHA software and compared to the original results for watershed U1. The hydrologic alteration (HA) values varied at each location for each significant parameter. In J358, the 1-, 3-, and 7-day minimum flows in each RVA category saw no HA except for the high RVA in the 7-day minimum flows, which did not follow what was shown from the U1 outlet. The high RVA in the 7-day minimum flows followed the U1 outlet as it increased in frequency. The 1-, 3-, 7-, 30-, and 90-day maximum flows follow the same HA as the U1 outlet except in the magnitude of the low RVA for the 1-, 3-, and 7-day maximum flows, where decrease in frequency was smaller. The HA for J358 can be seen in Figure 4.8.

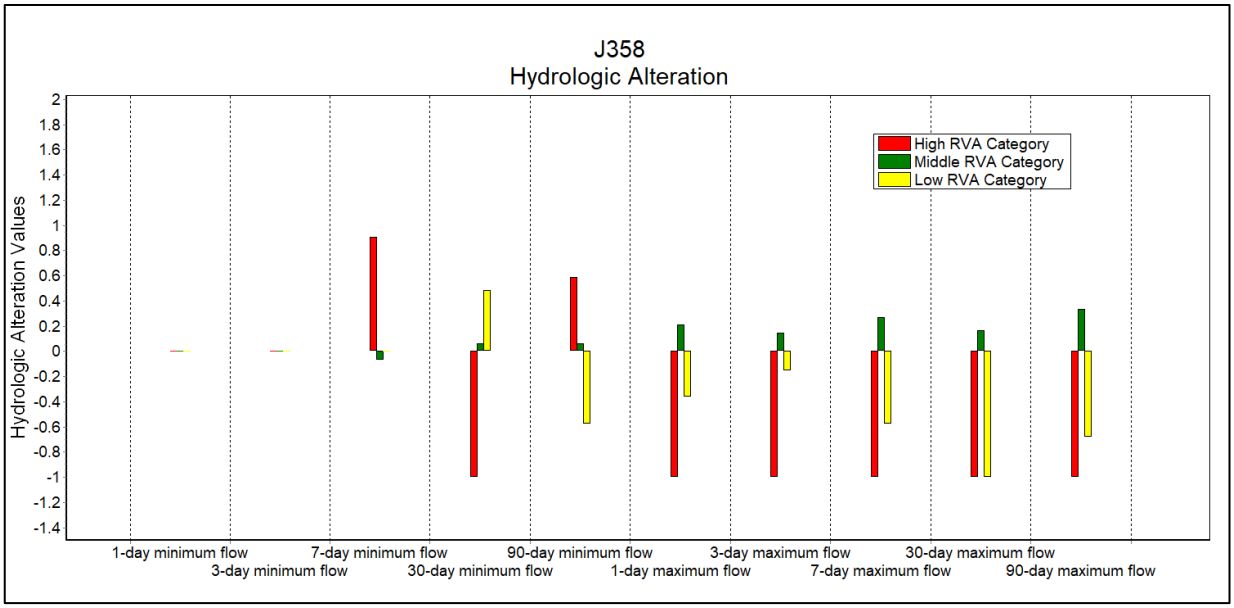

Figure 4.8: Hydrologic Alteration Values for J358

In J310, the 1-, 3-, 7-, 30-, and 90-day maximum flows followed the same HA as the U1 outlet except in the magnitude of the low RVA for the 1-, 3-, and 7-day maximum flows, where decrease in frequency was smaller for the U1 outlet. The middle RVA for the 1-, 3-, and 7-day minimum flows matched the U1 outlet, but the low and high RVA's showed opposite trends from the U1 outlet. The U1 outlet had an increase in frequencies for the high RVA and a decrease in frequency for the low RVA. In J310, the low RVA's for the minimum flows showed no HA and the High RVA's showed a significant decrease in frequency. The HA for J310 can be seen in Figure 4.9.

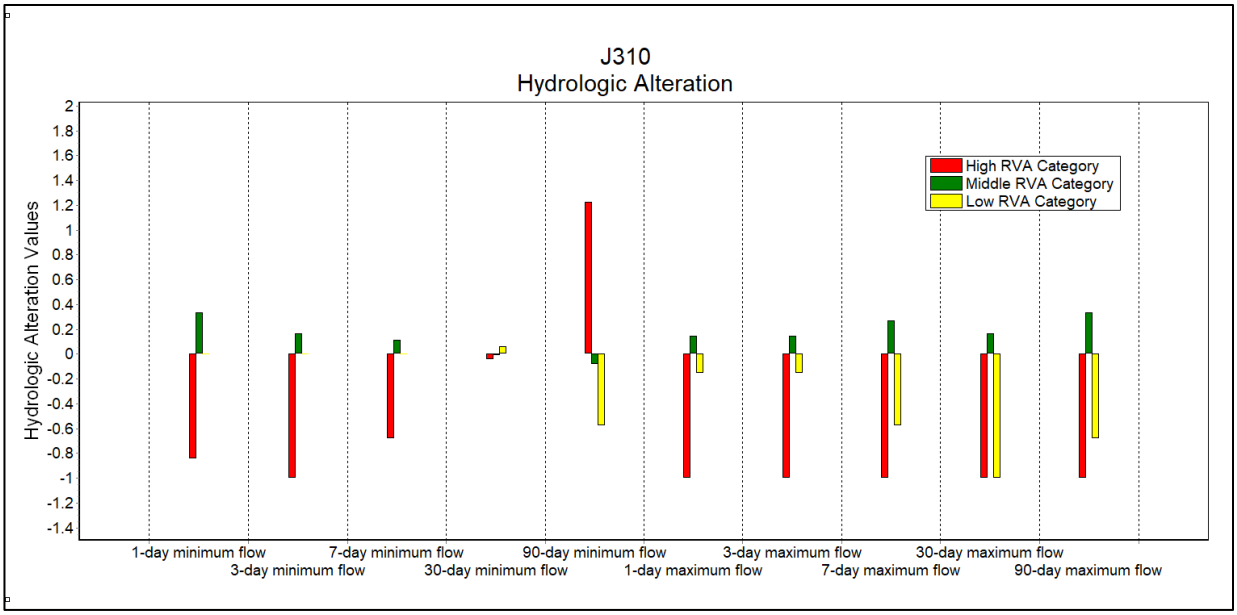

Figure 4.9: Hydrologic Alteration Values for J310

In J384, the 1-, 3-, 7-, 30-, and 90-day maximum flows followed the same HA as the U1 outlet except in the magnitude of the low RVA for the 1-, 3-, and 7-day maximum flows, where decrease in frequency was smaller at the U1 outlet. The middle RVA for the 1-, 3-, and 7-day minimum flows followed the same trend as at the U1 outlet, but the low and high RVA's differed. The high RVA's decreased in frequency at J384 whereas there was an increase at U1 outlet. The low RVA increased for the 7-day minimum flow, decreased for the 3-day minimum flow, and exhibited no HA for the 1-day minimum flow, whereas the U1 outlet had a significant decrease infrequency for all three. The HA for J384 can be seen in Figure 4.10.

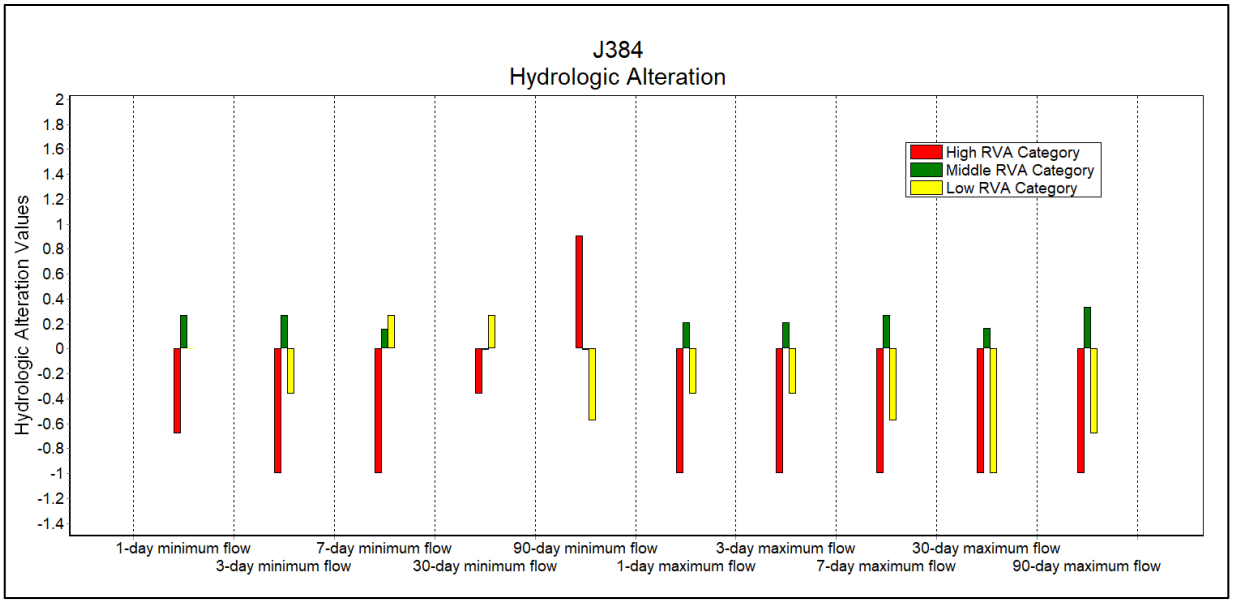

Figure 4.10: Hydrologic Alteration Values for J384

The J399 and J313 flows showed exactly the same trends except for a slight difference in magnitude for the 1-day minimum flows. The high RVA for the 1-day, 3-day, and 7-day minimum flows showed a significant increase in magnitude by a factor of 12 when compared to the U1 outlet. The middle RVA's for these flows showed an opposite trend than in U1 outlet, and the low RVA's experienced differing magnitudes but the same decreasing trend. All of the RVA categories for the 1-, 3-, 7-, 30-, and 90-day maximum flows showed a similar trend with the U1 outlet. The difference came in the magnitude of HA for each maximum flow. The HA for J399 and J313 can be seen in Figure 4.11 and Figure 4.12, respectively.

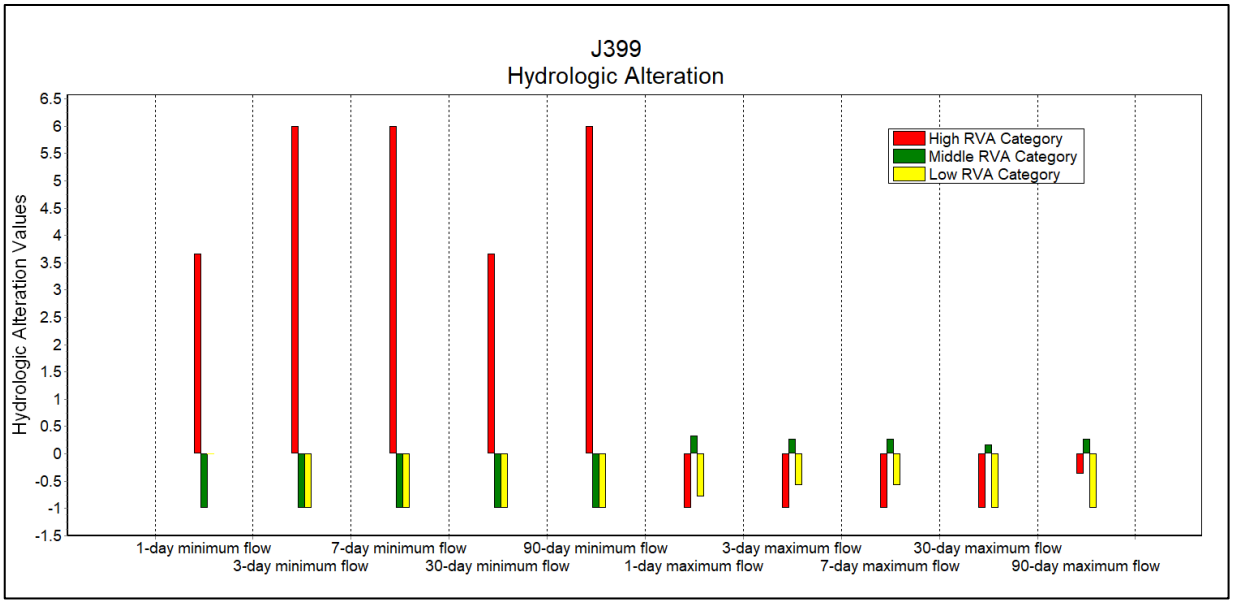

Figure 4.11: Hydrologic Alteration Values for J399

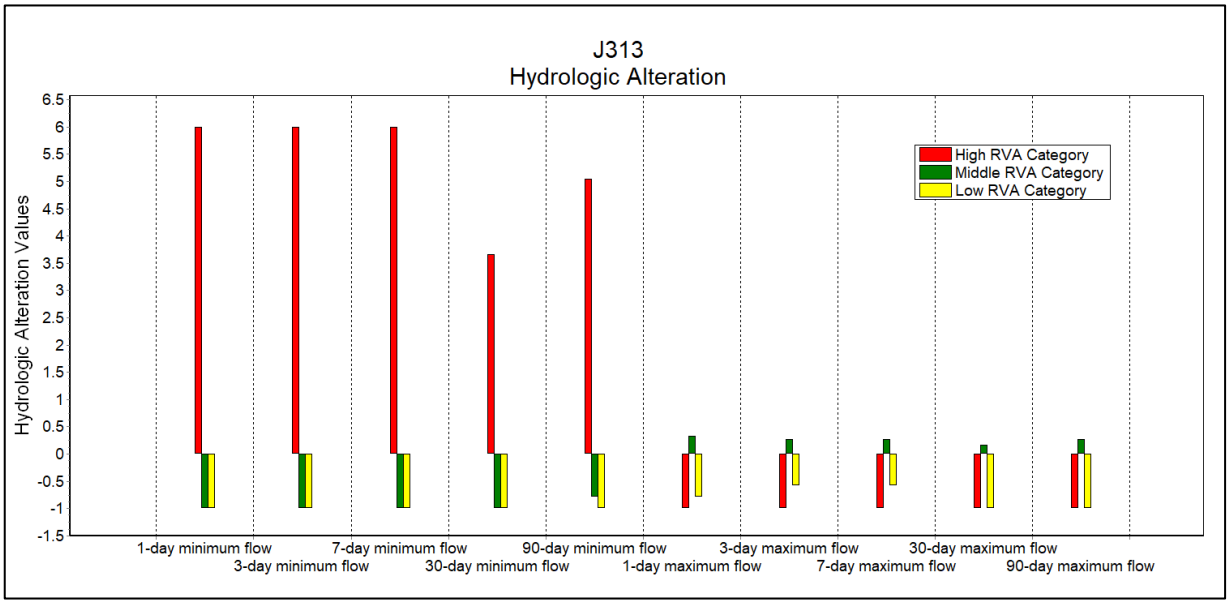

Figure 4.12: Hydrologic Alteration Values for J313

In J417, the RVA's for the 1-, 3-, and 7-day minimum flows differed completely from the U1 outlet. The 1-day minimum flows showed minimal HA in each RVA as did the 3-day and 7-day minimum flow low RVA. The high RVA for both the 3-day and 7-day minimum flows showed equal and opposite trends from the U1 outlet. The 1-, 3-, 7-, 30-, and 90-day maximum

flows all showed the same trends as the outlet except for slight differences in magnitude in the low RVA's. The HA for J417 can be seen in Figure 4.13.

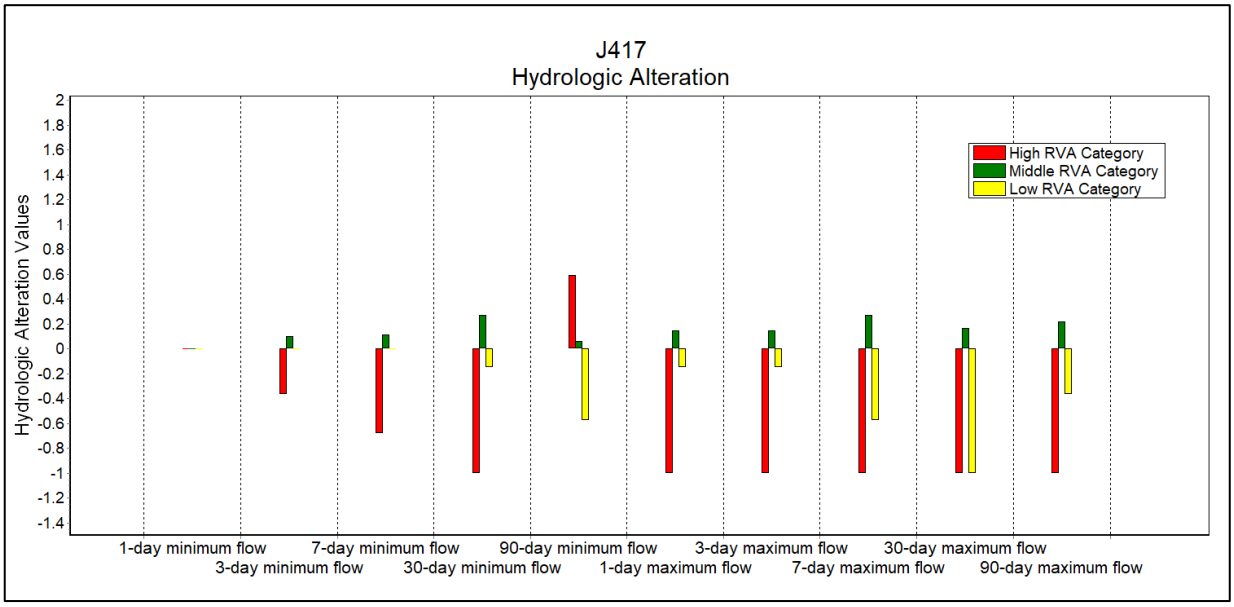

Figure 4.13: Hydrologic Alteration Values for J417

The J304 1-, 3-, and 7-day maximum flows experienced the same HA trend and magnitude as U1 outlet for the middle and high RVA, and the low RVA experienced the same trend but greater magnitude. The 30-day maximum flows experienced an opposite trend for the High RVA, was minimal for the middle RVA, and the same for the low RVA. The 90-day maximum flows experienced the same trend for the low RVA as U1 outlet, but the middle and high RVA's showed a different trend and magnitude. The 1-, 3-, and 7-day minimum flows for the high RVA showed a significant increase in the magnitude by a factor of about 12 when compared to the U1 outlet, and the low RVA was nonexistent when compared to U1 outlet. The middle RVA experienced a decrease in all three minimum flows, whereas the middle RVA for U1 outlet increased. The HA for J304 can be seen in Figure 4.14.

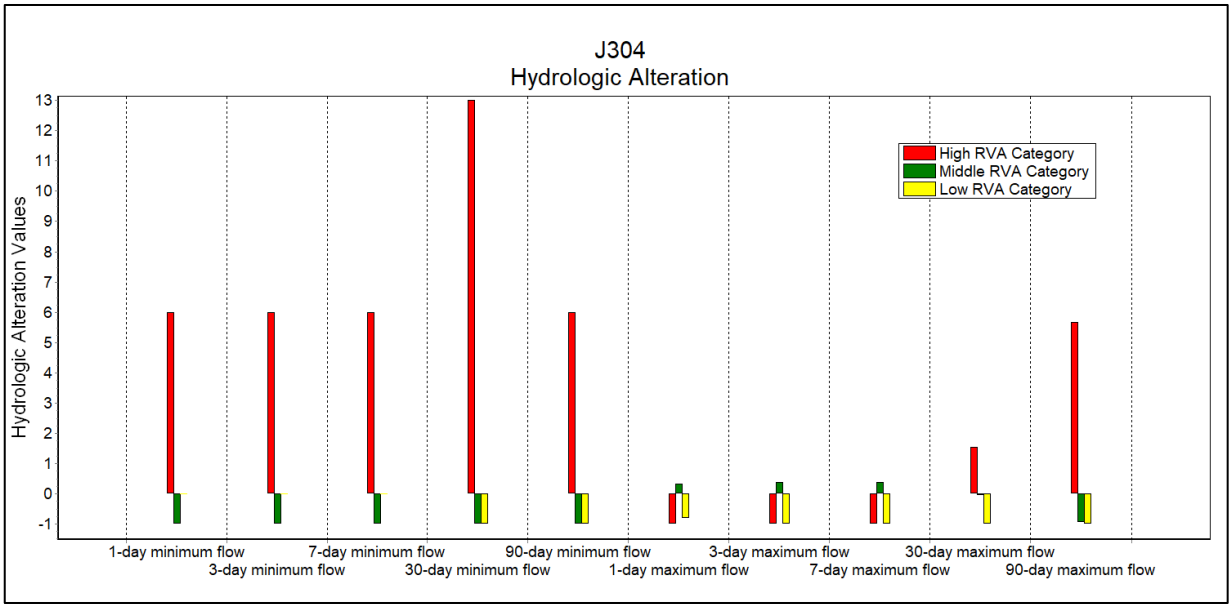

Figure 4.14: Hydrologic Alteration Values for J304

The IHA analysis showed there was great variation between each of the ungaged points when compared to the IHA analysis of the U1 outlet gage point. The maximum flow hydrologic alteration values were relatively close to the U1 outlet results when using the simulated streamflow except in a few cases. The minimum flow alterations were not close to the U1 outlet results in most cases especially in the high RVA categories. Significant increases in magnitude for the high RVA category in each minimum flow showed up at locations closest to the U1 outlet point. The farther away the ungaged location was upstream from the U1 outlet point, the less accurate the simulated flows seemed to be in measuring hydrologic alterations.

5. Conclusions

Increases to urbanization in the Southeastern United States over the past few decades as well as projected continual growth call for a better understanding of the impacts on hydrological processes in watersheds. The change in impervious surface in urban watersheds alters the surface runoff to streams causing major detriment to the ecological habitats. Streamflow signature and hydrologic alteration analyses were found useful in identifying hydrologic changes due to increases in urbanization over time in urban watersheds in Alabama (U1) and in Georgia (U2). However, IHA was a little better as the streamflow signature analysis did not detect significant changes in U1 even though impacts occurred. The U1 watershed had significant increase to the minimum flow values and significant decrease to the maximum flow values, which led to a less variable flow regime. This is verified by the decrease in slope of the flow duration curve. The changes to the flow regime have potential to greatly alter the aquatic habitat by reducing the diversity of biota, increasing invasive species, altering plant assemblages and dominant taxa, and reduce abundance of native fish species. The increases to the baseflow seen in the results may have been coincidental results of stormwater management control structures located in the watershed and nearby groundwater recharge locations.

The U2 watershed had significant increase to the minimum flow value leading to lower baseflow values, which was validated by the decrease in the baseflow index. The maximum flows were significantly decreased, which may be explained by stormwater management practices in Georgia for decreasing the peak flow values in post-development. This ultimately

led to a shift in the flow regime, and with an increase in the slope of the flow duration curve the stream became flashier, at a reduced magnitude. This can lead to alteration in aquatic habitat including decreased germination survival and growth of plants, lower species richness, altered assemblages, and increase in invasive species.

Changes to watershed characteristics have far reaching effects on the hydrological makeup as well as the ecological processes that take place. The HEC-HMS approach was meant determine the effectiveness of large-scale hydrological modeling methods in representing ungaged upstream tributary flows. Those simulated flows were then used with streamflow signature and IHA analysis to determine the hydrologic and ecological alterations. The findings show that results are variable and decrease in accuracy with increased distance upstream from the gage location. However, increasing and decreasing trends between the gage location and upstream tributary locations were mostly maintained even though the magnitude of alteration varied. This showed that gage locations can at least give a small picture of the hydrologic alterations across the entire watershed due to increases in urbanization. The trends found can help identify the type of changes to the aquatic habitat that should be expected, but not necessarily an accurate depiction of the magnitude of the change.

Limitations in available data prevented the study from encompassing a wider span of investigation to reach the objectives. The use of a larger quantity of watersheds would be useful in the future to better confirm these findings.

References

Barksdale, W. F., and Anderson, C. J. (2015). "The influence of land use on forest structure, species composition, and soil conditions in headwater-slope wetlands of coastal Alabama, USA." International Journal of Biodiversity Science, Ecosystem Services & Management, 11(1), 61–70.

Cook, M. B., and DeBell, K. M. (2002). "Improving Water Quality in Urban Watersheds." American Society of Civil Engineers, 24–34.

Copeland, C. (2016). Clean Water Act: A Summary of the Law. Congressional Research Service, Washington, DC.

Craymer, M. R. (2006). "The evolution of NAD83 in Canada." *Hydroscan*, 91.

Dale, J., Zou, C. B., Andrews, W. J., Long, J. M., Liang, Y., and Qiao, L. (2015). "Climate, water use, and land surface transformation in an irrigation intensive watershed—Streamflow responses from 1950 through 2010." Agricultural Water Management, 160, 144–152.

Diem, J. E., Hill, T. C., and Milligan, R. A. (2017). "Diverse multi-decadal changes in streamflow within a rapidly urbanizing region." Journal of Hydrology, 556, 61–71.

Dow, C. L. (2007). "Assessing regional land-use/cover influences on New Jersey Pinelands streamflow through hydrograph analysis." Hydrological Processes, 21(2), 185–197.

Eckhardt, K. (2008). "A comparison of baseflow indices, which were calculated with seven different baseflow separation methods." Journal of Hydrology, 352(1–2), 168–173.

Environmental Protection Agency South Australia (EPA South Australia). (2017). "Understanding Stormwater". <https://www.epa.sa.gov.au/environmental_info/water_quality/programs/stormwater/understanding_stormwater>. (July 8, 2018).

Environmental Systems Research Institute (ESRI). (2015). ArcGIS Release 10.3.1. Redlands, CA.

Fry, J.A., Coan, M.J., Homer, C.G., Meyer, D.K., and Wickham, J.D., (2009). Completion of the National Land Cover Database (NLCD) 1992-2001 Land Cover Change Retrofit product: U.S. Geological Survey Open-File Report 2008-1379, 18 p.

Fry, J., Xian, G., Jin, S., Dewitz, J., Homer, C., Yang, L., Barnes, C., Herold, N., and Wickham, J., (2011). Completion of the 2006 National Land Cover Database for the Conterminous United States, PE&RS, Vol. 77(9):858-864.

Galavotti, H. (2016). "Summary of State Post Construction Stormwater Standards." United States Environmental Protection Agency, <https://www.epa.gov/sites/production/files/2016-08/documents/swstdsummary_7-13-16_508.pdf> (Jul. 1, 2018).

Homer, C.G., Dewitz, J.A., Yang, L., Jin, S., Danielson, P., Xian, G., Coulston, J., Herold, N.D., Wickham, J.D., and Megown, K., (2015), Completion of the 2011 National Land Cover Database for the conterminous United States-Representing a decade of land cover change information. Photogrammetric Engineering and Remote Sensing, v. 81, no. 5, p. 345-354

Hopkins, K. G., Morse, N. B., Bain, D. J., Bettez, N. D., Grimm, N. B., Morse, J. L., Palta, M. M., Shuster, W. D., Bratt, A. R., and Suchy, A. K. (2015). "Assessment of Regional Variation in Streamflow Responses to Urbanization and the Persistence of Physiography." Environmental Science & Technology, 49(5), 2724–2732.

Lim, K. J., Engel, B. A., Tang, Z., Choi, J., Kim, K.-S., Muthukrishnan, S., and Tripathy, D. (2005). "AUTOMATED WEB GIS BASED HYDROGRAPH ANALYSIS TOOL, WHAT." JOURNAL OF THE AMERICAN WATER RESOURCES ASSOCIATION, 10.

Maidment, D.R. (1992). Handbook of hydrology. In D.R. Maidment (ed.) McGraw-Hill, New York, NY.

Marsalek, J. (Ed.). (2008). Urban water cycle processes and interactions. Urban water series – UNESCO-IHP, UNESCO Pub.; Taylor & Francis, Paris, France: Leiden, The Netherlands.

Moriasi, D. N., Arnold, J. G., Van Liew, M. W., Bingner, R. L., Harmel, R. D., and Veith, T. L. (2007). "Model Evaluation Guidelines for Systematic Quantification of Accuracy in Watershed Simulations." Transactions of the ASABE, 50(3), 885–900.

Nagy, R. C., Lockaby, B. G., Kalin, L., and Anderson, C. (2012). "Effects of urbanization on stream hydrology and water quality: the Florida Gulf Coast: URBANIZATION EFFECTS ON WATER RESOURCES." Hydrological Processes, 26(13), 2019–2030.

National Research Council. (2002). Riparian Areas: Functions and Strategies for Management. National Academies Press, Washington, D.C.

National Research Council. (2009). Urban Stormwater Management in the United States. National Academies Press, Washington, D.C.

Ouédraogo, W., Raude, J., and Gathenya, J. (2018). “Continuous Modeling of the Mkurumudzi River Catchment in Kenya Using the HEC-HMS Conceptual Model: Calibration, Validation, Model Performance Evaluation and Sensitivity Analysis.” Hydrology, 5(3), 44.

Paul, M. J., and Meyer, J. L. (2001). “Streams in the Urban Landscape.” Annu. Rev. Ecol. Syst., 32, 333–365.

Peel, M. C., and Blöschl, G. (2011). “Hydrological modelling in a changing world.” Progress in Physical Geography, 35(2), 249–261.

Poff, N. L., and Zimmerman, J. K. H. (2010). “Ecological responses to altered flow regimes: a literature review to inform the science and management of environmental flows: Review of altered flow regimes.” Freshwater Biology, 55(1), 194–205.

PRISM Climate Group. Oregon State University. Corvallis, OR. <http://prism.oregonstate.edu>. created 1 May 2018.

Richter, B. D., Baumgartner, J. V., Powell, J., and Braun, D. P. (1996). “A Method for Assessing Hydrologic Alteration within Ecosystems.” Conservation Biology, 10(4), 1163–1174.

Richter, B. D., Baumgartner, J. V., Braun, D. P., and Powell, J. (1998). “A Spatial Assessment of Hydrologic Alteration within a River Network.” Regulated Rivers: Research and Management, 14(4), 329–340.

Rosburg, T. T., Nelson, P. A., and Bledsoe, B. P. (2017). “Effects of Urbanization on Flow Duration and Stream Flashiness: A Case Study of Puget Sound Streams, Western Washington, USA.” JAWRA Journal of the American Water Resources Association, 53(2), 493–507.

Rose, S., and Peters, N. E. (2001). “Effects of urbanization on streamflow in the Atlanta area (Georgia, USA): a comparative hydrological approach.” Hydrological Processes, 15(8), 1441–1457.

Rouhani, H., and Malekian, A. (2013). “Automated Methods for Estimating Baseflow from Streamflow Records in a Semi-Arid Watershed.” 7.

Sanford, W. E., and Selnick, D. L. (2013). “Estimation of Evapotranspiration Across the Conterminous United States Using a Regression with Climate and Land-Cover Data 1: Estimation of Evapotranspiration Across the Conterminous United States Using a Regression with Climate and Land-Cover Data.” JAWRA Journal of the American Water Resources Association, 49(1), 217–230.

Sankarasubramanian, A., and Vogel, R. M. (2003). “Hydroclimatology of the continental United States: U.S. HYDROCLIMATOLOGY.” Geophysical Research Letters, 30(7).

Sankarasubramanian, A., Vogel, R. M., and Limbrunner, J. F. (2001). “Climate elasticity of streamflow in the United States.” Water Resources Research, 37(6), 1771–1781.

Sawicz, K. A., Kelleher, C., Wagener, T., Troch, P., Sivapalan, M., and Carrillo, G. (2014). “Characterizing hydrologic change through catchment classification.” Hydrology and Earth System Sciences, 18(1), 273–285.

Sawicz, K., Wagener, T., Sivapalan, M., Troch, P. A., and Carrillo, G. (2011). “Catchment classification: empirical analysis of hydrologic similarity based on catchment function in the eastern USA.” Hydrology and Earth System Sciences, 15(9), 2895–2911.

Schoonover, J. E., Lockaby, B. G., and Helms, B. S. (2006). “Impacts of Land Cover on Stream Hydrology in the West Georgia Piedmont, USA.” Journal of Environment Quality, 35(6), 2123.

Stenseth, N. C., Ottersen, G., Hurrell, J. W., Mysterud, A., Lima, M., Chan, K.-S., Yoccoz, N. G., and Adlandsvik, B. (2003). “Review article. Studying climate effects on ecology through the use of climate indices: The North Atlantic Oscillation, El Nino Southern Oscillation and beyond.” Proceedings of the Royal Society B: Biological Sciences, 270(1529), 2087–2096.

Teutschbein, C., Grabs, T., Karlsen, R. H., Laudon, H., and Bishop, K. (2015). “Hydrological response to changing climate conditions: Spatial streamflow variability in the boreal region: HYDROLOGICAL RESPONSE TO CHANGING CLIMATE CONDITIONS.” Water Resources Research, 51(12), 9425–9446.

United States Army Corps of Engineers (USACE). (2000). “Hydrologic Modeling System HEC-HMS.” Technical Reference Manual, United States Army Corps of Engineers, Hydrologic Engineering Center, 148.

United States Environmental Protection Agency (US EPA). (1992). Environmental impacts of storm water discharges: a national profile. Washington, DC.

United States Geological Survey (USGS). (2016). “Summary of the Water Cycle”. <https://water.usgs.gov/edu/watercyclesummary.html>. (July 8, 2018).

Walsh, C. J., Roy, A. H., Feminella, J. W., Cottingham, P. D., Groffman, P. M., and Morgan, R. P. (2005). “The urban stream syndrome: current knowledge and the search for a cure.” J. North Am. Benthol. Soc., 24(3), 706–723.

Wang, L., Lyons, J., Kanehl, P., and Bannerman, R. (2001). “Impacts of Urbanization on Stream Habitat and Fish Across Multiple Spatial Scales.” Environmental Management, 28(2), 255–266.

White, M. D., and Greer, K. A. (2006). “The effects of watershed urbanization on the stream hydrology and riparian vegetation of Los Peñasquitos Creek, California.” Landscape and Urban Planning, 74(2), 125–138.

Xian, G., Homer, C., Dewitz, J., Fry, J., Hossain, N., and Wickham, J., (2011). The change of impervious surface area between 2001 and 2006 in the conterminous United States. Photogrammetric Engineering and Remote Sensing, Vol. 77(8): 758-762.

Yadav, M., Wagener, T., and Gupta, H. (2007). Regionalization of constraints on expected watershed response, Adv.Water Resour., 30, 1756–1774.

Appendices

Appendix A: NLCD Information

Appendix B: IHA Results

Appendix C: Streamflow Signature Analysis Results

Appendix D: HEC-HMS Model Results

Appendix A: NLCD Information

NLCD Classification Changes

Table A-1: NLCD 1992/2001 Classification Change ID Numbers

NLCD 1992/2001 Classification Change ID Numbers		FROM 1992 CLASSIFICATION								
		Anderson Level 1	Open water	Urban	Barren	Forest	Grass/shrub	Agriculture	Wetland	Ice/snow
TO 2001 CLASSIFICATION	Anderson Level 1	-	1	2	3	4	5	6	7	8
	Open water	1	*	21	31	41	51	61	71	81
	Urban	2	12	*	32	42	52	62	72	82
	Barren	3	13	23	*	43	53	63	73	83
	Forest	4	14	24	34	*	54	64	74	84
	Grass/shrub	5	15	25	35	45	*	65	75	85
	Agriculture	6	16	26	36	46	56	*	76	86
	Wetland	7	17	27	37	47	57	67	*	87
	Ice/snow	8	18	28	38	48	58	68	78	*

Notes: * Classification Unchanged

Table A-2: NLCD 2001/2006 Classification Change ID Numbers

NLCD 2001/2006 Classification Change ID Numbers		FROM 2001 CLASSIFICATION																
		Unclassified	Open Water	Perennial Ice/Snow	Developed-Open Space	Developed-Low Intensity	Developed-Medium Intensity	Developed-High Intensity	Barren Land	Deciduous Forest	Evergreen Forest	Mixed Forest	Shrub/Scrub	Grassland/Herbaceous	Pasture/Hay	Cultivated Crops	Woody Wetlands	Herbaceous Wetlands
TO 2006 CLASSIFICATION	Unclassified	1 [1]	18	35	52	69	86	103	120	137	154	171	188	205	222	239	256	273
	Open Water	2	19 [1]	36	53	70	87	104	121	138	155	172	189	206	223	240	257	274
	Perennial Ice/Snow	3	20	37 [1]	54	71	88	105	122	139	156	173	190	207	224	241	258	275
	Developed-Open Space	4	21	38	55 [1]	72	89	106	123	140	157	174	191	208	225	242	259	276
	Developed-Low Intensity	5	22	39	56	73 [1]	90	107	124	141	158	175	192	209	226	243	260	277
	Developed-Medium Intensity	6	23	40	57	74	91 [1]	108	125	142	159	176	193	210	227	244	261	278
	Developed-High Intensity	7	24	41	58	75	92	109 [1]	126	143	160	177	194	211	228	245	262	279
	Barren Land	8	25	42	59	76	93	110	127 [1]	144	161	178	195	212	229	246	263	280
	Deciduous Forest	9	26	43	60	77	94	111	128	145 [1]	162	179	196	213	230	247	264	281
	Evergreen Forest	10	27	44	61	78	95	112	129	146	163 [1]	180	197	214	231	248	265	282
	Mixed Forest	11	28	45	62	79	96	113	130	147	164	181 [1]	198	215	232	249	266	283
	Shrub/Scrub	12	29	46	63	80	97	114	131	148	165	182	199 [1]	216	233	250	267	284
	Grassland/Herbaceous	13	30	47	64	81	98	115	132	149	166	183	200	217 [1]	234	251	268	285
	Pasture/Hay	14	31	48	65	82	99	116	133	150	167	184	201	218	235 [1]	252	269	286
	Cultivated Crops	15	32	49	66	83	100	117	134	151	168	185	202	219	236	253 [1]	270	287
	Woody Wetlands	16	33	50	67	84	101	118	135	152	169	186	203	220	237	254	271 [1]	288
	Herbaceous Wetlands	17	34	51	68	85	102	119	136	153	170	187	204	221	238	255	272	289 [1]

Notes: [1] Classification Unchanged

Table A-3: NLCD 2006/2011 Classification Change ID Numbers

NLCD 2006/2011 Classification Change ID Numbers		FROM 2006 CLASSIFICATION																
		Unclassified	Open Water	Perennial Ice/Snow	Developed-Open Space	Developed-Low Intensity	Developed-Medium Intensity	Developed-High Intensity	Barren Land	Deciduous Forest	Evergreen Forest	Mixed Forest	Shrub/Scrub	Grassland/Herbaceous	Pasture/Hay	Cultivated Crops	Woody Wetlands	Herbaceous Wetlands
TO 2011 CLASSIFICATION	Unclassified	1 [1]	18	35	52	69	86	103	120	137	154	171	188	205	222	239	256	273
	Open Water	2	19 [1]	36	53	70	87	104	121	138	155	172	189	206	223	240	257	274
	Perennial Ice/Snow	3	20	37 [1]	54	71	88	105	122	139	156	173	190	207	224	241	258	275
	Developed-Open Space	4	21	38	55 [1]	72	89	106	123	140	157	174	191	208	225	242	259	276
	Developed-Low Intensity	5	22	39	56	73 [1]	90	107	124	141	158	175	192	209	226	243	260	277
	Developed-Medium Intensity	6	23	40	57	74	91 [1]	108	125	142	159	176	193	210	227	244	261	278
	Developed-High Intensity	7	24	41	58	75	92	109 [1]	126	143	160	177	194	211	228	245	262	279
	Barren Land	8	25	42	59	76	93	110	127 [1]	144	161	178	195	212	229	246	263	280
	Deciduous Forest	9	26	43	60	77	94	111	128	145 [1]	162	179	196	213	230	247	264	281
	Evergreen Forest	10	27	44	61	78	95	112	129	146	163 [1]	180	197	214	231	248	265	282
	Mixed Forest	11	28	45	62	79	96	113	130	147	164	181 [1]	198	215	232	249	266	283
	Shrub/Scrub	12	29	46	63	80	97	114	131	148	165	182	199 [1]	216	233	250	267	284
	Grassland/Herbaceous	13	30	47	64	81	98	115	132	149	166	183	200	217 [1]	234	251	268	285
	Pasture/Hay	14	31	48	65	82	99	116	133	150	167	184	201	218	235 [1]	252	269	286
	Cultivated Crops	15	32	49	66	83	100	117	134	151	168	185	202	219	236	253 [1]	270	287
	Woody Wetlands	16	33	50	67	84	101	118	135	152	169	186	203	220	237	254	271 [1]	288
	Herbaceous Wetlands	17	34	51	68	85	102	119	136	153	170	187	204	221	238	255	272	289 [1]

Notes: [1] Classification Unchanged

NLCD Urbanization Area Change Comparison

NLCD 1992 to 2001 (U1)			
Classification Change	**Class Value**	**Count**	**Area (mi^2)**
Open Water to Urban	12	21	0.0073
Barren to Urban	32	17	0.0059
Forest to Urban	42	6019	2.0915
Grass/Shrub to Urban	52	30	0.0104

NLCD 1992 to 2001 (U2)			
Classification Change	**Class Value**	**Count**	**Area (mi^2)**
Open Water to Urban	12	77	0.0268
Forest to Urban	42	34162	11.8710
Agriculture to Urban	62	722	0.2509

NLCD 2001 to 2006 (U1)			
Classification Change	**Class Value**	**Count**	**Area (mi^2)**
Open Water to Developed - Open Space	21	23	0.0080
Open Water to Developed - Low Intensity	22	28	0.0097
Open Water to Developed - Medium Intensity	23	48	0.0167
Open Water to Developed - High Intensity	24	24	0.0083
Barren Land to Developed - Open Space	123	52	0.0181
Barren Land to Developed - Low Intensity	124	44	0.0153
Barren Land to Developed - Medium Intensity	125	51	0.0177
Barren Land to Developed - High Intensity	126	36	0.0125
Deciduous Forest to Developed - Open Space	140	1039	0.3610
Deciduous Forest to Developed - Low Intensity	141	629	0.2186
Deciduous Forest to Developed - Medium Intensity	142	237	0.0824
Deciduous Forest to Developed - High Intensity	143	71	0.0247
Evergreen Forest to Developed - Open Space	157	413	0.1435
Evergreen Forest to Developed - Low Intensity	158	309	0.1074
Evergreen Forest to Developed - Medium Intensity	159	155	0.0539
Evergreen Forest to Developed - High Intensity	160	63	0.0219
Mixed Forest to Developed - Open Space	174	272	0.0945
Mixed Forest to Developed - Low Intensity	175	178	0.0619
Mixed Forest to Developed - Medium Intensity	176	67	0.0233

Mixed Forest to Developed - High Intensity	177	13	0.0045
Shrub/Scrub to Developed - Open Space	191	306	0.1063
Shrub/Scrub to Developed - Low Intensity	192	205	0.0712
Shrub/Scrub to Developed - Medium Intensity	193	105	0.0365
Shrub/Scrub to Developed - High Intensity	194	34	0.0118
Grassland/Herbaceous to Developed - Open Space	208	214	0.0744
Grassland/Herbaceous to Developed - Low Intensity	209	195	0.0678
Grassland/Herbaceous to Developed - Medium Intensity	210	74	0.0257
Grassland/Herbaceous to Developed - High Intensity	211	24	0.0083
Pasture/Hay to Developed - Open Space	225	258	0.0897
Pasture/Hay to Developed - Low Intensity	226	193	0.0671
Pasture/Hay to Developed - Medium Intensity	227	90	0.0313
Pasture/Hay to Developed - High Intensity	228	26	0.0090
Cultivated Crops to Developed - Open Space	242	89	0.0309
Cultivated Crops to Developed - Low Intensity	243	91	0.0316
Cultivated Crops to Developed - Medium Intensity	244	65	0.0226
Cultivated Crops to Developed - High Intensity	245	21	0.0073
Woody Wetlands to Developed - Open Space	259	59	0.0205
Woody Wetlands to Developed - Low Intensity	260	39	0.0136
Woody Wetlands to Developed - Medium Intensity	261	16	0.0056
Woody Wetlands to Developed - High Intensity	262	5	0.0017

NLCD 2001 to 2006 (U2)			
Classification Change	**Class Value**	**Count**	**Area (mi^2)**
Open Water to Developed - Open Space	21	72	0.0250
Open Water to Developed - Low Intensity	22	13	0.0045
Open Water to Developed - Medium Intensity	23	5	0.0017
Barren Land to Developed - Open Space	123	343	0.1192
Barren Land to Developed - Low Intensity	124	761	0.2644
Barren Land to Developed - Medium Intensity	125	468	0.1626
Barren Land to Developed - High Intensity	126	113	0.0393
Deciduous Forest to Developed - Open Space	140	5833	2.0269
Deciduous Forest to Developed - Low Intensity	141	3921	1.3625
Deciduous Forest to Developed - Medium Intensity	142	1201	0.4173
Deciduous Forest to Developed - High Intensity	143	296	0.1029
Evergreen Forest to Developed - Open Space	157	5291	1.8386
Evergreen Forest to Developed - Low Intensity	158	4977	1.7295
Evergreen Forest to Developed - Medium Intensity	159	1656	0.5754

Evergreen Forest to Developed - High Intensity	160	293	0.1018
Mixed Forest to Developed - Open Space	174	124	0.0431
Mixed Forest to Developed - Low Intensity	175	92	0.0320
Mixed Forest to Developed - Medium Intensity	176	22	0.0076
Mixed Forest to Developed - High Intensity	177	15	0.0052
Shrub/Scrub to Developed - Open Space	191	276	0.0959
Shrub/Scrub to Developed - Low Intensity	192	194	0.0674
Shrub/Scrub to Developed - Medium Intensity	193	42	0.0146
Shrub/Scrub to Developed - High Intensity	194	15	0.0052
Grassland/Herbaceous to Developed - Open Space	208	692	0.2405
Grassland/Herbaceous to Developed - Low Intensity	209	725	0.2519
Grassland/Herbaceous to Developed - Medium Intensity	210	332	0.1154
Grassland/Herbaceous to Developed - High Intensity	211	90	0.0313
Pasture/Hay to Developed - Open Space	225	2219	0.7711
Pasture/Hay to Developed - Low Intensity	226	2297	0.7982
Pasture/Hay to Developed - Medium Intensity	227	805	0.2797
Pasture/Hay to Developed - High Intensity	228	255	0.0886
Woody Wetlands to Developed - Open Space	259	221	0.0768
Woody Wetlands to Developed - Low Intensity	260	65	0.0226
Woody Wetlands to Developed - Medium Intensity	261	29	0.0101

NLCD 2006 to 2011 (U1)			
Classification Change	**Class Value**	**Count**	**Area (mi^2)**
Open Water to Developed - Open Space	21	2	0.0007
Open Water to Developed - High Intensity	24	8	0.0028
Barren Land to Developed - Open Space	123	79	0.0275
Barren Land to Developed - Low Intensity	124	95	0.0330
Barren Land to Developed - Medium Intensity	125	68	0.0236
Barren Land to Developed - High Intensity	126	65	0.0226
Deciduous Forest to Developed - Open Space	140	292	0.1015
Deciduous Forest to Developed - Low Intensity	141	170	0.0591
Deciduous Forest to Developed - Medium Intensity	142	120	0.0417
Deciduous Forest to Developed - High Intensity	143	184	0.0639
Evergreen Forest to Developed - Open Space	157	177	0.0615
Evergreen Forest to Developed - Low Intensity	158	135	0.0469
Evergreen Forest to Developed - Medium Intensity	159	98	0.0341
Evergreen Forest to Developed - High Intensity	160	84	0.0292
Mixed Forest to Developed - Open Space	174	80	0.0278

Mixed Forest to Developed - Low Intensity	175	47	0.0163
Mixed Forest to Developed - Medium Intensity	176	45	0.0156
Mixed Forest to Developed - High Intensity	177	37	0.0129
Shrub/Scrub to Developed - Open Space	191	98	0.0341
Shrub/Scrub to Developed - Low Intensity	192	66	0.0229
Shrub/Scrub to Developed - Medium Intensity	193	43	0.0149
Shrub/Scrub to Developed - High Intensity	194	20	0.0069
Grassland/Herbaceous to Developed - Open Space	208	25	0.0087
Grassland/Herbaceous to Developed - Low Intensity	209	32	0.0111
Grassland/Herbaceous to Developed - Medium Intensity	210	16	0.0056
Grassland/Herbaceous to Developed - High Intensity	211	9	0.0031
Pasture/Hay to Developed - Open Space	225	248	0.0862
Pasture/Hay to Developed - Low Intensity	226	151	0.0525
Pasture/Hay to Developed - Medium Intensity	227	76	0.0264
Pasture/Hay to Developed - High Intensity	228	62	0.0215
Cultivated Crops to Developed - Open Space	242	40	0.0139
Cultivated Crops to Developed - Low Intensity	243	18	0.0063
Cultivated Crops to Developed - Medium Intensity	244	3	0.0010
Cultivated Crops to Developed - High Intensity	245	7	0.0024
Woody Wetlands to Developed - Open Space	259	18	0.0063
Woody Wetlands to Developed - Low Intensity	260	7	0.0024
Woody Wetlands to Developed - Medium Intensity	261	9	0.0031
Woody Wetlands to Developed - High Intensity	262	28	0.0097

NLCD 2006 to 2011 (U2)			
Classification Change	**Class Value**	**Count**	**Area (mi^2)**
Open Water to Developed - Open Space	21	23	0.0080
Open Water to Developed - Low Intensity	22	10	0.0035
Open Water to Developed - Medium Intensity	23	2	0.0007
Open Water to Developed - High Intensity	24	11	0.0038
Barren Land to Developed - Open Space	123	39	0.0136
Barren Land to Developed - Low Intensity	124	67	0.0233
Barren Land to Developed - Medium Intensity	125	34	0.0118
Barren Land to Developed - High Intensity	126	45	0.0156
Deciduous Forest to Developed - Open Space	140	1627	0.5654
Deciduous Forest to Developed - Low Intensity	141	912	0.3169
Deciduous Forest to Developed - Medium Intensity	142	305	0.1060
Deciduous Forest to Developed - High Intensity	143	88	0.0306

Evergreen Forest to Developed - Open Space	157	2097	0.7287
Evergreen Forest to Developed - Low Intensity	158	1345	0.4674
Evergreen Forest to Developed - Medium Intensity	159	340	0.1181
Evergreen Forest to Developed - High Intensity	160	86	0.0299
Mixed Forest to Developed - Open Space	174	40	0.0139
Mixed Forest to Developed - Low Intensity	175	12	0.0042
Mixed Forest to Developed - Medium Intensity	176	8	0.0028
Mixed Forest to Developed - High Intensity	177	8	0.0028
Shrub/Scrub to Developed - Open Space	191	102	0.0354
Shrub/Scrub to Developed - Low Intensity	192	59	0.0205
Shrub/Scrub to Developed - Medium Intensity	193	9	0.0031
Grassland/Herbaceous to Developed - Open Space	208	463	0.1609
Grassland/Herbaceous to Developed - Low Intensity	209	368	0.1279
Grassland/Herbaceous to Developed - Medium Intensity	210	89	0.0309
Grassland/Herbaceous to Developed - High Intensity	211	16	0.0056
Pasture/Hay to Developed - Open Space	225	1602	0.5567
Pasture/Hay to Developed - Low Intensity	226	1153	0.4007
Pasture/Hay to Developed - Medium Intensity	227	304	0.1056
Pasture/Hay to Developed - High Intensity	228	177	0.0615
Woody Wetlands to Developed - Open Space	259	54	0.0188
Woody Wetlands to Developed - Low Intensity	260	21	0.0073
Woody Wetlands to Developed - Medium Intensity	261	1	0.0003
Woody Wetlands to Developed - High Intensity	262	1	0.0003

Appendix B: IHA Results

IHA Parameter Significance Test

IHA Parameter Significance Test				
IHA Parameter	**U1 p-Value**	**C1 p-Value**	**U2 p-Value**	**C2 p-Value**
October	0.5	0.5	0.5	0.5
November	0.5	0.5	0.5	0.5
December	0.5	0.5	0.5	0.5
January	0.5	0.5	0.5	0.5
February	0.25	0.25	0.25	0.1
March	0.25	0.25	0.25	0.5
April	0.25	0.25	0.25	0.05
May	0.5	0.5	0.5	0.5
June	0.25	0.5	0.25	0.5
July	0.5	0.5	0.5	0.5
August	0.05	0.25	0.1	0.5
September	0.5	0.5	0.5	0.5
1-day minimum	0.025	0.5	0.25	0.05
3-day minimum	0.025	0.5	0.25	0.05
7-day minimum	0.025	0.5	0.25	0.025
30-day minimum	0.25	0.5	0.25	0.005
90-day minimum	0.25	0.5	0.25	0.1
1-day maximum	0.05	0.5	0.5	0.25
3-day maximum	0.05	0.5	0.5	0.25
7-day maximum	0.05	0.5	0.5	0.5
30-day maximum	0.05	0.25	0.5	0.25
90-day maximum	0.05	0.25	0.5	0.5
Number of zero days	0.5	0.5	0.5	0.1
Base flow index	0.5	0.5	0.1	0.05
Date of minimum	0.25	0.5	0.5	0.5
Date of maximum	0.5	0.5	0.25	0.5
Low pulse count	0.05	0.5	0.025	0.025
Low pulse duration	0.5	0.5	0.5	0.1

High pulse count	0.25	0.5	0.5	0.5
High pulse duration	0.25	0.025	0.25	0.5
Rise rate	0.025	0.25	0.5	0.5
Fall rate	0.01	0.1	0.5	0.5
Number of reversals	0.1	0.05	0.1	0.5
October Low Flow	0.5	0.5	0.5	0.5
November Low Flow	0.5	0.5	0.5	0.5
December Low Flow	0.5	0.5	0.5	0.025
January Low Flow	0.5	0.5	0.5	0.1
February Low Flow	0.5	0.5	0.5	0.025
March Low Flow	0.025	0.5	0.5	0.5
April Low Flow	0.5	0.5	0.5	0.05
May Low Flow	0.5	0.5	0.25	0.005
June Low Flow	0.25	0.5	0.1	0.25
July Low Flow	0.25	0.5	0.5	0.25
August Low Flow	0.25	0.5	0.5	0.5
September Low Flow	0.5	0.25	0.5	0.5
Extreme low peak	0.1	0.25	0.25	0.05
Extreme low duration	0.5	0.1	0.5	0.1
Extreme low timing	0.25	0.5	0.5	0.5
Extreme low freq.	0.01	0.5	0.005	0.01
High flow peak	0.25	0.5	0.5	0.005
High flow duration	0.1	0.5	0.25	0.5
High flow timing	0.5	0.5	0.25	0.5
High flow frequency	0.5	0.5	0.5	0.5
High flow rise rate	0.1	0.5	0.005	0.001
High flow fall rate	0.005	0.5	0.025	0.001
Small Flood peak	0.5	0.5	0.1	0.1
Small Flood duration	0.5	0.5	0.25	0.5
Small Flood timing	0.5	0.5	0.5	0.5
Small Flood freq.	0.5	0.5	0.5	0.25
Small Flood rise rate	0.05	0.5	0.5	0.5
Small Flood fallrate	0.5	0.5	0.5	0.5
Large flood peak	0.1	0.5	0.5	0.5
Large flood duration	0.5	0.5	0.5	0.5
Large flood timing	0.5	0.1	0.001	0.5
Large flood freq.	0.1	0.5	0.5	0.5
Large flood rise rate	0.5	0.1	0.5	0.5
Large flood fallrate	0.1	0.5	0.5	0.5

Ecological Impacts

(Reference: Poff and Zimmerman, 2010)

Flow component	Organism(s) studied	Total no. papers	No. papers reporting decreased ecological responses	No. papers reporting increased ecological responses	Primary flow alteration	No. papers	Common ecological responses
Magnitude	Aquatic	71	66	5	Stabilisation (loss of extreme high and/or low flows)	31	Loss of sensitive species Reduced diversity Altered assemblages and dominant taxa Reduced abundance Increase in non-natives
					Greater magnitude of extreme high and/or low flows	23	Life cycle disruption Reduced species richness Altered assemblages and relative abundance of taxa Loss of sensitive species
	Riparian	28	24	7	Stabilisation (loss of peak flows)	18	Altered recruitment; failure of seedling establishment Terrestrialisation of flora Increased success of nonnatives Lower species richness Vegetation encroachment into channels Increased riparian cover Altered assemblages
Frequency	Aquatic	12	12	1	Decreased frequency of peak flows	8	Aseasonal reproduction Reduced reproduction Decreased abundance or extirpation of native fishes Decreased richness of endemic and sensitive species Reduced habitat for young fishes
	Riparian	4	4	2	Decreased frequency of peak flows	4	Shift in community composition Reductions in species richness Increase in wood production

Flow component	Organism(s) studied	Total no. papers	No. papers reporting decreased ecological responses	No. papers reporting increased ecological responses	Primary flow alteration	No. papers	Common ecological responses
Duration	Aquatic	7	7	1	Decreased duration of floodplain inundation	4	Decreased abundance of young fish Change in juvenile fish assemblage Loss of floodplain specialists in mollusk assemblage
	Riparian	18	17	1	Decreased duration of floodplain inundation	13	Reduced growth rate or mortality Altered assemblages Terrestrialisation or desertification of species composition Reduced area of riparian plant or forest cover Increase in abundance of nonnatives
Timing	Aquatic	12	12	0	Shifts in seasonality of peak flows	12	Disruption of spawning cues Decreased reproduction and recruitment Change in assemblage structure
					Increased predictability	5	Change in diversity and assemblages structure Disruption of spawning cues Decreased reproduction and recruitment
	Riparian	4	4	0	Loss of seasonal flow peaks	4	Reduced riparian plant recruitment Invasion of exotic riparian plant species Reduced plant growth and increased mortality Reduction in species richness and plant cover
Rate of change	Aquatic	3	2	2	Reduced variability	2	Increase in crayfish abundance Increase in schistosomiasis
	Riparian	2	2	0	Increased variability	2	Decreased germination survival and growth of plants Decreased abundance and change in species assemblage of waterbirds
Not specified	Aquatic	4	2	2	River regulation; type unspecified	4	Decrease in species richness Increased abundance of some macroinvertebrate taxa No change

Appendix C: Streamflow Signature Analysis Results

Flow Duration Curves

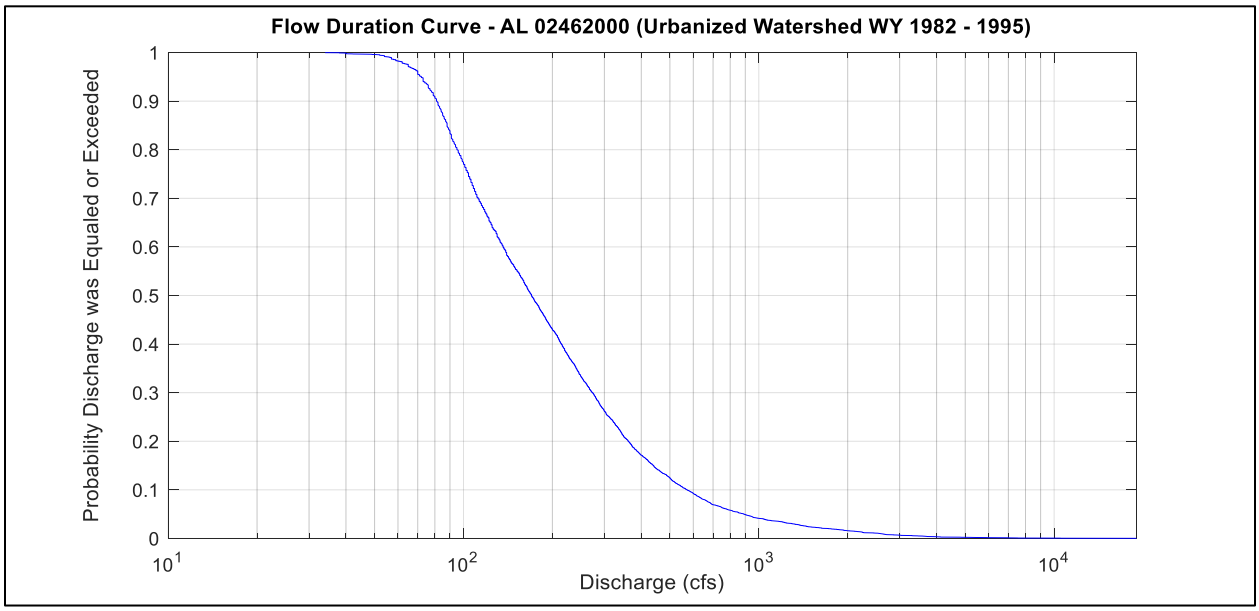

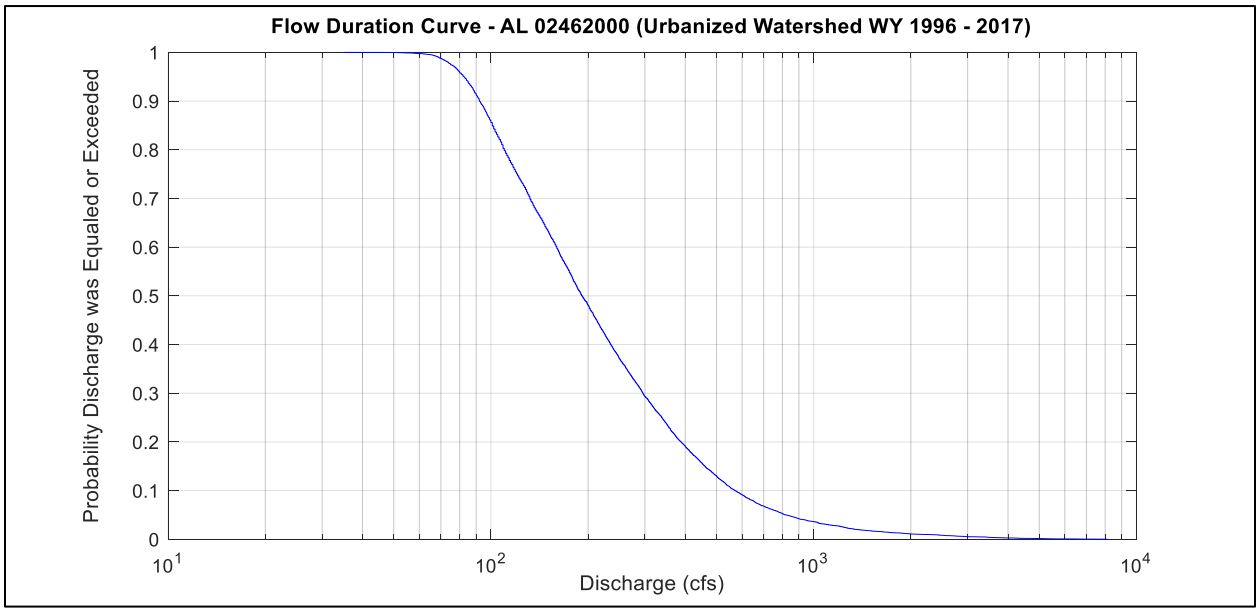

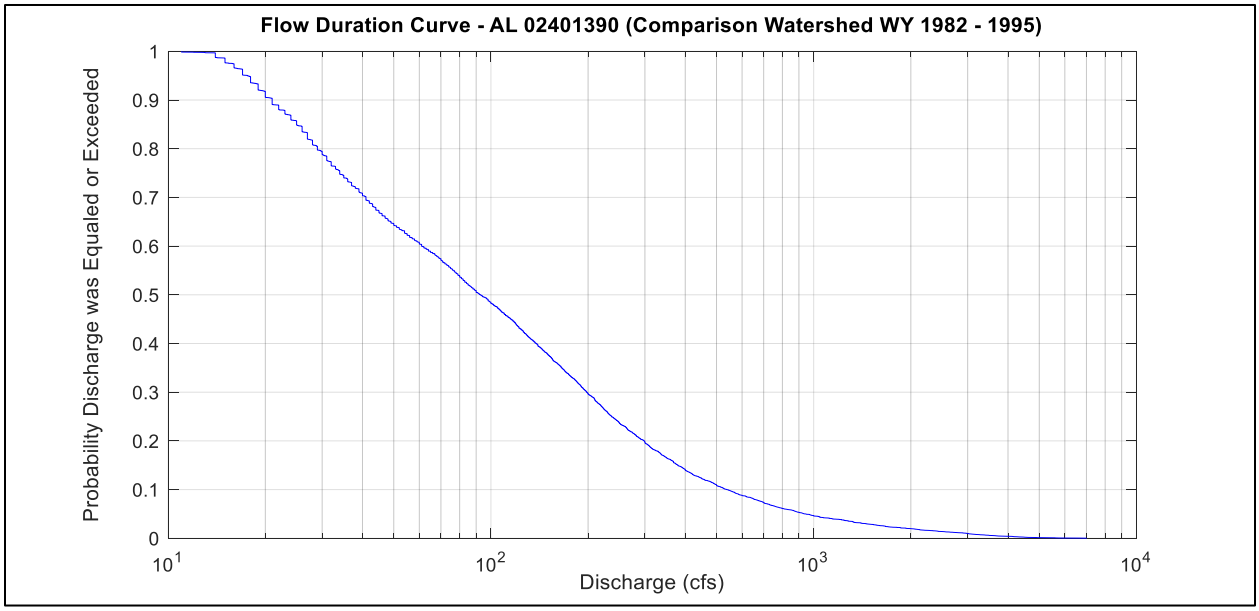
Flow Duration Curve - AL 02401390 (Comparison Watershed WY 1982 - 1995)
Probability Discharge was Equaled or Exceeded
Discharge (cfs)
0
0.1
0.2
0.3
0.4
0.5
0.6
0.7
0.8
0.9
1
10^1
10^2
10^3
10^4

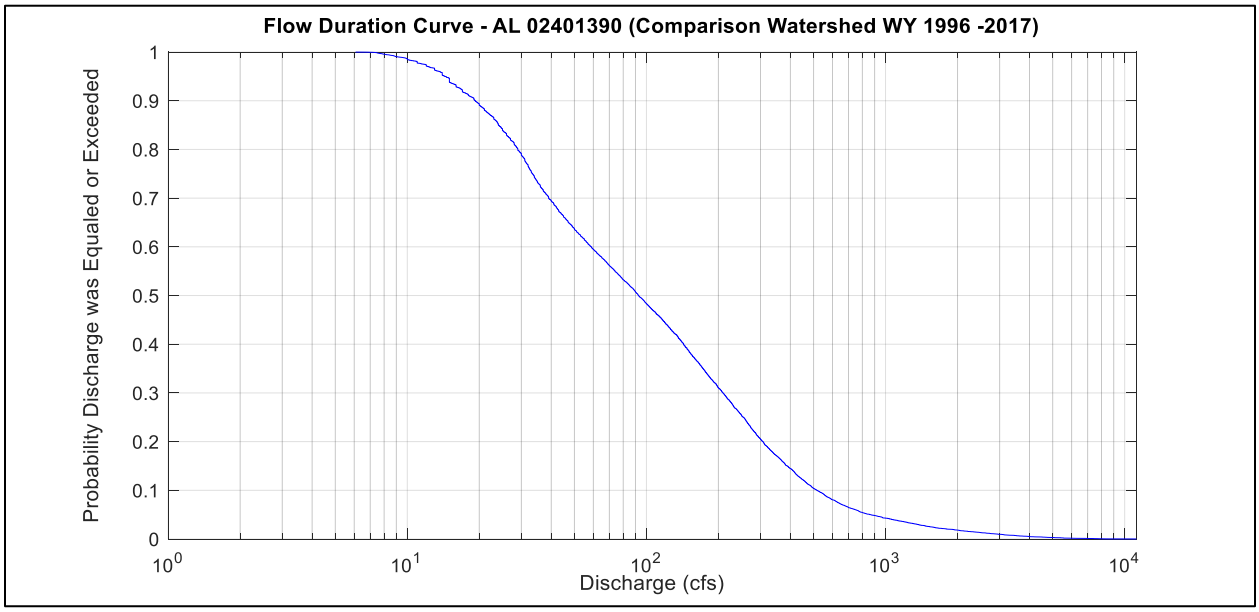
Flow Duration Curve - AL 02401390 (Comparison Watershed WY 1996 -2017)
Probability Discharge was Equaled or Exceeded
Discharge (cfs)
0
0.1
0.2
0.3
0.4
0.5
0.6
0.7
0.8
0.9
1
10^0
10^1
10^2
10^3
10^4

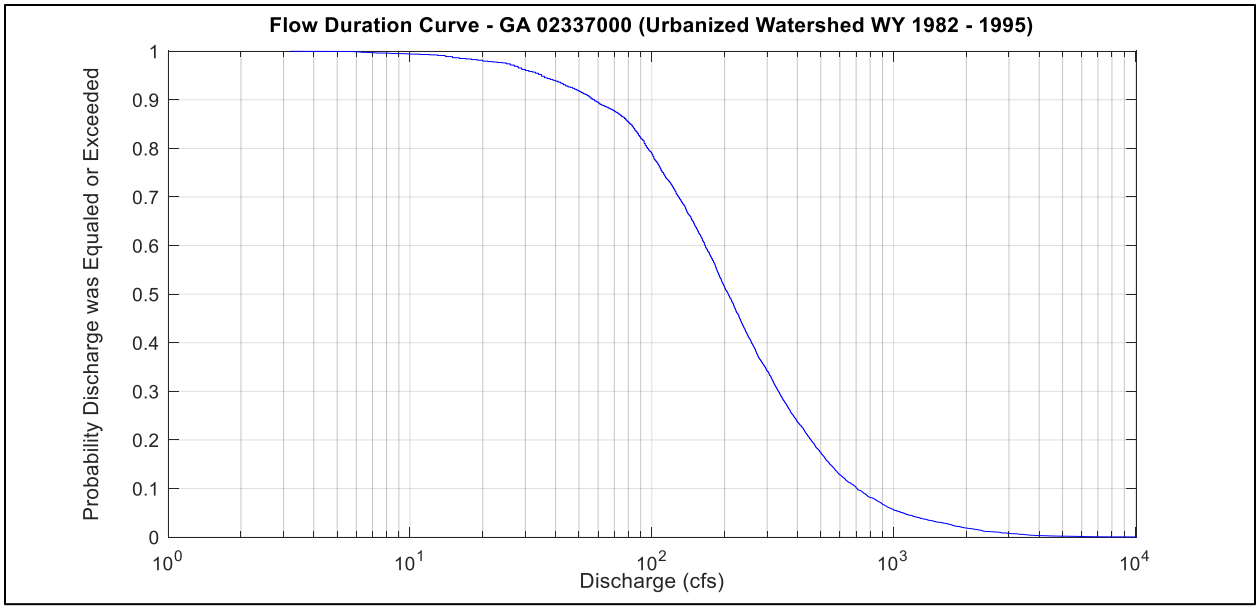
Flow Duration Curve - GA 02337000 (Urbanized Watershed WY 1982 - 1995)
Probability Discharge was Equaled or Exceeded
Discharge (cfs)

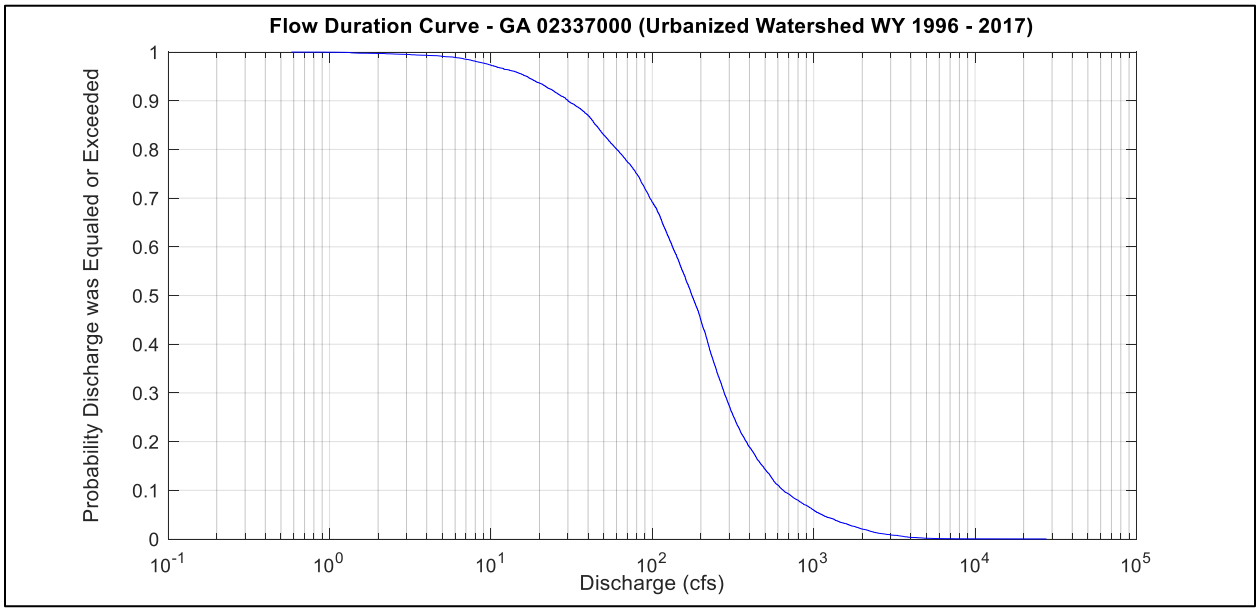
Flow Duration Curve - GA 02337000 (Urbanized Watershed WY 1996 - 2017)
Probability Discharge was Equaled or Exceeded
Discharge (cfs)

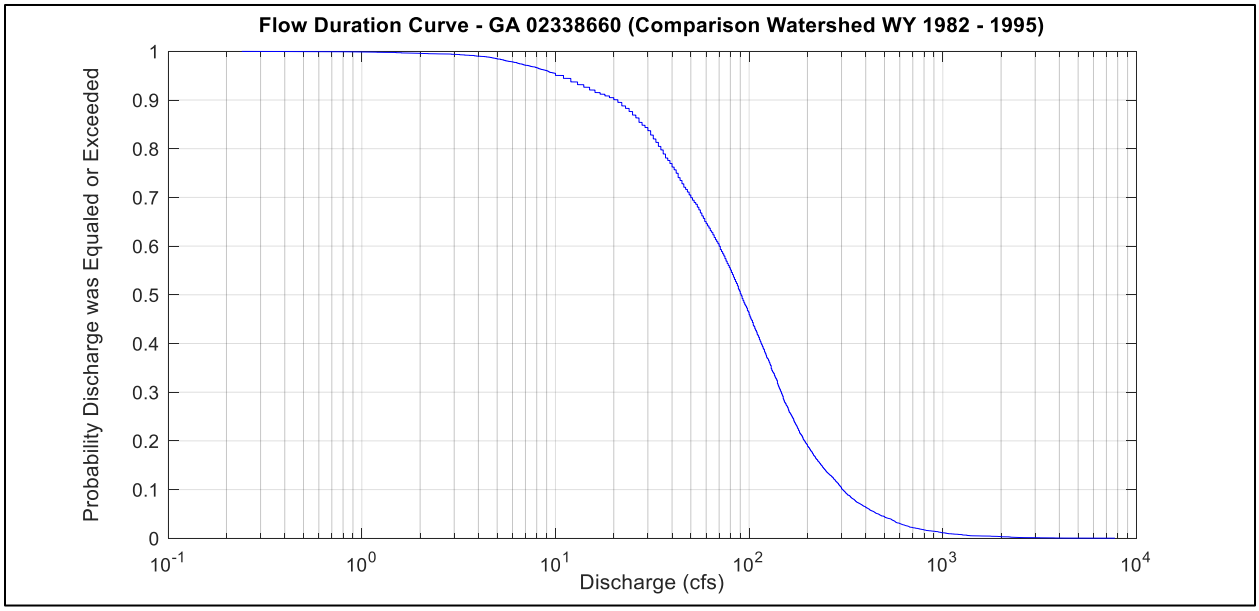
Flow Duration Curve - GA 02338660 (Comparison Watershed WY 1982 - 1995)
Probability Discharge was Equaled or Exceeded
Discharge (cfs)

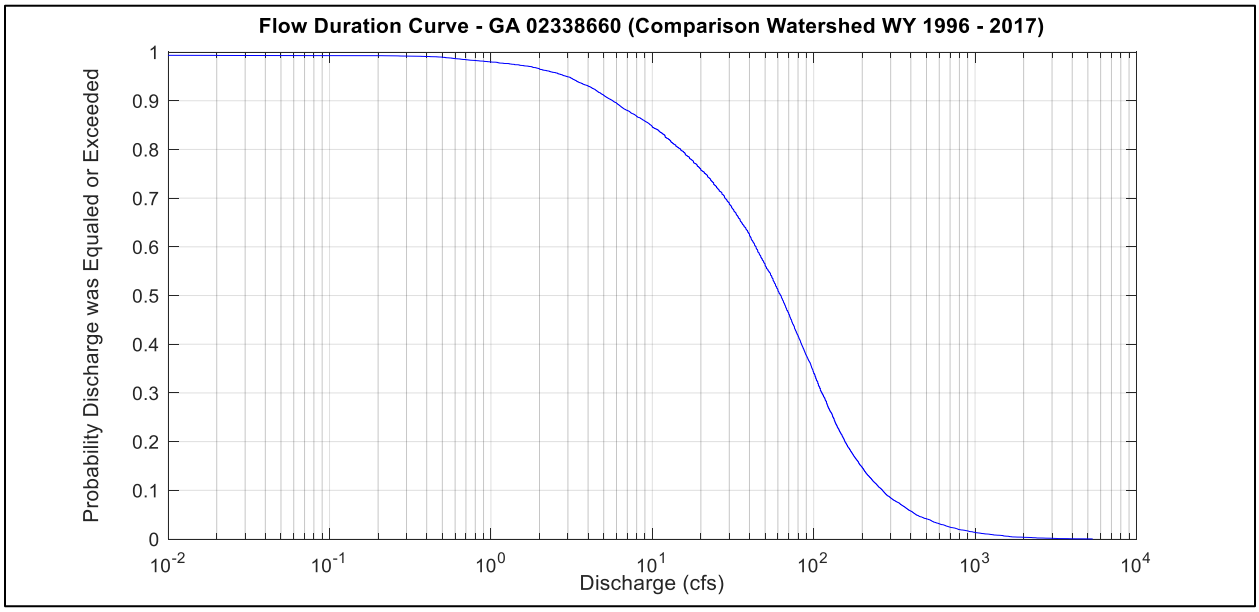
Flow Duration Curve - GA 02338660 (Comparison Watershed WY 1996 - 2017)
Probability Discharge was Equaled or Exceeded
Discharge (cfs)

Hydrographs

U1 Hydrographs:

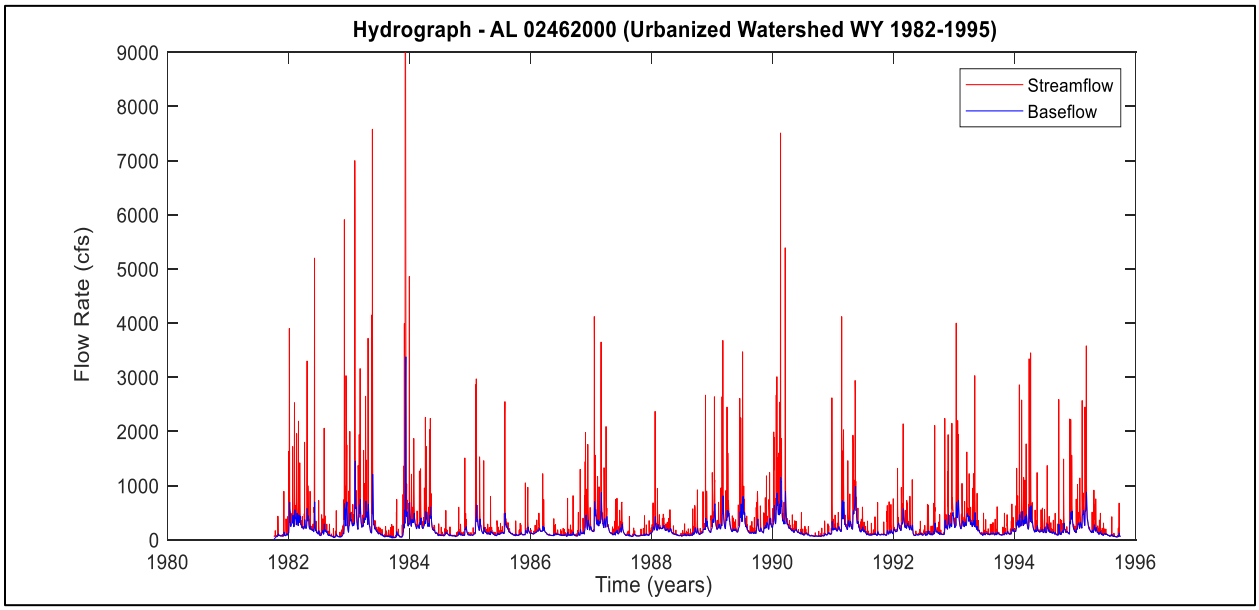

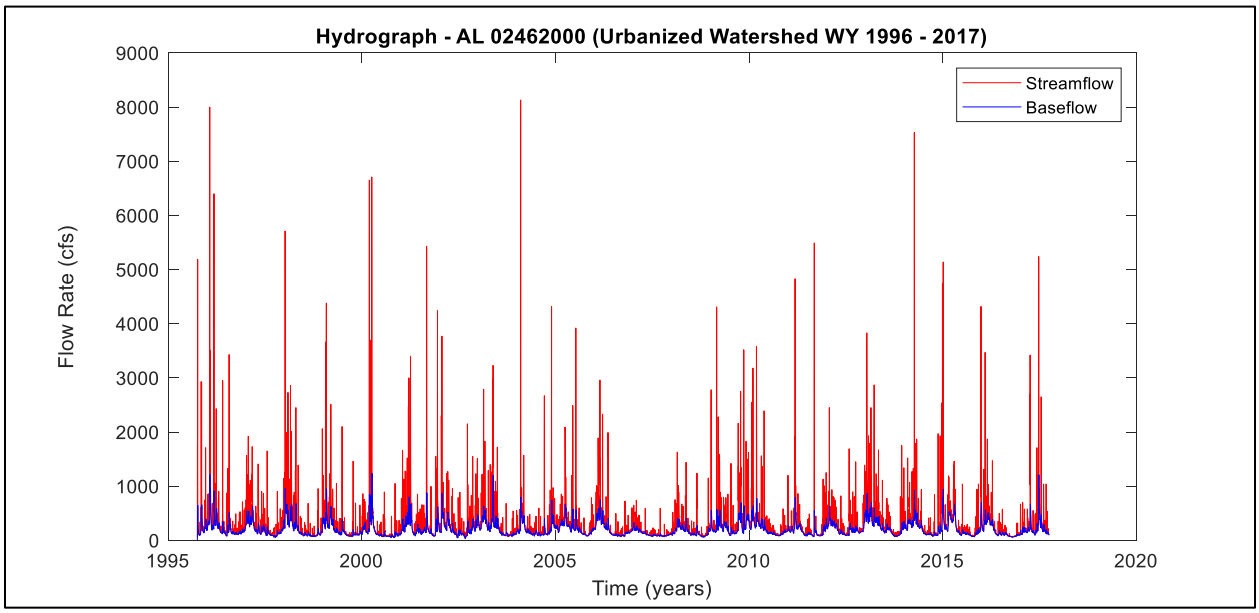

C1 Hydrographs:

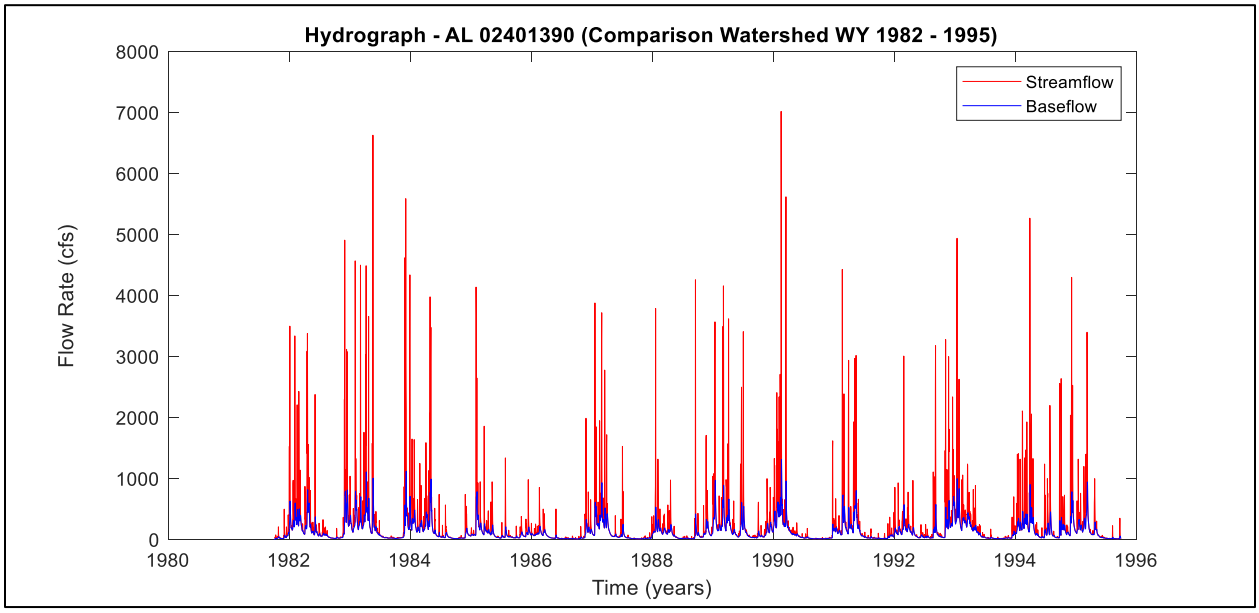

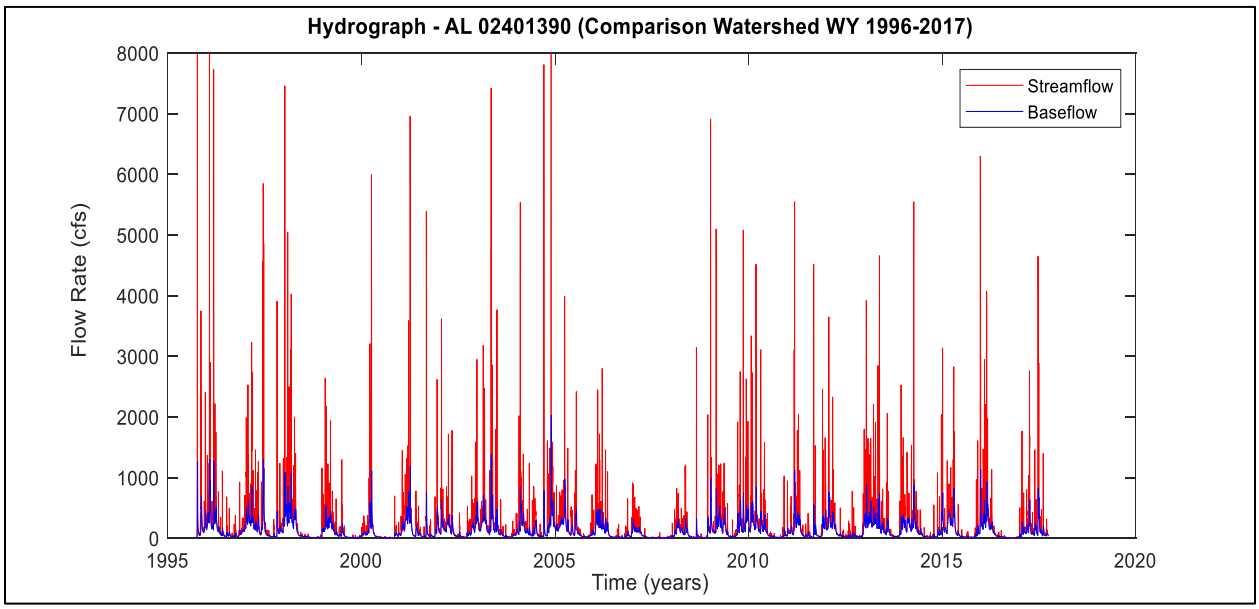

U2 Hydrographs:

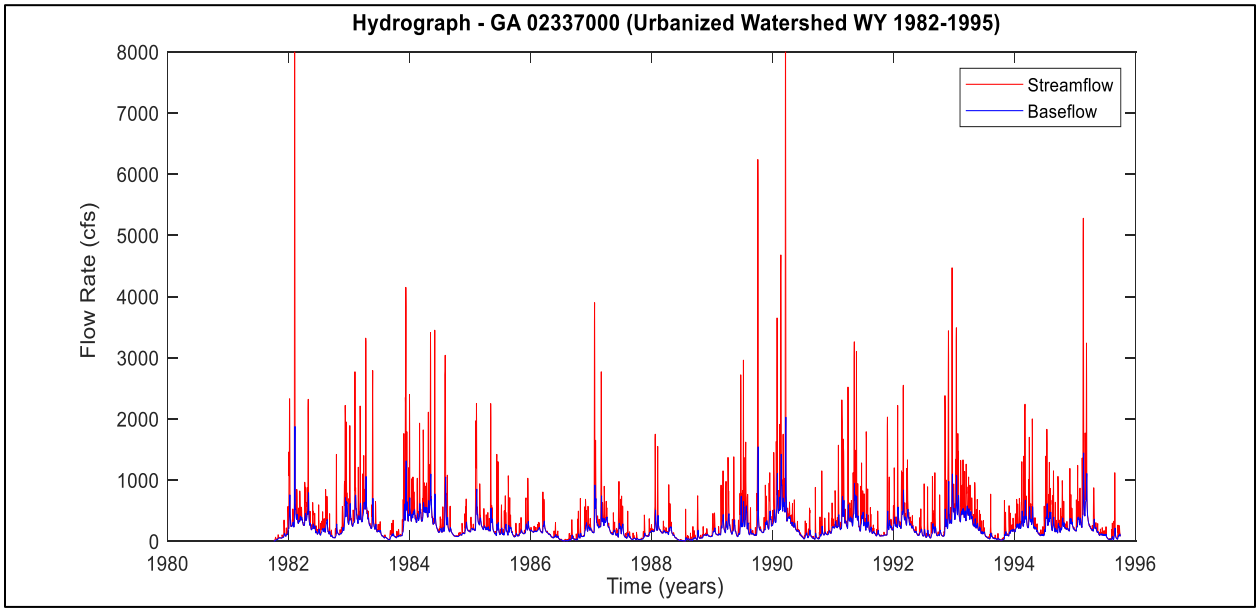

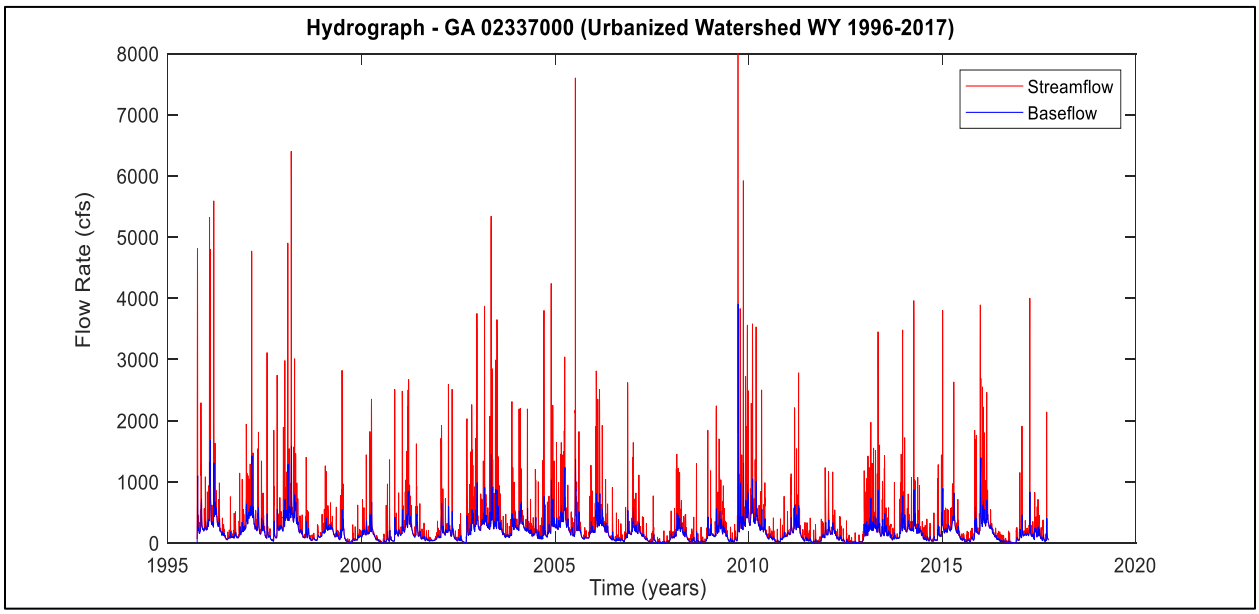

C2 Hydrographs:

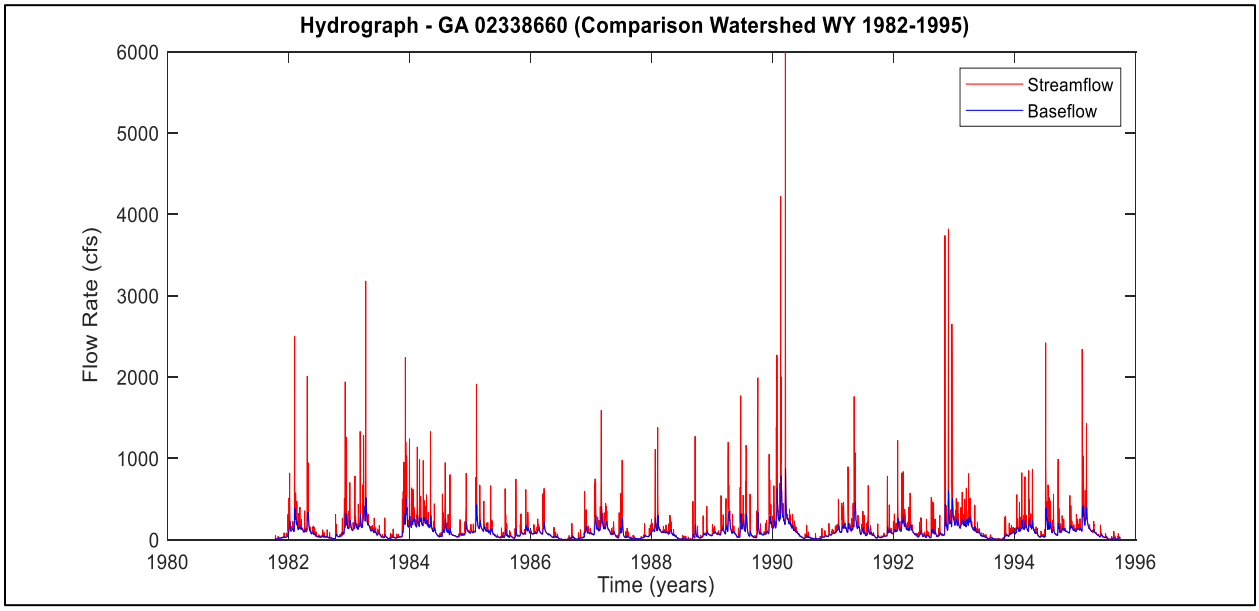

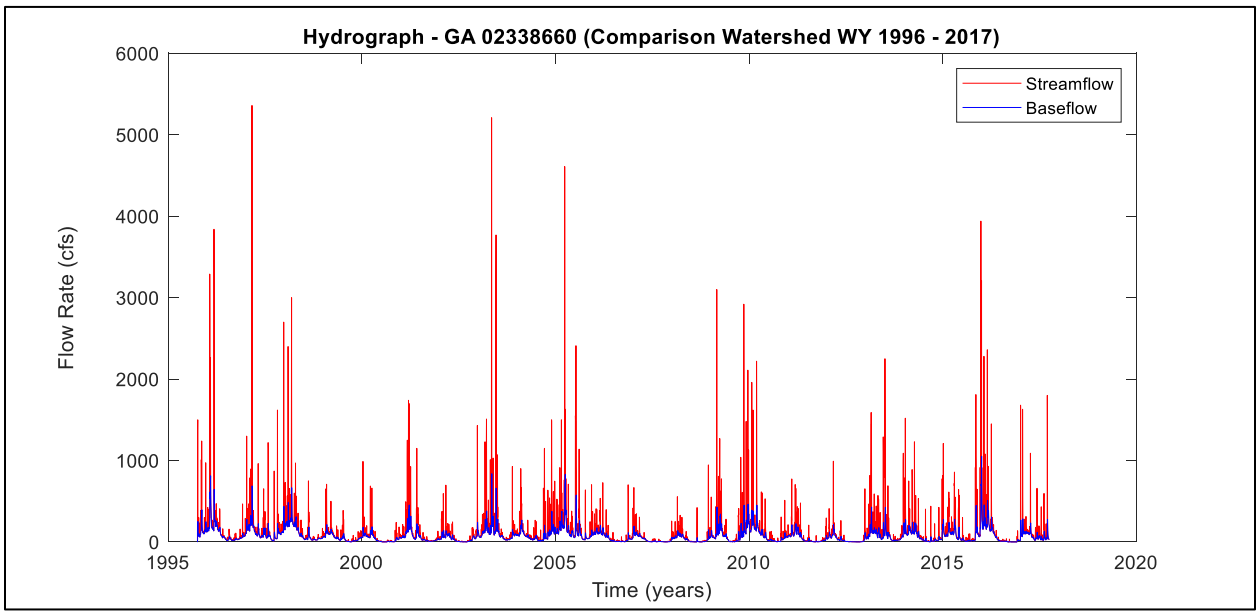

Appendix D: HEC-HMS Model Results

Model Calibration/Validation

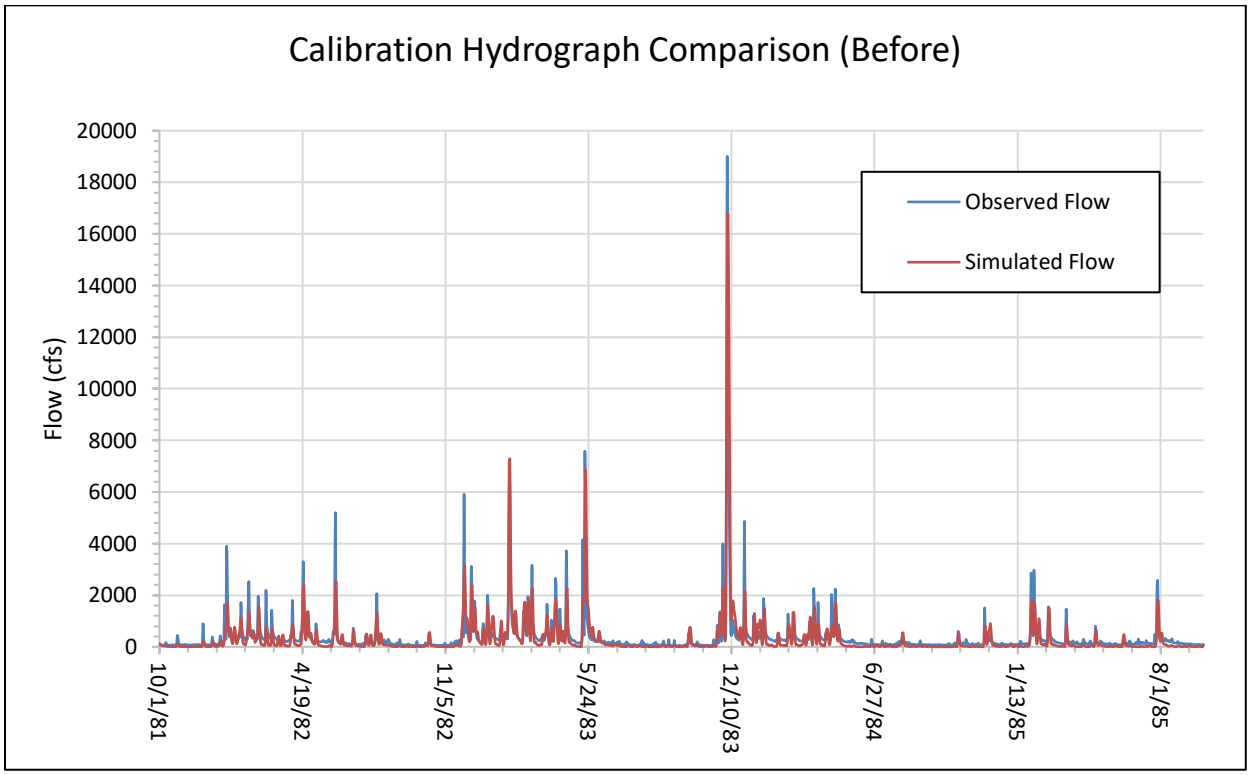

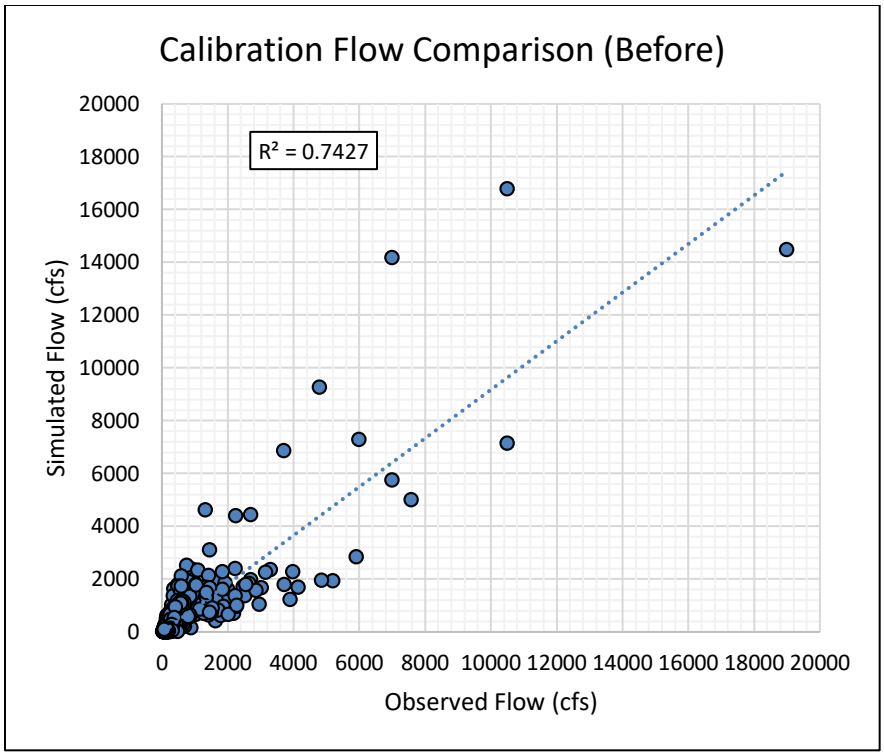
Calibration Flow Comparison (Before)
R² = 0.7427
Simulated Flow (cfs)
Observed Flow (cfs)
0
2000
4000
6000
8000
10000
12000
14000
16000
18000
20000

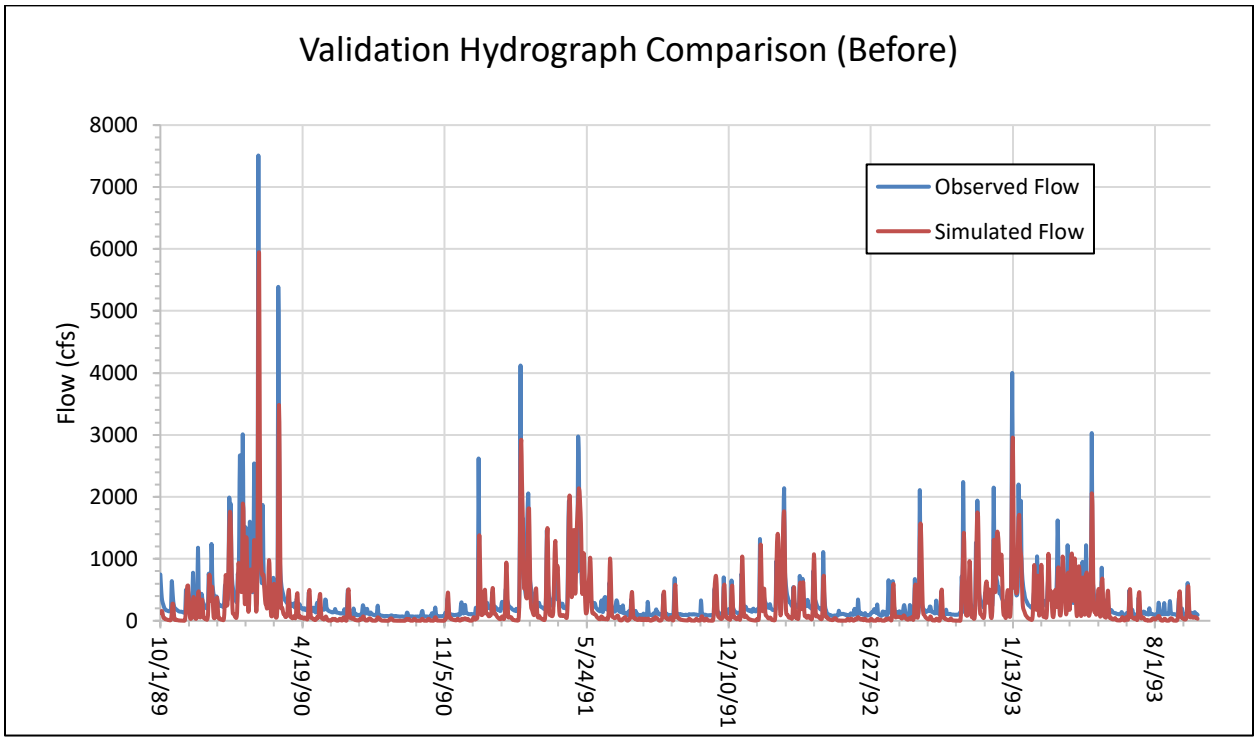
Validation Hydrograph Comparison (Before)
Observed Flow
Simulated Flow
Flow (cfs)
0
1000
2000
3000
4000
5000
6000
7000
8000
10/1/89
4/19/90
11/5/90
5/24/91
12/10/91
6/27/92
1/13/93
8/1/93

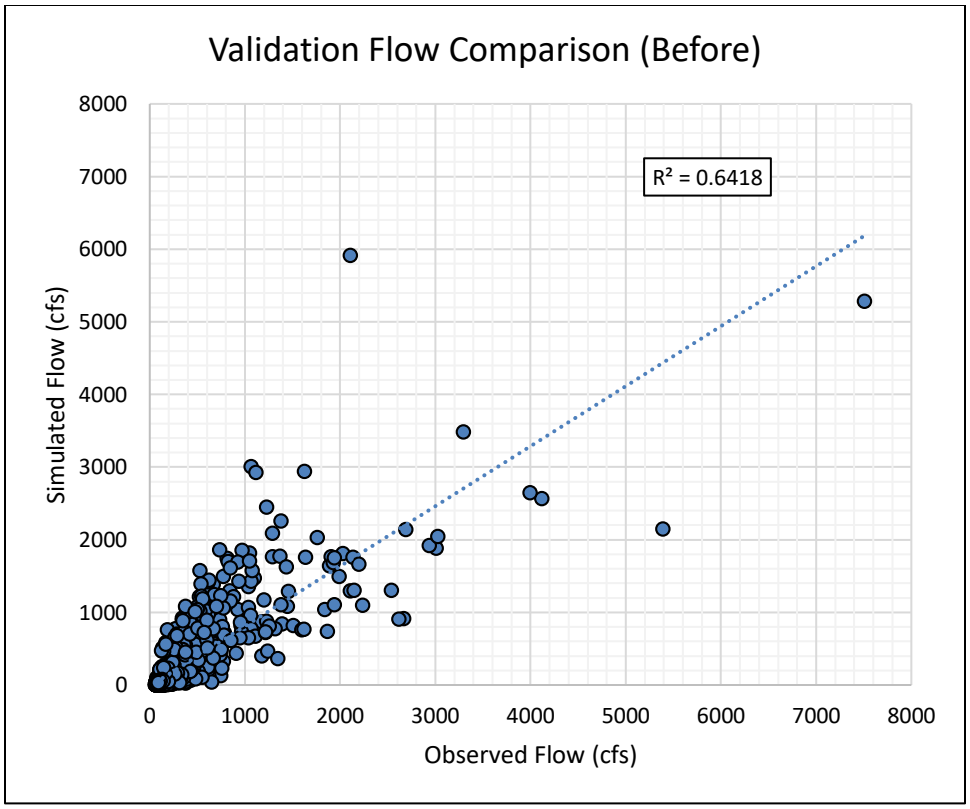
Validation Flow Comparison (Before)
R² = 0.6418
Simulated Flow (cfs)
Observed Flow (cfs)
0
1000
2000
3000
4000
5000
6000
7000
8000

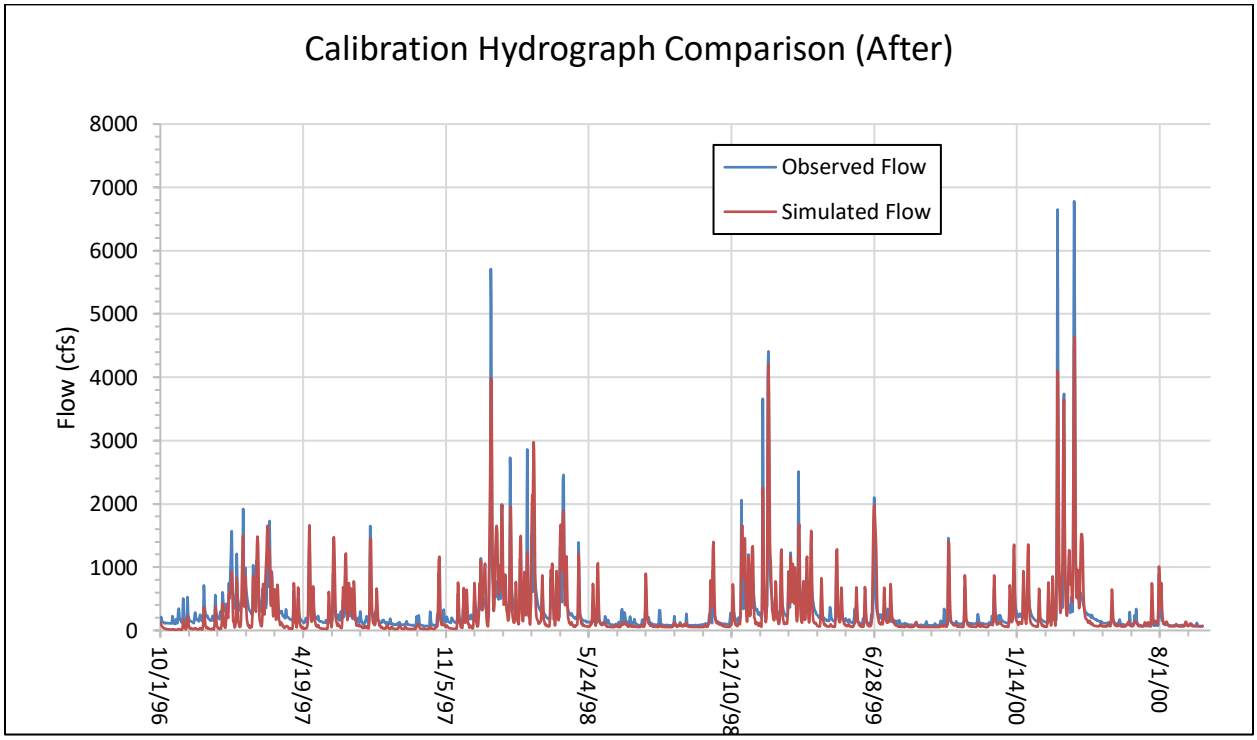
Calibration Hydrograph Comparison (After)
Observed Flow
Simulated Flow
Flow (cfs)
0
1000
2000
3000
4000
5000
6000
7000
8000
10/1/96
4/19/97
11/5/97
5/24/98
12/10/98
6/28/99
1/14/00
8/1/00

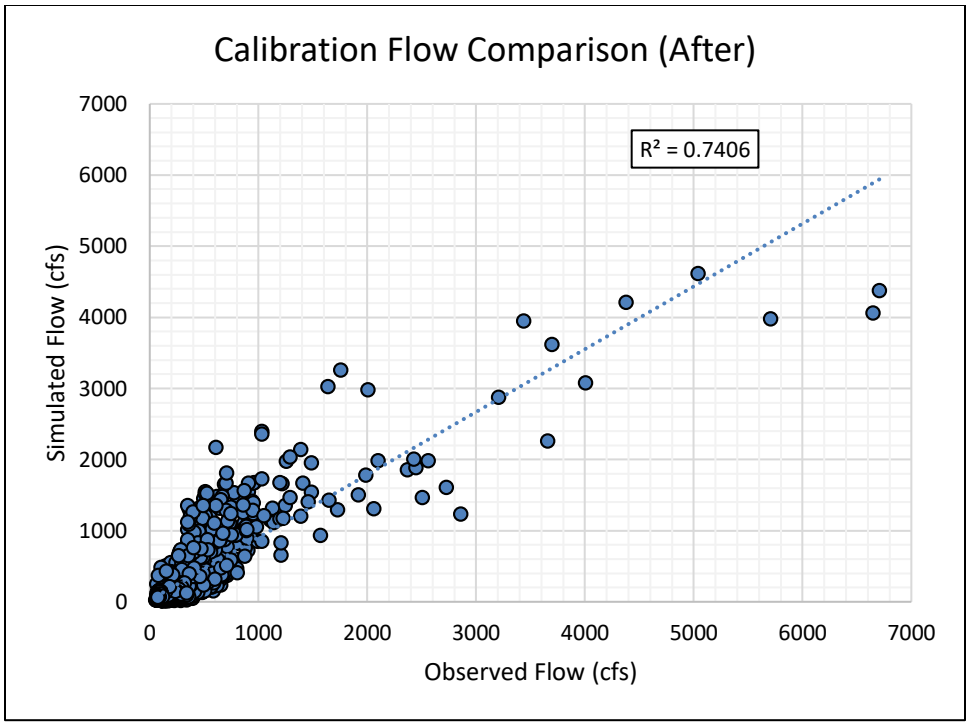
Calibration Flow Comparison (After)
R² = 0.7406
Simulated Flow (cfs)
Observed Flow (cfs)
0
1000
2000
3000
4000
5000
6000
7000

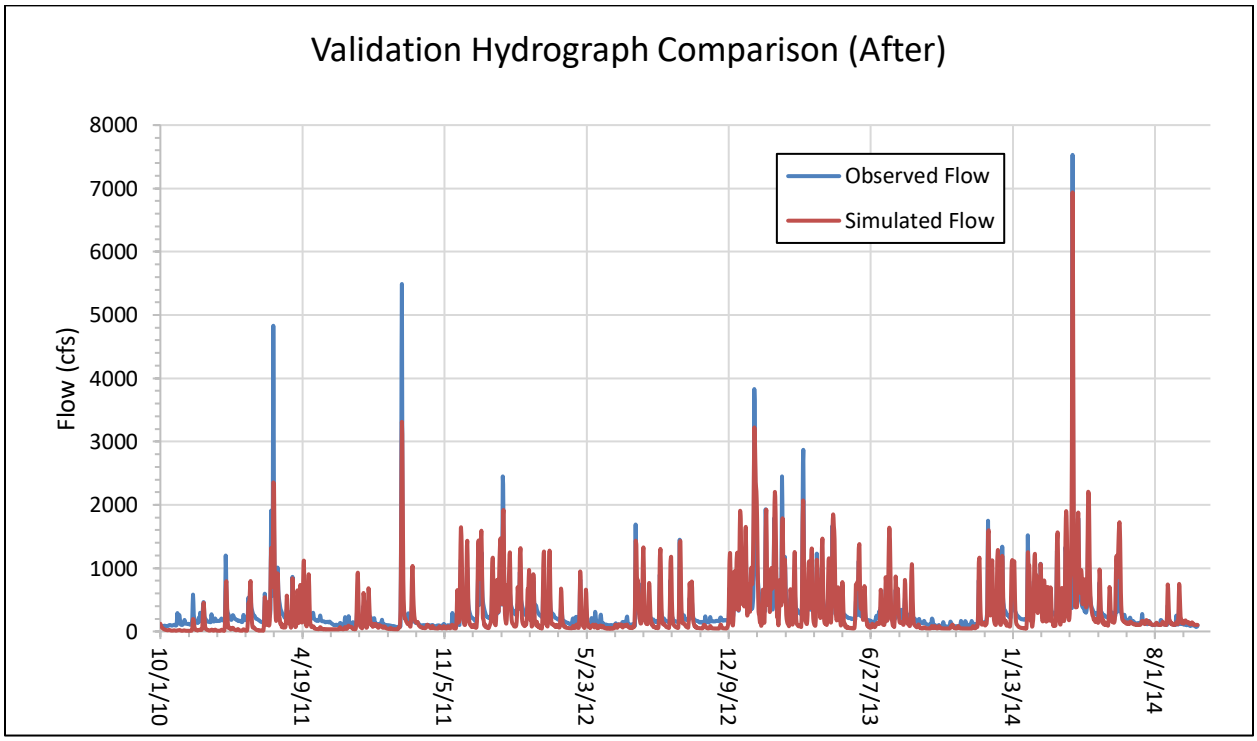
Validation Hydrograph Comparison (After)
Observed Flow
Simulated Flow
Flow (cfs)
0
1000
2000
3000
4000
5000
6000
7000
8000
10/1/10
4/19/11
11/5/11
5/23/12
12/9/12
6/27/13
1/13/14
8/1/14

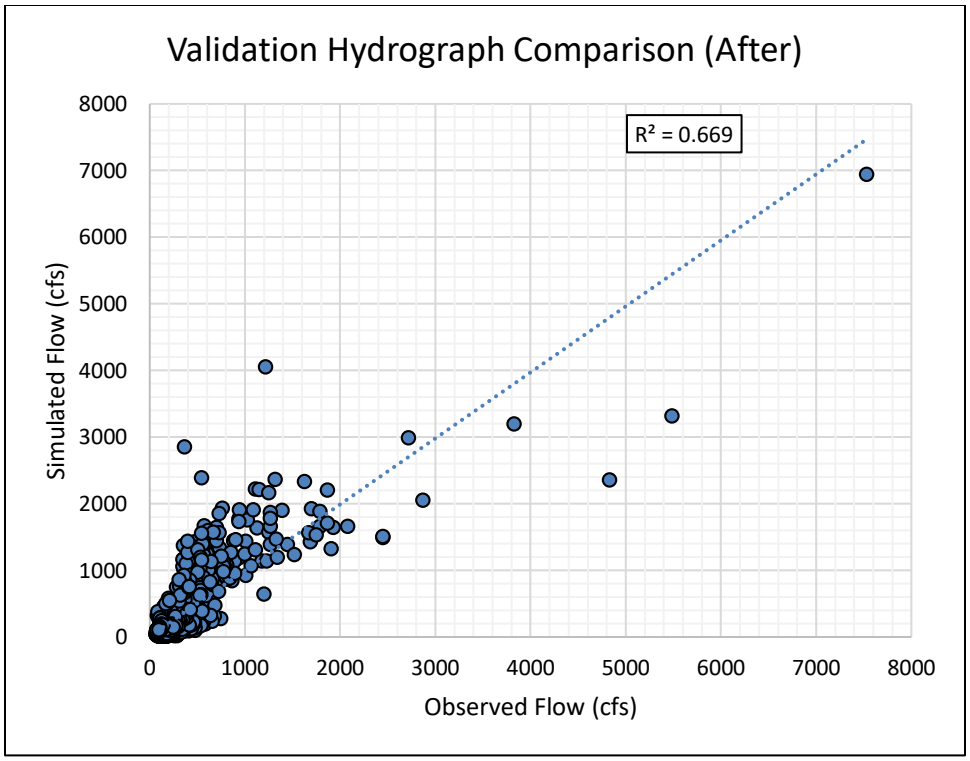
Validation Hydrograph Comparison (After)
R² = 0.669
Simulated Flow (cfs)
Observed Flow (cfs)
0
1000
2000
3000
4000
5000
6000
7000
8000

Model Optimization Parameter Values

Model Optimization Parameter Values (Before)				
Element	**Model Optimization Parameter**	**Initial Value**	**Optimized Value**	**Objective Function Sensitivity**
R1030	Muskingum - K	1.8319	1.6749	0.01
R1040	Muskingum - K	0.22217	0.20725	0
R1090	Muskingum - K	0.97611	0.81884	0.01
R1120	Muskingum - K	1.0438	0.91272	0.01
R140	Muskingum - K	3.7784	3.734	0
R170	Muskingum - K	0.89337	0.84319	0
R200	Muskingum - K	0.2183	0.2549	0
R270	Muskingum - K	2.0484	2.0415	0
R320	Muskingum - K	1.0305	1.0283	0
R340	Muskingum - K	0.13265	0.0650179	0
R360	Muskingum - K	1.4614	1.3966	0
R370	Muskingum - K	1.7917	1.4521	0.08
R380	Muskingum - K	0.72647	0.35782	0.02
R390	Muskingum - K	0.0557862	0.0321428	0
R420	Muskingum - K	0.83359	0.75091	0.01
R430	Muskingum - K	2.1177	2.1124	0
R510	Muskingum - K	1.32799	1.2775	0
R540	Muskingum - K	1.637	1.6333	0
R550	Muskingum - K	0.70204	0.7018	0
R580	Muskingum - K	0.51728	0.51294	0
R620	Muskingum - K	1.2853	1.1975	0.01
R630	Muskingum - K	0.60554	0.48302	0
R640	Muskingum - K	0.88451	0.81375	0
R670	Muskingum - K	1.6757	1.673	0
R680	Muskingum - K	2.5715	2.2641	0.1
R700	Muskingum - K	0.57759	0.24392	0.01
R730	Muskingum - K	3.2352	3.1645	0.03
R740	Muskingum - K	1.5477	1.2212	0.06
R770	Muskingum - K	1.2482	1.1444	0.02
R780	Muskingum - K	0.36364	0.31844	0
R820	Muskingum - K	1.1144	0.77365	0.02
R840	Muskingum - K	1.3441	1.2435	0.02
R860	Muskingum - K	1.2321	1.1181	0.02

R870	Muskingum - K	1.9544	1.6491	0.05
R880	Muskingum - K	1.2566	1.1479	0.02
R890	Muskingum - K	0.90766	0.70297	0.02
R910	Muskingum - K	0.80174	0.71337	0
R970	Muskingum - K	1.3071	1.014	0.03
R980	Muskingum - K	2.1274	1.8881	0.05
All Subbasins	Initial Abstraction Scale Factor	1	0.93743	0
R1030	Muskingum - x	0.26823	0.23592	0
R1040	Muskingum - x	0.40543	0.24217	0
R1090	Muskingum - x	0.29153	0.33525	0
R1120	Muskingum - x	0.38006	0.31844	0
R140	Muskingum - x	0.41119	0.36089	0
R170	Muskingum - x	0.43002	0.38707	0
R200	Muskingum - x	0.42338	0.37904	0
R270	Muskingum - x	0.42388	0.3716	0
R320	Muskingum - x	0.43333	0.37633	0
R340	Muskingum - x	0.42092	0.38594	0
R360	Muskingum - x	0.40539	0.34852	0
R370	Muskingum - x	0.13271	0.18997	0
R380	Muskingum - x	0.23025	0.23992	0
R390	Muskingum - x	0.42968	0.38414	0
R420	Muskingum - x	0.40624	0.42295	0
R430	Muskingum - x	0.43059	0.37761	0
R510	Muskingum - x	0.41186	0.34942	0
R540	Muskingum - x	0.41573	0.36518	0
R550	Muskingum - x	0.4205	0.32848	0
R580	Muskingum - x	0.41731	0.38458	0
R620	Muskingum - x	0.43146	0.37986	0
R630	Muskingum - x	0.42009	0.35623	0
R640	Muskingum - x	0.42451	0.36974	0
R670	Muskingum - x	0.41761	0.36647	0
R680	Muskingum - x	0.1657	0.18929	0
R700	Muskingum - x	0.42208	0.36742	0
R730	Muskingum - x	0.22164	0.23768	0
R740	Muskingum - x	0.27495	0.18724	0
R770	Muskingum - x	0.34747	0.31006	0
R780	Muskingum - x	0.43805	0.39441	0
R820	Muskingum - x	0.28334	0.23651	0
R840	Muskingum - x	0.2835	0.23099	0

R860	Muskingum - x	0.28848	0.25659	0
R870	Muskingum - x	0.27133	0.16881	0
R880	Muskingum - x	0.30668	0.27337	0
R890	Muskingum - x	0.41915	0.36756	0
R910	Muskingum - x	0.41587	0.37348	0
R970	Muskingum - x	0.26905	0.18734	0
R980	Muskingum - x	0.16964	0.20717	0
W1460	Recession - Initial Discharge	5	5.0458	0
W1470	Recession - Initial Discharge	5	5.0385	0
W1550	Recession - Initial Discharge	5	5.0277	0
W1600	Recession - Initial Discharge	5	5.1207	0
W1610	Recession - Initial Discharge	5	5.1614	0
W1650	Recession - Initial Discharge	5	5.0374	0
W1720	Recession - Initial Discharge	5	5.1436	0
W1750	Recession - Initial Discharge	5	5.0481	0
W1760	Recession - Initial Discharge	5	5.0198	0
W1930	Recession - Initial Discharge	5	5.0248	0
W1980	Recession - Initial Discharge	5	5.0437	0
W2040	Recession - Initial Discharge	5	5.0531	0
W2050	Recession - Initial Discharge	5	5.0368	0
W2060	Recession - Initial Discharge	5	5.0296	0
W2070	Recession - Initial Discharge	5	5.0849	0
W2090	Recession - Initial Discharge	5	5.0319	0
W2200	Recession - Initial Discharge	5	5.1154	0
W2310	Recession - Initial Discharge	5	5.0239	0
W2370	Recession - Initial Discharge	5	5.0799	0
W2390	Recession - Initial Discharge	5	5.0291	0
W2420	Recession - Initial Discharge	5	5.1651	0
W2460	Recession - Initial Discharge	5	5.0387	0
W2500	Recession - Initial Discharge	5	5.0614	0
W2640	Recession - Initial Discharge	5	5.0556	0
W1460	Recession - Ratio to Peak	0.2	0	0
W1470	Recession - Ratio to Peak	0.2	0.0948082	0
W1550	Recession - Ratio to Peak	0.2	0	0
W1600	Recession - Ratio to Peak	0.2	0.10451	0
W1610	Recession - Ratio to Peak	0.2	0.19691	0
W1650	Recession - Ratio to Peak	0.2	0.3541	0
W1720	Recession - Ratio to Peak	0.2	0.0287219	0
W1750	Recession - Ratio to Peak	0.2	0.1058	0
W1760	Recession - Ratio to Peak	0.2	0.0909698	0

W1930	Recession - Ratio to Peak	0.2	0.0756027	0
W1980	Recession - Ratio to Peak	0.2	0.18024	0
W2040	Recession - Ratio to Peak	0.2	0.13114	0
W2050	Recession - Ratio to Peak	0.2	0.17236	0
W2060	Recession - Ratio to Peak	0.2	0.0496284	0
W2070	Recession - Ratio to Peak	0.2	0.47704	0.01
W2090	Recession - Ratio to Peak	0.2	0.0787097	0
W2200	Recession - Ratio to Peak	0.2	0.0222399	0
W2310	Recession - Ratio to Peak	0.2	0.12859	0
W2370	Recession - Ratio to Peak	0.2	0.0352219	0
W2390	Recession - Ratio to Peak	0.2	0.0683327	0
W2420	Recession - Ratio to Peak	0.2	0.23838	0.01
W2460	Recession - Ratio to Peak	0.2	0.0046496	0
W2500	Recession - Ratio to Peak	0.2	0.0481897	0
W2640	Recession - Ratio to Peak	0.2	0.12717	0
W1460	Recession - Recession Constant	0.875	0.81301	0
W1470	Recession - Recession Constant	0.875	0.80839	0
W1550	Recession - Recession Constant	0.875	0.87842	0
W1600	Recession - Recession Constant	0.875	0.8023	0
W1610	Recession - Recession Constant	0.875	0.80812	0.01
W1650	Recession - Recession Constant	0.875	0.7821	0.01
W1720	Recession - Recession Constant	0.875	0.78622	0
W1750	Recession - Recession Constant	0.875	0.80815	0
W1760	Recession - Recession Constant	0.875	0.78916	0
W1930	Recession - Recession Constant	0.875	0.80173	0
W1980	Recession - Recession Constant	0.875	0.78874	0.01
W2040	Recession - Recession Constant	0.875	0.78167	0
W2050	Recession - Recession Constant	0.875	0.82228	0
W2060	Recession - Recession Constant	0.875	0.80859	0
W2070	Recession - Recession Constant	0.875	0.79644	0.01
W2090	Recession - Recession Constant	0.875	0.78455	0
W2200	Recession - Recession Constant	0.875	0.86754	0
W2310	Recession - Recession Constant	0.875	0.79023	0
W2370	Recession - Recession Constant	0.875	0.81281	0
W2390	Recession - Recession Constant	0.875	0.79761	0
W2420	Recession - Recession Constant	0.875	0.77684	0.01
W2460	Recession - Recession Constant	0.875	0.79439	0
W2500	Recession - Recession Constant	0.875	0.80242	0
W2640	Recession - Recession Constant	0.875	0.81084	0

Model Optimization Parameter Values (After)				
Element	**Model Optimization Parameter**	**Initial Value**	**Optimized Value**	**Objective Function Sensitivity**
R1030	Muskingum - K	1.6044	1.4953	0.01
R1040	Muskingum - K	0.2023	0.11303	0
R1090	Muskingum - K	0.77182	0.61653	0
R1120	Muskingum - K	0.25256	0.13152	0
R140	Muskingum - K	3.8614	4.0271	-0.01
R170	Muskingum - K	0.97668	1.0924	0
R200	Muskingum - K	0.43814	1.1296	0
R270	Muskingum - K	2.2331	2.3495	0
R320	Muskingum - K	1.1869	1.3338	0
R340	Muskingum - K	0.01843	0.016529	0
R360	Muskingum - K	1.3763	1.2963	0
R370	Muskingum - K	0.02237	0.016703	0
R380	Muskingum - K	0.01874	0.0168409	0
R390	Muskingum - K	0.01869	0.0167554	0
R420	Muskingum - K	0.46403	0.23454	0
R430	Muskingum - K	2.2805	2.4518	0
R510	Muskingum - K	1.325	1.2622	0
R540	Muskingum - K	1.7923	1.9041	0
R550	Muskingum - K	0.8965	1.0225	0
R580	Muskingum - K	0.68687	0.83068	0
R620	Muskingum - K	1.0729	0.85463	0
R630	Muskingum - K	1.0797	1.036	0
R640	Muskingum - K	0.8527	0.78123	0
R670	Muskingum - K	1.8237	1.9848	0
R680	Muskingum - K	1.0202	0.24517	0.01
R700	Muskingum - K	0.02985	0.016	0
R730	Muskingum - K	3.1588	3.0763	0.01
R740	Muskingum - K	0.02691	0.016	0
R770	Muskingum - K	0.98833	0.70731	0.01
R780	Muskingum - K	0.22134	0.13235	0
R820	Muskingum - K	0.19962	0.0822545	0
R840	Muskingum - K	0.47346	0.20203	0
R860	Muskingum - K	0.49458	0.22284	0
R870	Muskingum - K	0.86476	0.11506	0
R880	Muskingum - K	0.92575	0.598	0.01
R890	Muskingum - K	0.18332	0.0846081	0

R910	Muskingum - K	0.38984	0.30217	0
R970	Muskingum - K	0.20628	0.0541688	0
R980	Muskingum - K	1.3775	0.97746	0.02
All Subbasins	Initial Abstraction Scale Factor	1	0.98222	0
R1030	Muskingum - x	0.29965	0.30447	0
R1040	Muskingum - x	0.21289	0.30742	0
R1090	Muskingum - x	0.27142	0.31956	0
R1120	Muskingum - x	0.30363	0.30612	0
R140	Muskingum - x	0.18048	0.23636	0
R170	Muskingum - x	0.35064	0.32854	0
R200	Muskingum - x	0.34402	0.30627	0
R270	Muskingum - x	0.37346	0.35748	0
R320	Muskingum - x	0.39559	0.37928	0
R340	Muskingum - x	0.34583	0.40649	0
R360	Muskingum - x	0.36069	0.33728	0
R370	Muskingum - x	0.22162	0.22941	0
R380	Muskingum - x	0.22987	0.17585	0
R390	Muskingum - x	0.34627	0.3351	0
R420	Muskingum - x	0.38146	0.3706	0
R430	Muskingum - x	0.37624	0.35954	0
R510	Muskingum - x	0.36323	0.34095	0
R540	Muskingum - x	0.31121	0.28339	0
R550	Muskingum - x	0.34149	0.33001	0
R580	Muskingum - x	0.36745	0.34672	0
R620	Muskingum - x	0.3572	0.32122	0
R630	Muskingum - x	0.39151	0.37559	0
R640	Muskingum - x	0.3716	0.34723	0
R670	Muskingum - x	0.35693	0.33471	0
R680	Muskingum - x	0.19978	0.24179	0
R700	Muskingum - x	0.34879	0.32539	0
R730	Muskingum - x	0.18959	0.12565	0
R740	Muskingum - x	0.32798	0.30422	0
R770	Muskingum - x	0.30701	0.27718	0
R780	Muskingum - x	0.37002	0.33828	0
R820	Muskingum - x	0.26351	0.25019	0
R840	Muskingum - x	0.25235	0.25099	0
R860	Muskingum - x	0.23534	0.23109	0
R870	Muskingum - x	0.22201	0.28499	0
R880	Muskingum - x	0.25679	0.20318	0

R890	Muskingum - x	0.36867	0.34747	0
R910	Muskingum - x	0.36356	0.33783	0
R970	Muskingum - x	0.25038	0.23593	0
R980	Muskingum - x	0.23525	0.19791	0
W1460	Recession - Initial Discharge	5.0131	5.0322	0
W1470	Recession - Initial Discharge	5.0654	5.107	0
W1550	Recession - Initial Discharge	5.496	5.5195	0
W1600	Recession - Initial Discharge	5.1239	5.1245	0
W1610	Recession - Initial Discharge	5.1852	5.1081	0
W1650	Recession - Initial Discharge	5.426	5.4359	0
W1720	Recession - Initial Discharge	5.092	5.104	0
W1750	Recession - Initial Discharge	5.0086	5.055	0
W1760	Recession - Initial Discharge	4.9805	5.0639	0
W1930	Recession - Initial Discharge	5.0722	5.0981	0
W1980	Recession - Initial Discharge	5.0401	4.9825	0
W2040	Recession - Initial Discharge	4.7248	4.6932	0
W2050	Recession - Initial Discharge	5.0833	5.0842	0
W2060	Recession - Initial Discharge	5.0616	5.2929	0
W2070	Recession - Initial Discharge	5.0907	5.0153	0
W2090	Recession - Initial Discharge	4.9897	4.7951	0
W2200	Recession - Initial Discharge	5.111	5.1273	0
W2310	Recession - Initial Discharge	4.9945	4.9453	0
W2370	Recession - Initial Discharge	5.188	5.107	0
W2390	Recession - Initial Discharge	5.0841	5.1499	0
W2420	Recession - Initial Discharge	5.1422	5.1163	0
W2460	Recession - Initial Discharge	5.0408	5.0295	0
W2500	Recession - Initial Discharge	5.077	4.9923	0
W2640	Recession - Initial Discharge	5.0936	5.024	0
W1460	Recession - Ratio to Peak	0.01246	0.0043946	0
W1470	Recession - Ratio to Peak	0.1671	0.1134	0
W1550	Recession - Ratio to Peak	0.01293	0	0
W1600	Recession - Ratio to Peak	0.13324	0.11346	0
W1610	Recession - Ratio to Peak	0.12461	0.14071	0
W1650	Recession - Ratio to Peak	0.47016	0.44601	0
W1720	Recession - Ratio to Peak	0.03948	0.0713686	0
W1750	Recession - Ratio to Peak	0.13435	0.12453	0
W1760	Recession - Ratio to Peak	0.12988	0.14199	0
W1930	Recession - Ratio to Peak	0.14548	0.13951	0
W1980	Recession - Ratio to Peak	0.30343	0.29384	0
W2040	Recession - Ratio to Peak	0.13033	0.12554	0

W2050	Recession - Ratio to Peak	0.20757	0.15586	0
W2060	Recession - Ratio to Peak	0.10929	0.0915064	0
W2070	Recession - Ratio to Peak	0.49035	0.69909	0
W2090	Recession - Ratio to Peak	0.14445	0.14099	0
W2200	Recession - Ratio to Peak	0.06264	0.0835119	0
W2310	Recession - Ratio to Peak	0.16602	0.1438	0
W2370	Recession - Ratio to Peak	0.08571	0.0913649	0
W2390	Recession - Ratio to Peak	0.12341	0.11836	-0.01
W2420	Recession - Ratio to Peak	0.10928	0.10961	0
W2460	Recession - Ratio to Peak	0.04172	0.0541083	0
W2500	Recession - Ratio to Peak	0.11495	0.13131	0
W2640	Recession - Ratio to Peak	0.12688	0.10879	0
W1460	Recession - Recession Constant	0.89219	0.88988	0
W1470	Recession - Recession Constant	0.80393	0.787	0
W1550	Recession - Recession Constant	0.84946	0.84694	0
W1600	Recession - Recession Constant	0.7805	0.68606	0
W1610	Recession - Recession Constant	0.63588	0.58513	0
W1650	Recession - Recession Constant	0.75756	0.72148	0
W1720	Recession - Recession Constant	0.85907	1	-0.27
W1750	Recession - Recession Constant	0.81797	0.88583	0
W1760	Recession - Recession Constant	0.50288	0.48854	0
W1930	Recession - Recession Constant	0.79309	0.81881	0
W1980	Recession - Recession Constant	0.64997	0.62188	-0.01
W2040	Recession - Recession Constant	0.75835	0.73565	0
W2050	Recession - Recession Constant	0.85152	0.58536	0
W2060	Recession - Recession Constant	0.81338	0.76231	0
W2070	Recession - Recession Constant	0.37126	0.20847	0
W2090	Recession - Recession Constant	0.78987	0.77396	0
W2200	Recession - Recession Constant	0.86345	0.84496	0
W2310	Recession - Recession Constant	0.73486	0.7168	0
W2370	Recession - Recession Constant	0.55127	0.5532	0
W2390	Recession - Recession Constant	1	1	-0.29
W2420	Recession - Recession Constant	0.76023	0.7137	0
W2460	Recession - Recession Constant	0.75835	0.7007	0
W2500	Recession - Recession Constant	0.41563	0.39366	0
W2640	Recession - Recession Constant	0.67069	0.61969	0